

INFORMATION TO USERS

This manuscript has been reproduced from the microfilm master. UMI films the text directly from the original or copy submitted. Thus, some thesis and dissertation copies are in typewriter face, while others may be from any type of computer printer.

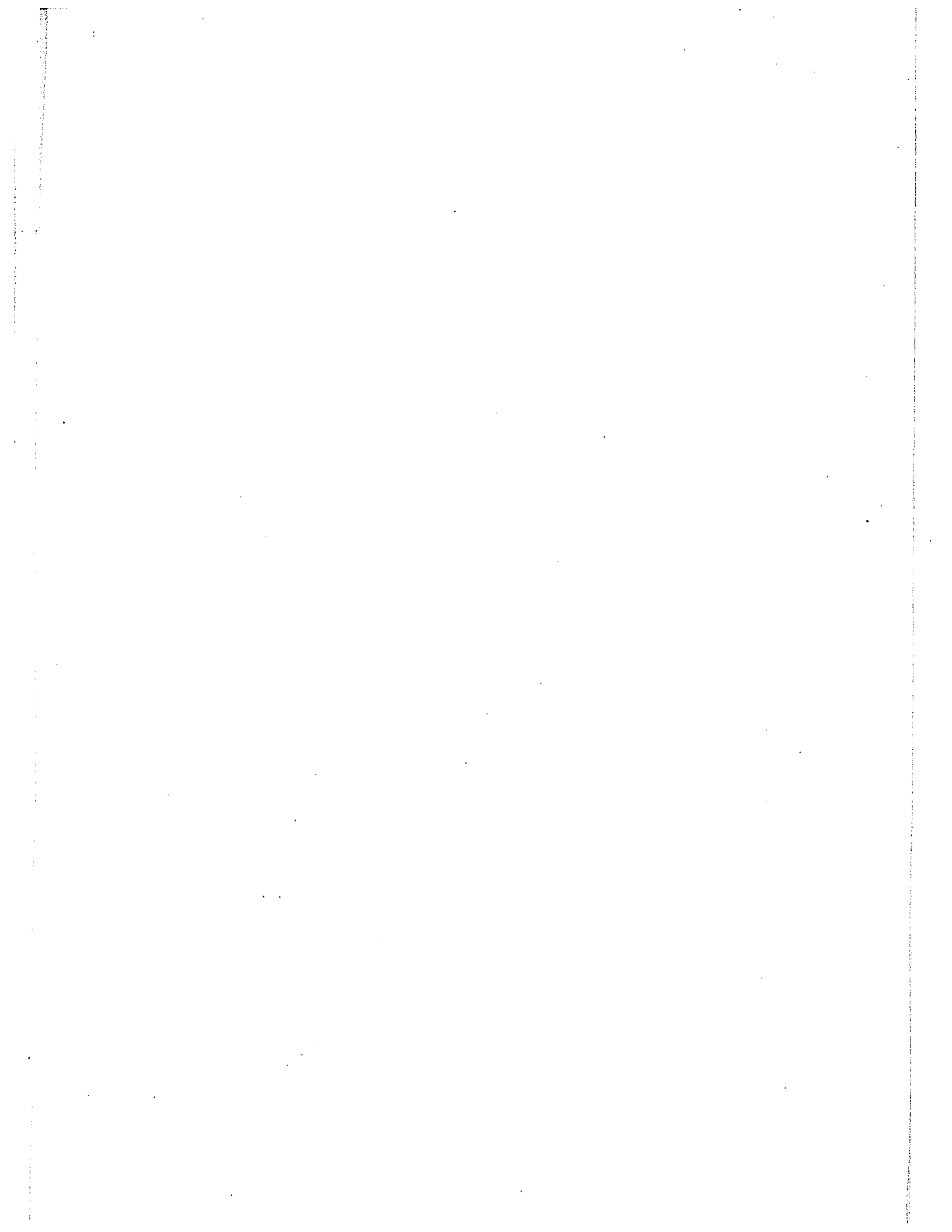
The quality of this reproduction is dependent upon the quality of the copy submitted. Broken or indistinct print, colored or poor quality illustrations and photographs, print bleedthrough, substandard margins, and improper alignment can adversely affect reproduction.

In the unlikely event that the author did not send UMI a complete manuscript and there are missing pages, these will be noted. Also, if unauthorized copyright material had to be removed, a note will indicate the deletion.

Oversize materials (e.g., maps, drawings, charts) are reproduced by sectioning the original, beginning at the upper left-hand corner and continuing from left to right in equal sections with small overlaps.

ProQuest Information and Learning
300 North Zeeb Road, Ann Arbor, MI 48106-1346 USA
800-521-0600

UMI[®]

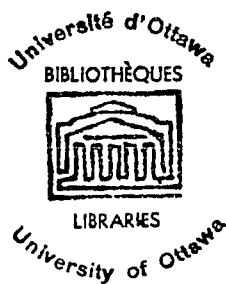


A FORM AND PROCESS RESPONSE
STUDY OF A TERMINAL ICE CORED
ABLATION MORAINÉ

by
A. BLAIR ROSS

Thesis submitted to the School of Graduate Studies of the University
of Ottawa in partial fulfillment of the requirements for the degree
of Master of Arts in Geography and Regional Planning.

Ottawa, June 6, 1975



UMI Number: EC52423

INFORMATION TO USERS

The quality of this reproduction is dependent upon the quality of the copy submitted. Broken or indistinct print, colored or poor quality illustrations and photographs, print bleed-through, substandard margins, and improper alignment can adversely affect reproduction.

In the unlikely event that the author did not send a complete manuscript and there are missing pages, these will be noted. Also, if unauthorized copyright material had to be removed, a note will indicate the deletion.

UMI[®]

UMI Microform EC52423
Copyright 2007 by ProQuest LLC
All rights reserved. This microform edition is protected against
unauthorized copying under Title 17, United States Code.

ProQuest LLC
789 East Eisenhower Parkway
P.O. Box 1346
Ann Arbor, MI 48106-1346

TABLE OF CONTENTS

		<u>Page Number</u>
ABSTRACT		i
ACKNOWLEDGMENTS		vi
LIST OF FIGURES		vii
LIST OF PLATES		ix
CHAPTER 1.	INTRODUCTION	1
	1.1 Preface	1
	1.2 Study Area	3
	1.3 Literature Review	9
	1.3.1. Ice Cored Moraines	9
	1.3.2. Identification of Ice Type	15
	1.4 Methodology	19
CHAPTER 2.	NATURE OF ICE CORE	27
	2.1 Introduction	27
	2.2 Methodology	28
	2.3 Results of Analysis	31
	2.3.1. Crystal Orientation	31
	2.3.2. Crystal Size	37
	2.3.3. Crystal Shape	44
	2.4 Summary	46
CHAPTER 3.	MORPHOLOGY OF THE DONJEK END MORaine	50
	3.1 General Form	50
	3.2 Slope Analysis	55
	3.2.1. Introduction	55
	3.2.2. Methodology	56
	3.2.3. Data Analysis	57
	-- Proximal-Distal Sides	60
	Mean Slope Angles	60
	Frequency Distributions	61
	-- Slope Orientation	61
	Mean Slope Angles	61
	Frequency Distribution	62
	3.2.4. Summary	63
	3.3 Summary on Form of End Moraine	66

TABLE OF CONTENTS

- 2 -

	<u>Page Number</u>
CHAPTER 4. CLIMATIC AND GLACIAL SURGE INPUT FACTORS AND GROUND TEMPERATURES	69
4.1 Climatic Inputs	69
4.1.1. Introduction	69
4.1.2. Micro Climatic Trends at Moraine Stations	70
Air Temperature	70
Cloud Cover	73
Relative Humidity	75
Wind Speed	80
Wind Direction	83
Evaporation	85
Precipitation	88
4.2 Soil Temperatures	90
4.3 Glacial Surge Input	96
4.4 Summary	97
CHAPTER 5. DEPTH OF FREEZE-THAW OCCURRING ON THE MORAINE AND ICE CORE ABLATION	99
5.1 Introduction	99
5.2 Grain Size Analysis	100
Methodology	100
Results of Analysis	101
5.3 General Conditions and Assumptions For Calculation of Freeze-Thaw Depths	103
5.3.1. Depth of Penetration of A Periodic Wave	104
5.3.2. Depth of Freeze	108
(1) Simplified Stefan Method	108
(2) Modified Berggren Method	113
5.3.3. Depth of Thaw	117
(1) Simplified Stefan Method	117
(2) Modified Berggren Method	118
(3) Terzaghi	118
5.3.4 Summary	120
5.4 Ablation of Debris Covered Ice	122
5.4.1. Calculations	122
5.4.2 Summary	124
5.5 Ablation of Exposed Ice	125
5.5.1. Direct and Diffuse Radiation	125
5.5.2. Evaporation on Exposed Ice Faces	128

TABLE OF CONTENTS

- 3 -

	<u>Page Number</u>
5.6 Ablation of Ice Core as a Result of Terrestrial Heat Flow	130
5.7 Summary	130
5.8 Summary of the Depth of Freeze-Thaw and Ice Core Ablation on the Moraine	133
 CHAPTER 6. DEGRADATIONAL PROCESSES	 136
6.1 Introduction	136
6.2 Ablation	136
6.3 Mass Movements and the Action of Melt Water Streams and Ponds	137
6.4 Rates of Headwall Retreat	144
6.4.1. Results of Analysis	144
6.4.2. Summary	149
6.5 Headwall Retreat and Micro Climate	150
6.5.1. Results of Analysis	150
6.5.2. Summary	157
6.6 Variations Around the Moraine	157
6.7 Resultant Topographic Forms	159
6.8 Summary	162
 CHAPTER 7. CONCLUSIONS	 164
 BIBLIOGRAPHY	 170
 APPENDIX	
1. Grain Size Analysis	A-1
1.1 Statistical Analysis	A-1
(a) Mean Grain Size	A-1
(b) Sorting	A-4
(c) Skewness	A-6
(d) Kurtosis	A-7
(e) Frequency Distributions	A-9
 2. General Discussion of Heat Flow Through Soil	 A-18
2.1 Soil Thermal Parameters	A-18
2.2 Unidirectional Heat Transfer	A-25

ABSTRACT

The initiation and distribution of certain types of degradational processes together with resultant topographical changes on an ice cored moraine were studied in terms of the variation in micro climatic and glacial surge inputs operating on it. The study was conceived in terms of a process-response model.

The study area was located on a large arcuate shaped ice cored end moraine, which rims the terminus of the Donjek Valley Glacier located in the Donjek Valley, St. Elias Mountains, Yukon Territory. The end moraine lies approximately 0.8 to 2.7 Km downvalley from the present position of the glacier, and is detached from it.

The regional climate of the area was determined from data collected from a nearby government operated meteorological station. Climatic inputs occurring on or near the moraine surface, from June 1 to July 25, 1972, were obtained from two micro meteorological stations located directly on its surface. All data was abstracted and shown on graphs as mean daily values. The number of days that one station exceeded the other either/or on a mean daily basis and over three hour intervals, was also noted over the study period.

Similarly, the resultant temperature gradient in the moraine material was measured, at each meteorological station, by continuously recording thermographs, located at 15 cm, 31 cm and 46 cm depths. Mean daily values were graphed while mean values for the entire study period were also noted. The depth to which a periodic wave extends both daily and on a seasonal basis, together with the depth of freeze-thaw occurring on the moraine, was calculated. The quantity of heat being transmitted through the soil, as a result of the climatic interaction occurring at the air-ground boundary together with that being transmitted as a result of terrestrial heat flow, was also calculated for each station with the use of standard soil engineering equations. Similarly, the amount of ice core ablation, due to the above heat transfer process, together with that due to a short wave radiation and evaporation on an exposed ice face, was derived.

Both micro climatic parameters and heat flow values were related to degradational processes, i.e. ablation and resultant processes such as mudflows (slumps, slides), and glacial melt water stream and pond action, occurring on the moraine. Rates of headwall retreat were calculated for exposures on the moraine. In most of the above mentioned cases trends rather than specific values were noted.

The morphology of the moraine was presented both qualitatively and quantitatively (by taking slope angle measurements on both

its proximal and distal sides); and together with type and frequency of vegetation type, were related to the occurrence of these processes. Similarly soil samples were taken around the moraine and analyzed for grain size; and these results were used in heat transfer equations.

Glacial surge inputs on the moraine were determined by aerial photographs; and their results were monitored in terms of headwall retreat at exposures caused by these advances.

Finally, a sample of the buried ice, from the Donjek ice cored moraine, was subjected to fabric analysis to determine the effectiveness of this method in identifying buried ice types.

Results showed that the variation in micro climatic inputs, occurring on the moraine, do not fully explain the occurrence of certain types of degradational processes operating on it. However, the initiation and increases in rates of these processes may be explained, to a degree, by corresponding increases in certain micro climatic parameters, such as ambient air temperatures, precipitation, relative humidity, incoming radiation; and decreases in the intensity of others, such as evaporation and wind. Climatic inputs, not soil variation, account primarily for the variation in the quantity of heat being transmitted through the soil at the two stations and their differential ablation rates. Due to the heterogeneous character of the moraine material, no specific soil

thermal parameters could be presented.

The occurrence of ice core exposures, and resultant mass movements, depend primarily upon the variations in both the depth of overlying material and soil thermal parameters. Rates of headwall retreat, for slumps active throughout the study period, are comparable to those for similar features in the Arctic.

Maximum melt out rates, under present climatic conditions, suggest 60 years for complete wastage of the ice core.

Melt water streams and ponds, on the moraine, are effective triggering mechanisms for slumps and slides and, indirectly, are responsible for the same processes becoming inactive.

The moraine is extremely massive in size, with steeper distal than proximal slope angles. The slope angles were also greater on the lee area than elsewhere; and this, combined with a micro climate more conducive to greater quantities of heat flow through the soil and a thinner debris cover, has resulted in more active degradational processes here. The surface of the moraine is highly complex, both morphologically and in composition of the materials, reflecting the variety of environments, which either have or presently are, operating there. The size of the moraine and quantity of till present are deceiving, as the depth of overlying material (on the western portion) was only a thin mantle when

compared to the quantity of ice beneath. Differential ablation of the ice core has resulted in both the form of the overlying material conforming to that of the underlying ice, and the hummocky appearance of the moraine.

Fabric analysis on the ice sample revealed that it was glacier ice. However, because other ice types may possess similar fabric characteristics under certain circumstances, caution must be used when employing this technique.

ACKNOWLEDGMENTS

I wish to express my gratitude to my advisor, Dr. P. G. Johnson, for his guidance in helping me to compile and write this thesis. A very personal note of appreciation is also extended to my father for his words of encouragement, counsel and suggestions in the final stages of preparation of the manuscript, and to Marian whose continued faith in me provided additional inspiration throughout its writing.

Recognition is also accorded to Dr. R. Ramseier, Head, Floating Ice Section, Division of Inland Waters, Ottawa, for his interest and direction in preparation of ice samples and for use of laboratory facilities.

I am extremely grateful to the Department of Geography for their educational training and support.

Finally I would like to acknowledge the assistance of Dr. B. Rust, Department of Geology, University of Ottawa, for his guidance during the data collection, T. Kent who acted as my field assistant, and E. Koster for his aid with the analysis of the data.

LIST OF FIGURES

FIGURE	Page Number
1. Location of Study Area -----	4
2. Glacier Features of Study Area -----	7
3. Fabric Diagram of Ice Sample-Contour -----	32
4. Fabric Diagram of Ice Sample-Points -----	33
5.(a) Mean Size of Ice Crystals -----	38
(b) Longest Axis and Size Variation on Colour and Black and White Photographs -----	39
6. Slope Angles - Individual Traverses -----	58
7. Slope Angles - Integrated Results -----	59
8. Mean Daily Air Temperatures -----	71
9. Mean Monthly and Maximum-Minimum Air Temperatures-----	72
10. Mean Daily Air Temperature for Three Hour Intervals and Percentage of Time When A or B Exceeded One Another-	74
11. Mean Daily Relative Humidity -----	76
12. Mean Daily Short Wave Radiation -----	78
13. Mean Daily and Mean Maximum Daily Short Wave Radiation and Percentage of Time A Exceeded B -----	79
14. Mean Daily Wind Speed -----	82
15. Mean Wind Speed - Three Hour Intervals -----	83
16. Total Potential Daily Evaporation -----	86
17. Wind Speed <u>vs</u> Evaporation -----	87
18. Total Daily Precipitation -----	89
19. Mean Daily Soil Temperatures - A Station -----	91
20. Mean Daily Soil Temperature - B Station -----	92
21. Mean Daily Soil Temperature for Study Period -----	93
22. Mean Daily Maximum and Minimum Soil Temperatures-----	94
23. Percent of Time A or B Exceeded One Another -----	95
24. Mean Monthly Air Temperature Burwash Landing -----	105
25. Mean Annual Air Temperature Sine Wave -----	106
26. Simplified Stefan Model -----	110
27. Annual Variation in Air Temperature Burwash Landing -----	111

FIGURE	Page Number
28. Modified Berggren Model -----	114
29. Mean Daily Ablation <u>vs</u> Till Thickness -----	127
30. Distribution of Ice Exposures -----	142
31. Rates of Retreat of Ice Exposures -----	145
32. Slumping of Debris Along Ice-Till Interface -----	148
33. Synopsis of Micro Climate and Soil Temperatures ----	153
34. Rates of Headwall Retreat - Percentage of Study Time -----	154
35. Daily Soil Temperatures <u>vs</u> Precipitation -----	156
36. Grain Size Analysis -----	A-12
37.(1-5) Cumulative Percent Curves -----	A-13
38. Thermal Conductivity for Various Substances -----	A-20
39. Thermal Conductivity <u>vs</u> Moisture Content -----	A-21
40. Heat Capacity <u>vs</u> Moisture Content -----	A-22
41. Field Capacity - Wilting Point for Various Substances -----	A-24
42. Thermal Diffusivity <u>vs</u> Water Content -----	A-28
43. Diffusivity Values for Various Substances -----	A-29
44. Slope Profile -----	A-32

LIST OF PLATES

PLATE	Page Number*
1.1	6
Aerial view of terminus of Donjek Glacier and terminal moraine-----	
2.1,11,111,1V,V,VI,V11.	44
Horizontal and vertical view of ice crystal sample-----	
3.1	50
Oblique view of terminal moraine-----	
3.11	52
Ridge separating drift A and B-----	
3.111	54
A conical hill and melt water ponds located along the terminal moraine-----	
5.1	125
Exposure II-----	
6.1	139
Erosion and ice core exposure by melt water stream action-----	
6.11	140
Ice core exposure on side of melt water pond-----	

* Plates are located opposite the given page number in the text.

1. INTRODUCTION

1.1 Preface

In this work ice cored moraines are defined as features in which an ice mass occupies a portion of the internal structure of the landform while the remaining portion consists of detritus deposited directly or indirectly by glacier action. This definition is similar to that used by Østrem (1964) and Loomis (1970) in which it was recognized that both glacier or snowbank ice may exist as an ice core under morainic debris.

The conception of this study was in the form of a model. Past glacial action resulted in the formation of an ice cored end moraine and as a result of the dynamic interaction of inputs, (micro climatic factors and the effect of glacial surges), both on and within the moraine, certain degradational processes occurred. The effect of these processes has been to modify the form of the moraine.

It has been the latter part of this model, i.e. ablation of buried ice, with resulting degradational processes and morphological changes, that has occupied much of the contemporary work of Østrem throughout the nineteen sixties and that of Loomis (1970) and Johnson (1971, 1972). However, each author

has chosen a particular segment to investigate rather than analyzing this section on an integral basis. A brief summary of their work is given in section 1.2.

The problem under investigation in this study is the determination of the influence of micro climatic parameters, and the effect of glacial surge action in the production and distribution of certain degradational processes, and the resultant morphological changes occurring on ice cored moraines.

The study involved the measurement of micro climatic parameters existing on the ice cored terrain, together with measurements of certain material and morphological parameters such as grain size analysis, slope angles (orientation and inclination), morphology, cracking, percentage frequency of melt water ponds, and vegetation cover, and the collection of soil thermal data showing the resulting heat flux through the morainic material. This latter measurement allowed determination of the minimum depth of material required to prevent ablation of the underlying ice, and quantitative and qualitative analysis of other processes such as rates of headwall retreat, melt water stream and pond action.

The rates were then compared to the climatic parameters operating near these sites; and those which influenced both the rates

and initiation of these processes were determined. The climatic parameters were then compared with the distribution of these processes and their resultant topographical changes.

1.2 The Study Area

The study area is located in the southwestern corner of the Yukon Territory, Canada, in the St. Elias Mountain Range, latitude $61^{\circ} 30''$, longitude $139^{\circ} 45''$. This mountain chain forms a major element of the Pacific Mountain Ranges of North America. They form a shallow arc, some 500 km in length, running parallel to one another, and the resultant topography is that of a high alpine region with active ice fields and valley glaciers. Many authors such as Taylor-Barge (1969), Havens and Saarela (1969), and Marcus and Ragle (1970) and others, have recognized the important role that these mountains play in moderating the climate around them. They form an effective topographic barrier between the Gulf of Alaska, where they promote a cool Maritime West Coast climate on the Pacific littoral, and the continental interior, some 250 km away, where a subarctic regime exists.

The field site chosen for this particular work was in the Donjek Valley (FIG.1). The valley is located along

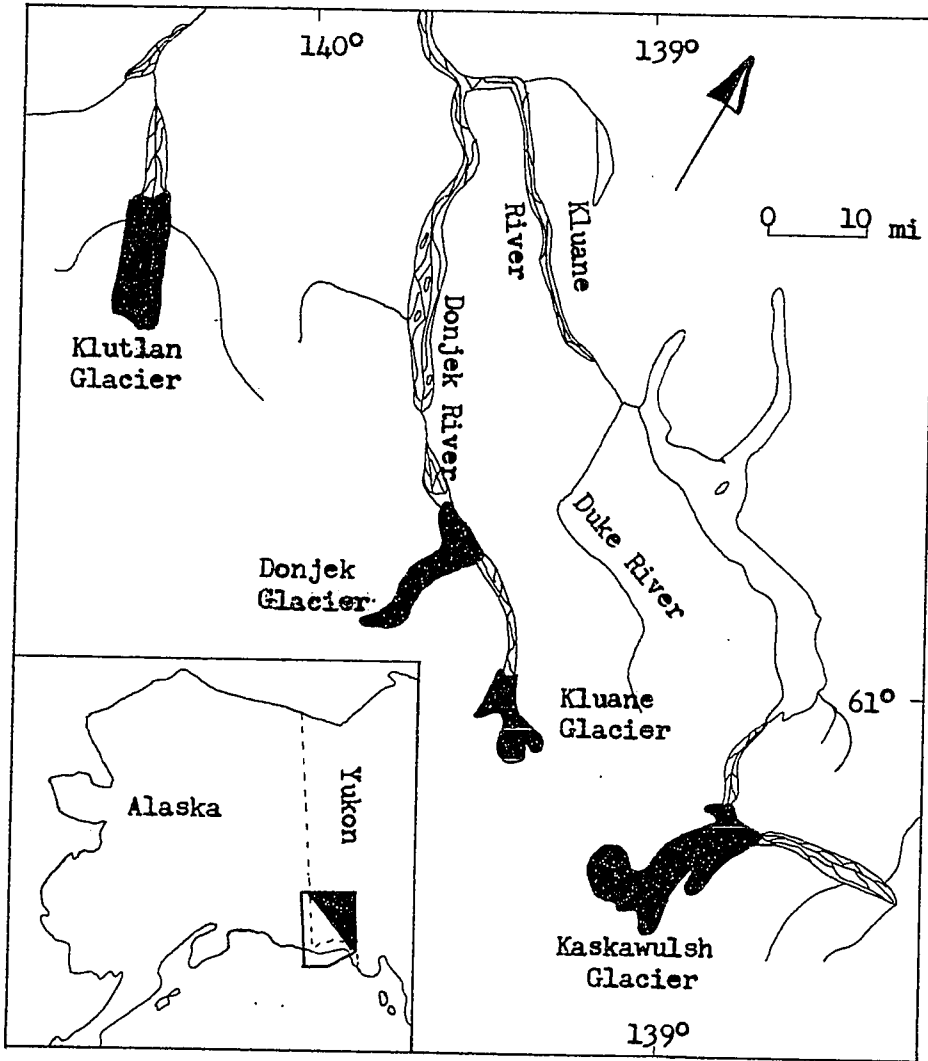


FIG. 1 LOCATION OF THE STUDY AREA

the north eastern flanks of the St. Elias Range and thus falls under the influence of a strong continental type climate. The valley trends north north west to south south east and the study site lies at an elevation of 1,100 meters above mean sea level, surrounded on either side by mountains rising 1,300 meters above the valley floor.

The valley presently drains a number of large valley glaciers, the most notable of which are the Kluane, Steele and Donjek. The valley floor is covered by fluvio-glacial outwash material and wind blown loess, and displays a marked braided river pattern.

The Donjek Glacier is a typical valley glacier extending almost 56 km from the source area to its terminus. The glacier source area is a high plateau snowfield, some 1,800 sq. km., lying along the axis of the St. Elias Mountains at an elevation of 2,800 meters above the Donjek Valley floor. The glacier terminates at the point where the Donjek Glacier Valley joins the Donjek River Valley (FIG.2). Here the glacier ends in a lobate form which varies in width from 1.6 km to 4.8 km.

The specific area under study represents a large discontinuity between the broad, relatively flat and gentle sloping outwash plain, which lies in front of the north west facing lobe of the Donjek Glacier, and the present terminus of the Donjek Glacier. Most work was done on the large end moraine structure which is arcuate in form and lies approximately 0.8 km to 2.7 km from the ice front (FIG. 2). The massive end moraine rises 18 meters to 45 meters above the Donjek Valley train and is thought to represent the maximum extent of the Donjek Glacier during its Neoglacial advance (Denton and Stuiver 1966; Borns and Goldthwait 1966; and Johnson 1971). This time era extends between 1500-1900 A.D.; and corresponds to Matthes 'little ice age', (1942), and the 'Neuzeitlich' ice extent as defined by Whalley (1974). Neoglacial advances have been reported in other areas along the West Coast mountains of North America (Borns and Goldthwait 1966; Denton and Stuiver 1966, 1967; Porter and Denton 1967; Benedict 1967, 1968; Rampton 1970; and Reid 1970).

Denton and Stuiver (1966) have proposed A.D. 1825 as the date for the recession of the Donjek terminus from the outermost moraine. They first stated that this end moraine was ice cored. They associated fresh cracks, near vertical till

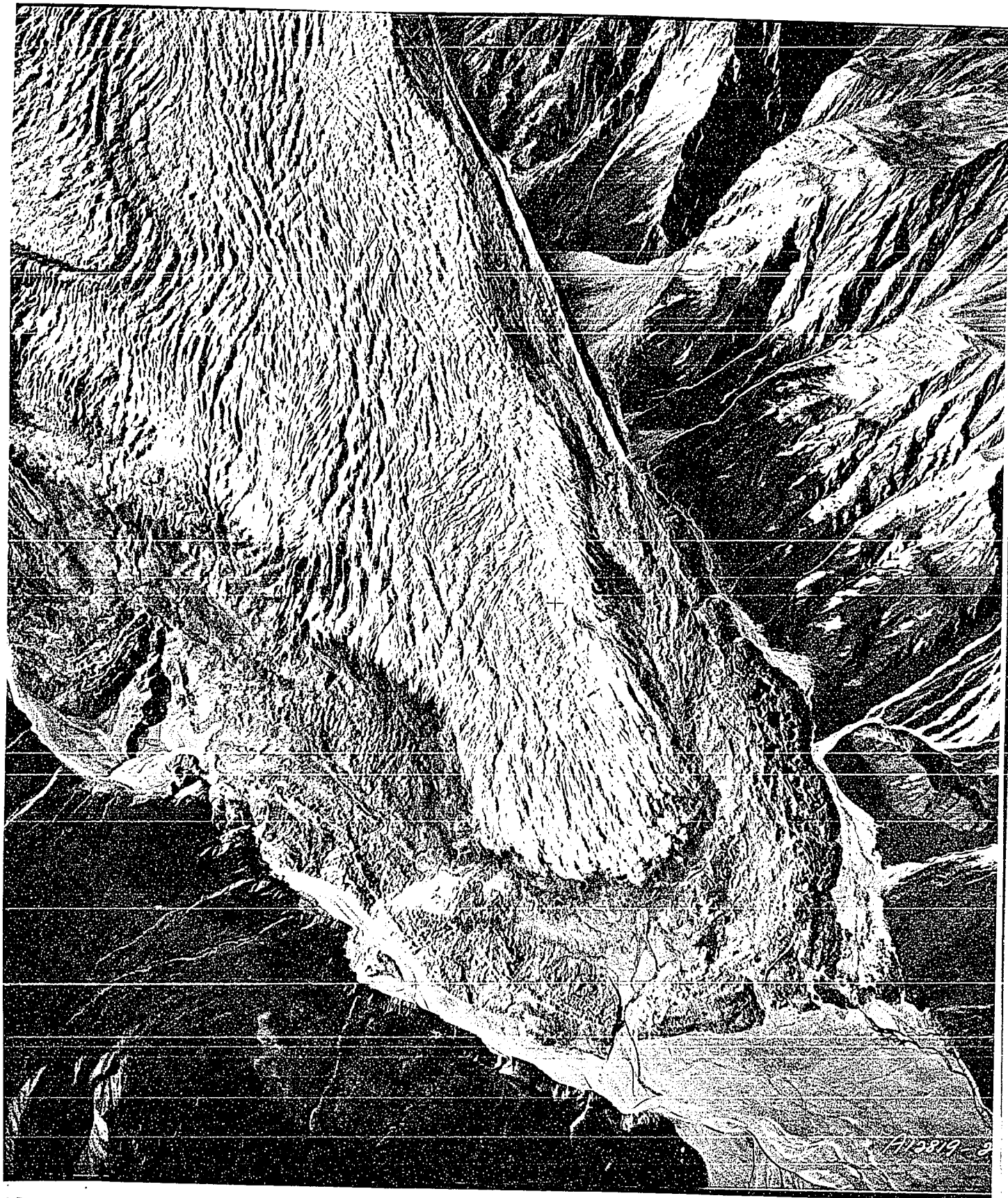


Plate 1.1 Vertical air photograph of terminus of Donjek Glacier and terminal moraine. Scale approximately 1:37,000.

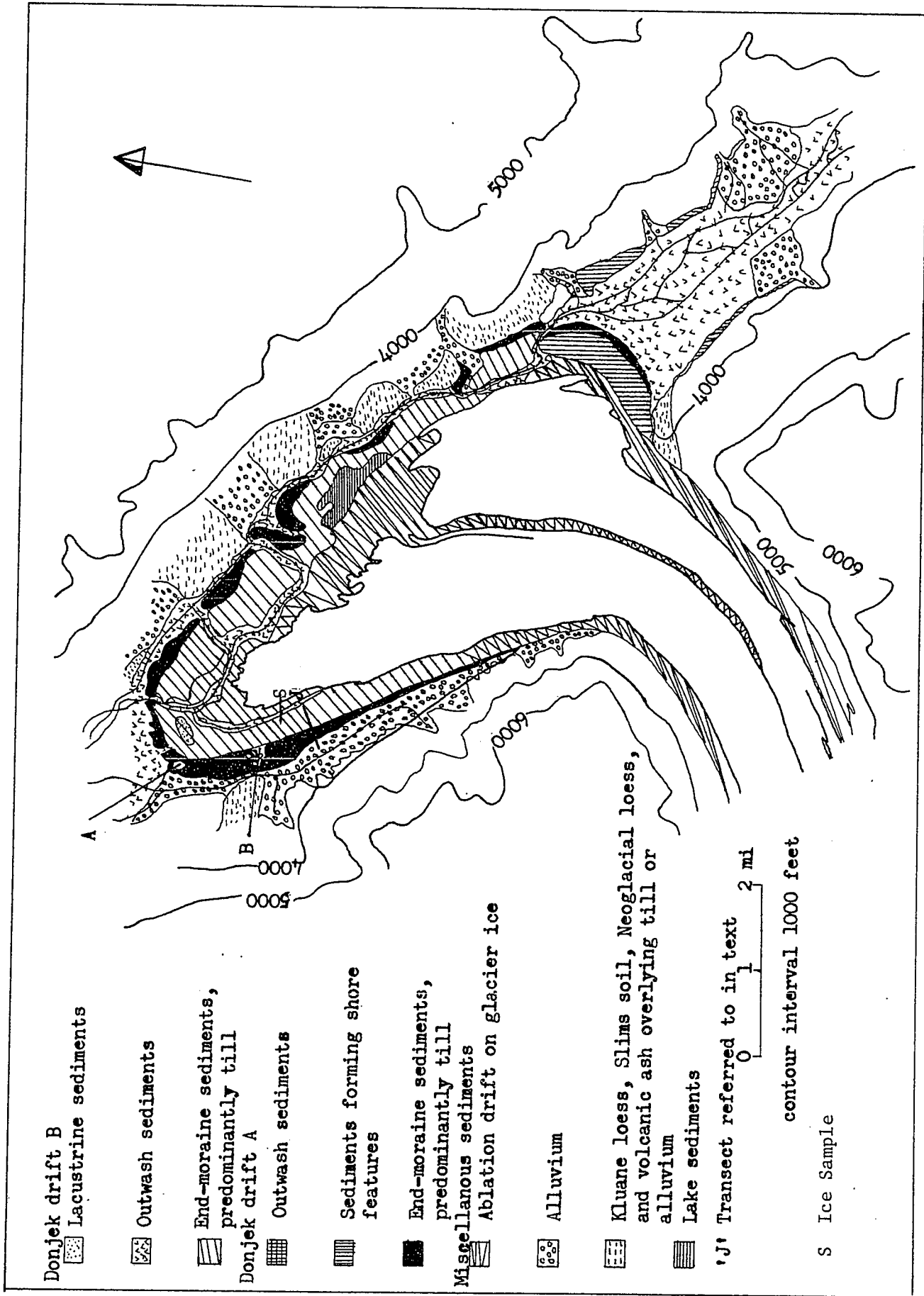


FIG. 2 GLACIAL FEATURES IN TERMINAL AREA OF DONJEK GLACIER (from Denton & Stuiver, 1966)

faces, and the increase in the system of lakes on the northwest portion of the moraine, as features representative of melting and settling of an ice core. Johnson (1971) cited the occurrence of ice core exposures on the end moraine itself, the occurrence of numerous kettle forms on parts of its degraded surface, and the possible ice coring of the outwash plain, between the present downvalley glacier terminus and the Neoglacial end moraine, as criteria for the presence of an extensive ice core. Østrem (1971) has used size, exposures, and lack of lichen growth, the ramp like appearance of the moraine and the 'porridge like' appearance of the ice cored moraine on air photographs as further criteria in judging whether moraines are ice cored; and these features fit the appearance of the Donjek end moraine (see Chapter 3).

Relatively recent surges or fluctuations of the Donjek Glacier have been identified by Denton and Stuiver (1966); Muller (1967); and Johnson (1971). Denton and Stuiver calculated various distances and recessions from August 1935 to July 1964. In August 1935 the ice front was 805 meters behind the distal portion of the end moraine. Between August 1935 and summer of 1941 net retreat was about 532 meters; between the summer of 1941 and the summer of 1955 it was again about 532 meters;

between the summer of 1955 and summer of 1956 it was 61 meters. Sometime between the summer of 1956 and August 1961 the ice front advanced to a position some 421 meters in front of its 1956 position. Muller (1967) compared aerial photographs of the Donjek Glacier snout taken in summers of 1947 and 1956 and concluded that the glacier had retreated 610 meters to the southeast. Muller also determined that an advance had occurred around 1930. Johnson noticed prominent features on the Donjek Glacier in 1969 which are associated with actively surging glaciers. However since the last reported surge of 1969, the terminus of the Donjek Glacier has been stagnating and downwasting.

1.3 Literature Review

1.3.1 Ice Cored Moraines

Ice cored moraines have been recognized and described in literature since the late 19th century. Matthes (1948) described what he considered to be ice cored moraines located in the Sierra Nevada Range. On the basis that these features contained cores of stagnant or dead glacier ice, Matthes proposed that they were formed at the terminus of the glaciers by 'ground moraine' being brought to the surface along thrust planes. This material was added to ablation material and

slowly covered the terminus until the debris mantled surface was left standing, while the remainder of the glacier wasted back during recession.

The theory of debris incorporation into bands and transportation to the surface of the glacier in the terminus area along shear planes, resulting in ice core moraine formation, was further elaborated upon by Goldthwait (1951); Bishop (1957); Schytt (1959) and Souchez (1967, 1971). Most of these studies were on polar ice caps and outlet glaciers. Another hypothesis, refuting the shear plane mechanism of material incorporation and transportation, was proposed by Weertman (1961) for cold ice sheets, whereby material which has been eroded by the glacier at its base; becomes frozen into the base of the glacier by the action of melt water freezing. The material, which is now incorporated into the glacier, is carried along as debris bands which slowly rise to the surface as it flows into the terminal area of the glacier. This mechanism was further supported by Boulton (1970); Hooke (1970, 1973); Shaw (1971); and Souchez (1971). However many of the above authors, and others such as Anderson and Sollid (1971), have employed both mechanisms to describe the formation of ice core formations in their respective

study areas. Hooke (1973) used Weertman's hypothesis to show how superimposed ice, which has formed in the lee of an ice sheet, may become incorporated into the terminal ice by the over riding action of an advancing ice sheet and later, during stagnation, result in moraines which include both ice types together as their ice core.

In all of these studies the ice cored moraines were just beginning to form on the terminal area of the glacier. Features resulting from the accumulation of supraglacial debris on the terminal area of glaciers have been described by Sharp (1949); Swithinbank (1950); Gravenor and Kupsch (1959); Clayton (1964); Boulton (1967) and Reid (1970). In all of the above cases, except Gravenor and Kupsch (1959), the stagnant ice was still attached to the glacier. Thus these features could have undergone modification if the glacier became reactivated. Also melt water action, from ice melting upglacier from the debris covered ice, may modify the existing forms. According to Gravenor and Kupsch (1959), the underlying ice was thought to have completely melted out producing a very complex ablation landscape.

Much less attention has been given to the rate of ablation of these ice cored features with respect to the depth, lithology, and texture of the overlying material, the climatic variables promoting ablation, and resulting degradational processes. Brief accounts are given by Sharp (1949); Swithinbank (1950); Goldthwait (1951); Bishop (1957); Gravenor and Kupsch (1959); Souchez (1967,1971); Boulton (1967); and Hooke (1970). More detailed studies into this particular aspect have been undertaken by Østrem (1959,1965); McKenzie (1969); and Loomis (1970).

Loomis (1970) measured rates of ablation, degradational processes and morphological changes on a medial ice cored moraine located on a presently active glacier. His study area was similar to those previously discussed in that it was on the surface of a presently active glacier, where the till cover was very shallow averaging 6 to 10 cm in depth. Also his relationships between atmospheric energy relations and ice ablation, as they are affected by an intervening layer of morainic debris, were limited mainly because of the short period of data collection and the paucity of climatic parameters measured. Loomis concentrated primarily on the single process of ablation as affected by the depth of overlying debris.

McKenzie (1969) measured the amount of heat transfer by conduction through a medium (gravel) and the resultant melting of the underlying ice core. His climatic data was not taken from his study area but from a nearby weather station. Although McKenzie recognized various processes, such as slumping and sliding of material and the action of running water, he made no quantitative measurements of the effect these processes had in changing the topography of the landform.

Østrem (1959,1965) has made the most detailed measurements on rates of ablation of debris covered ice and exposed ice. However, his work was only experimental. Different grades and thicknesses of sand were placed over exposed ice in the field and rates of ice ablation were measured. From this data Østrem (1959) constructed a graph showing the rate of ablation with increasing depth, but no detailed measurements of climatic parameters at the study site were made with which the ablation data could be correlated. He did not measure any processes operating on ice cored moraines but concentrated more on the nature and extent of ice cores, and their distribution under a debris cover, as well as the distribution of ice cored moraines in Scandinavia and Canada.

Boulton (1967, 1970) and Johnson (1971, 1972) have both measured and described degradation processes operating on ice cored moraines. However this data has not been correlated in detail with climatic and soil thermal data in the areas under investigation. Both have shown the complexity of environments which have been or are operating on ice cored moraines. Boulton's work concentrated more on the nature of the tills making up individual structures on the moraines and the debris bands in the glacier. Johnson described more the morphology and nature of degradational processes on ice cored moraines, as well as the mechanism of ice core moraine formation in the Donjek Valley.

In summary most work on ice cored moraines has been done in areas in which only a thin veneer of debris covers the underlying core. Most detailed work has been done on the mode of ice core moraine formation, debris bands within the terminal areas of both polar and temperate glaciers, and resulting structures either on thin debris covered stagnant ice or in areas in which no ice core is now thought to be present. Rates of ablation and processes operating on ice cored moraines have been measured in little detail, and the effect of various climatic parameters operating together over the feature have been scantily dealt with.

1.3.2 Identification of Ice Type

In view of the discussion on snowbank ice and glacier ice in ice cored moraines, it is important to be able to identify the origin of the ice. Recent studies on buried ice have been directed towards a means of identifying the various ice types, i.e. glacier ice-polar or temperate, segregated ice or massive ice, and snowbank or superimposed ice. The criteria most commonly used for identification have been crystal size, shape, and orientation of the major crystallographic 'c' axis.

Detailed measurements of crystal size from various locations along valley glaciers have been done by Seligman (1948); Ahlmann and Droessler (1949); Ekerbom and Palosuo (1963); Gow (1969); and Anderton (1970, 1974). Their results indicated the wide variety of crystal sizes which may exist along the length of glaciers. As well they show how ice temperature and length of time of ice crystal formation may cause variations in the size that an ice crystal may obtain. Gow (1969) also points out the fact that the average crystal size, obtained from thin section analysis, will be less than the true value simply because a section seldom cuts crystals at their maximum diameters.

Gell (1973) has shown that two trends of thought are in vogue as to the effect of stress and strain on crystal size. Bader (1939); Perutz (1940); and Steinemann (1959), believe that under a high stress ice crystals tend to increase in size, and when the load is released the crystal size will increase further. Kamb (1949); Seligman (1949); Glen (1958); and Schumskii (1958), believe that under stress conditions crystals decrease in size.

The shape and structure of crystals may reflect the environment in which the crystals have originated as well as the environment(s) in which they have existed or presently exist in. For example, glacier ice crystals form by the process of firnification and densification in a relatively stress-free environment. However due to the nature of glacial activity the ice crystals environs may vary from a stress free environment, such as that found at the surface of stagnant glacier ice, to one in which stress and strain may be such as to cause severe crystal deformation or recrystallization, such as along the sides of a moving valley glacier or along shear planes where active ice is or has sheared over stagnant or dead ice. Deformed crystals show such features as slip bands, grain boundary migration, kink bands, distortion of grain boundaries and cracks and cavities.

Snowbank or superimposed ice is thought to have formed and continued to exist in a relatively stress free environment and thus would undergo little or no deformation. Crystals formed in this type of environment have straight boundaries. The resulting shapes and structures of individual crystals have been studied by Rigsby (1960); Gold (1963); and Gell (1973).

Another characteristic of crystals, which may reflect their past and or present environments, is the degrees of concentration of the primary or crystallographic 'c' axis. Fabric analysis on ice crystals has been described in detail by Haff (1938); Bader (1951); and Rigsby (1951), in which a universal stage and Schmidt equal area net was used to plot individual 'c' axis orientations.

Textural analysis, performed on crystals from different locations on temperate glacier ice, has been done by many authors (e.g. Rigsby (1951, 1960); Kamb (1959); Allen, Kamb, Meier, and Sharp (1960); Taylor (1963); Kizaki (1969); Østrem (1963, 1964); Anderton (1970); and Hooke (1970, 1973). In general they found that glacier ice tended towards a three or four maxima 'c' axis orientation or concentration. This multiple maxima seems to reflect a number of stress-strain environments to which glacier ice

crystals are subjected. Similar petrofabric and textural analysis has been done on polar ice sheets (Pery and Pounder 1958; Gow 1969; Kizaki 1969; Patterson 1969; and Anderton 1974), where generally a single maxima of c axis was found.

Observations have shown that snow or snowbanks may accumulate in the terminal area of large ice sheets or temperate glaciers, as a result of wind blowing predominantly down over the ice. Snowbanks may also occur in the lee area of ridges of already existing moraines. In both cases the snow may become buried by morainic debris and eventually become buried ice. Østrem (1963) has termed this ice type as snowbank ice whereas Hooke (1970, 1973) has called this superimposed ice or a superimposed ice wedge. Both Østrem and Hooke performed fabric and textural analysis on this ice type in attempts to differentiate it from other types of buried ice. Their orientation measurements tended to show a weak or non-existent fabric, reflecting the random orientation of the crystals as they form, and the stress free environment in which they exist.

A final type of subsurface ice which has been recognized in this work is segregated or massive ice (Mackay 1971; Rampton and Mackay 1971; Gell 1973). Textural analysis performed on a segregated ice lens in leda clay by Penner

(1961) showed a high concentration towards a single maxima, reflecting the unidirectional cooling effect on fresh water ice crystal formation. Gell's work on fabric analysis revealed the presence of both a single and multiple maxima c axis concentration. These results indicated the complexity of crystal orientation found in ground ice.

The most detailed work on identification of ice types has been that in which all three variables of texture have been employed. As this has been done by most of the above mentioned authors, an ice sample was also taken at the end of this study period and shipped to a laboratory for study to determine the ice type by textural analysis.

1.4 Methodology

The macro climate of the study area was determined from data gathered from government operated meteorological stations at Whitehorse and at Burwash Landing (this latter station was located approximately 48 km from the study area). Data was abstracted from Monthly Records, Environment Canada (1970, 1972, 1973), as well as from other previous works on climate within the same general study area (Benjey 1969; and Webber 1974).

Within this regional weather pattern, local variations may be expected to occur. To determine any local variations in the weather over the study area, two micro climatic weather stations were installed.

One station was located approximately 2.7 km north of the present position of the terminus of the Donjek Glacier in a central valley position. The second station was placed almost directly west of the present position of the glacier terminus near the center of the ridge of the end moraine. (FIG. 2). The station located downvalley is designated A Station while that on the west side of the valley is designated B Station.

A Station was located on a flat portion of the morainic material near the central ridge. There was no vegetation surrounding the site and the morainic material was a light grey in colour. North of the site the moraine was covered by a variety of vegetation types, while to the south a sparse vegetation cover existed.

B Station was located near the center portion of the end moraine on a ridge separating a number of very large melt water ponds. There was sparse vegetation on the ridge and the material on which the site was constructed was a darker grey than that of A Station.

Precipitation, ambient air temperature, humidity, evaporation, wind and solar radiation were recorded at each site over a 55 day period. All equipment requiring housing was placed in large wooden leevered shelters. In order to more closely record the climate operating over the moraine surface, the shelters were placed at ground level rather than at the standard meteorological heights. Because of the ground level siting of the instruments, care had to be taken when making comparisons with the standard meteorological data from Burwash Landing and Whitehorse.

Precipitation was measured by four rain gauges. Readings were taken directly after each rainfall to avoid inaccuracies caused by high evaporation rates. Rates and occurrences of mass movement in the form of slumps, slides and mudflows were observed both during and after periods of precipitation. This was done in order to determine any relationship which may exist between mass movement and addition of rain water to the morainic material. The effects that precipitation had upon heat transfer through the same media were also noted. The amount of precipitation was recorded as a 24 hr. value. The times when it began and ceased were also noted.

Ambient air temperature and relative humidity were measured continuously by Weathermeasure H311 hygrothermographs. The accuracy of the recorders is plus or minus 1 percent between 20 and 80 percent and plus or minus 3 percent at the extremes. Potential evaporation was determined by use of continuously recording Weathermeasure E 801 evaporation recorders. The instrument is purported to have an accuracy of plus or minus 0.1 mm or 1 percent. Average wind speed was measured by two anemometers which were calibrated to measure in miles. They were placed 1 meter above the ground surface. The intensity of total short wave radiation energy from the sun was measured by Weathermeasure R 401 solar radiation recorders. The glass hemisphere or dome is transparent to wave lengths of electro magnetic radiation energy between .36 microns and 2.5 microns. Temperature, humidity, and solar radiation values were abstracted for 3 hourly periods and daily values of wind run and evaporation were calculated.

The amount of energy exchange occurring both on and within the moraine debris requires a study of the temperature gradients through the material. Soil temperatures were measured by two maximum recording thermometers as well as by continuously recording Weathermeasure T 603 three

point thermographs. The recorders have an accuracy of plus or minus 1.0°C. Values were taken from the charts at 3 hourly intervals and a mean value for each 24 hour period was calculated.

An attempt was made to determine whether or not heat flow, both on a daily or seasonally basis, was penetrating down to the ice core. A general theoretical review of heat flux through soils is given by Sellers (1967), and a summary of his work is presented in the appendix. Equations used in determining this heat flux were those given by Terzaghi 1952; Yong and Warkentin (1966); Williams and Nickling (1971); and Tuma and Abdel-Hady (1973). The quantity of heat reaching the ice surface, by conduction only, and the resultant amount of ablation was determined by an equation given by McKenzie (1969). From this the quantity of ice which could be expected to melt under ideal conditions was determined for the season. As well, both the quantity of heat flow due to terrestrial heat flow and the quantity of ice melt expected from this was calculated.

Graphs were drawn to show data results; and rather than trying to compare data on a daily basis for the total study time, patterns or trends shown on the graphs were noted and compared.

The above mentioned climatic parameters and heat flow data were also related to the occurrence of certain geomorphic processes. These were identified as:

1) Ablation of exposed ice cores. Rates of ablation were determined and the resultant lowering of the ice calculated.

2) Mass movements (slumping, sliding). These were monitored on a weekly basis. Markers were used to measure headwall retreat and to calculate the rate of backwasting at various orientations within each exposure. Values are expressed in terms of cm per day.

3) The action of melt water streams and melt water ponds. The effects on degradation of the morainic debris were noted but no quantitative measurements were obtained.

In order to obtain a more quantitative description of the moraine, the angles of slope, on the surface of the end moraine, were measured by taking a number of slope profiles across its proximal and distal sides. Slope angles were measured at 30 foot intervals,

and additional measurements taken where noticeable breaks in slope occurred, as well as slope orientation measurements. Slope angles and orientations were measured especially where ice core exposures and other distinct morphological features occurred. The degree of correlation between slope angle and orientation, and the types and frequency of occurrence of processes of degradation were studied.

Tensional cracks, thought to be the result of the underlying ice core melting out, causing large masses of morainic material to slip down slope, were investigated as to width, depth and orientation.

Soil samples were taken at random across and along the end moraine, as well as where marked changes in slope occurred, and where other specific morphological parameters were apparent. Mechanical analysis as to size and shape was performed by use of sieves and a microscope. The results were also used in the analysis of thermal heat data in the morainic material.

The effect of recent glacial surges, on morainic degradation, was examined by monitoring the rate of retreat of certain ice core exposures which were thought to have resulted from glacial surges. Markers were placed at equal intervals around the exposures and their respective aspects noted. Charts showing weekly rates of recession of these features, and those initiated by other means in terms of total percentage loss over the study period, were constructed.

The percentage of, and the type of vegetation cover over the morainic material, was determined in conjunction with the slope angle and orientation measurements. This data was correlated with type and number of geomorphic processes, e.g. slumping and mudflow, operating on the end moraine. Tree coring, by use of an increment borer, was carried out on the morainic material to verify possible germination periods, and thus help in identification of the age of moraine deposition.

In this way the interaction of micro climatic and glacial surge inputs was examined, as well as the effect of these inputs in producing certain geomorphic degradational processes and associated morphological changes on the Donjek ice cored end moraine.

2. NATURE OF ICE CORE

2.1 Introduction

An ice sample, obtained from an ice exposure on the western portion of the Donjek end moraine, was subjected to a textural analysis under laboratory conditions. Many authors have performed such analysis, but their main concern was in describing characteristics of that particular ice sample to complement their work on another aspect under investigation such as structural analysis on glaciers with respect to foliation planes, faults and folding in ice, and in locating differential movement within flowing ice. Less direct emphasis has been placed on using textural analysis alone to differentiate between various forms of buried ice. Therefore, the purpose of this chapter is to attempt to evaluate the effectiveness of using textural analysis as a tool in differentiating between types of buried ice, with special reference to the Donjek Glacier moraine sample. The identification of the ice type may help explain the mode of end moraine formation and assist in the description of ice cored moraines following the format of Østrem and Arnold (1970).

The chapter presents an outline of the procedures used in the laboratory analysis of the ice sample and the results of the study. These results are then compared with the findings of other workers who used similar methods of analysis on particular ice types. Possible errors in this type of study are discussed and conclusions are drawn on the effectiveness of this method.

2.2 Methodology

Thin sections were obtained from the ice sample by cutting 10 x 10 cm blocks with the aid of a band saw. The ice blocks were then mounted on glass plates of equivalent size. The mounting was accomplished by taking the glass plates from room temperature (20°C) into the cold room (-10°C) and pressing the glass plate onto the base of a trimmed block of ice. The plate was moved in a circular motion over the entire ice surface, melting a thin layer of the ice at first and then allowing the melt water to refreeze, forming an air-free bond between the ice and glass plate. The thin sections were placed on a Leitz base sledge microtome type 1300 and the ice block was reduced to a thickness of between 0.2-0.4 mm. Four horizontal thin sections were made as well as one vertical thin section.

Ice is a uniaxial anisotropic mineral which has a hexagonal or cubic form, probably in the ditrigonal pyramidal class (Rigsby 1951; Patterson 1969). According to Pery and Pounder (1958), its birefringence is relatively small but sufficient to show the crystal structure under polarized light. "The fabric of a crystalline mass is found by the statistical study of the orientation of the individual crystals and their relationship to each other." (Rigsby 1960, p. 590).

The determination of the crystal fabric of the ice sample was done on a four ~~axis~~ Universal Stage, which permits orientation of the crystals optically. The method used in principal axis determination and point plotting closely follows that of Langway (1958). The position of the optic or c axis of the ice crystal was determined and plotted by measuring the azimuth and polar or equatorial angle of individual crystals. The desirability of showing the relative spatial concentration of the data dictated the use of the Schmidt equal area net (20 cm diameter). This net eliminates nearly all aerial distortion, as a unit area in any position on the net corresponds to a unit area on the spherical projection from which the net was derived. Data are plotted on the net as points corresponding to the optic or c axis of the ice crystal. The standard procedure in glacier fabric studies is to use the upper hemisphere of the spherical

projection as the basis for plotting points. Before plotting the data, the universal stage measurements were tabulated and angular corrections were made. Contour lines of equal density were constructed, showing numerical densities expressed as the number of points per one percent of the total area, and these values were then shown on the net in degrees of shading.

The crystals were photographed under cross polarized light in both black and white and colour. Each section was photographed twice, one position rotated ninety degrees from the other position. This procedure was designed to minimize the chances of photographing crystals located next to each other and possessing the same extinction position. A centimeter square grid was placed over each section in the black and white photographs, and a ruler, marked off in centimeters, was used for scale with the colour photographs. In the latter photographs the long and short axis, as seen in the horizontal sections of each crystal, were used in computing the crystal cross sectional area.

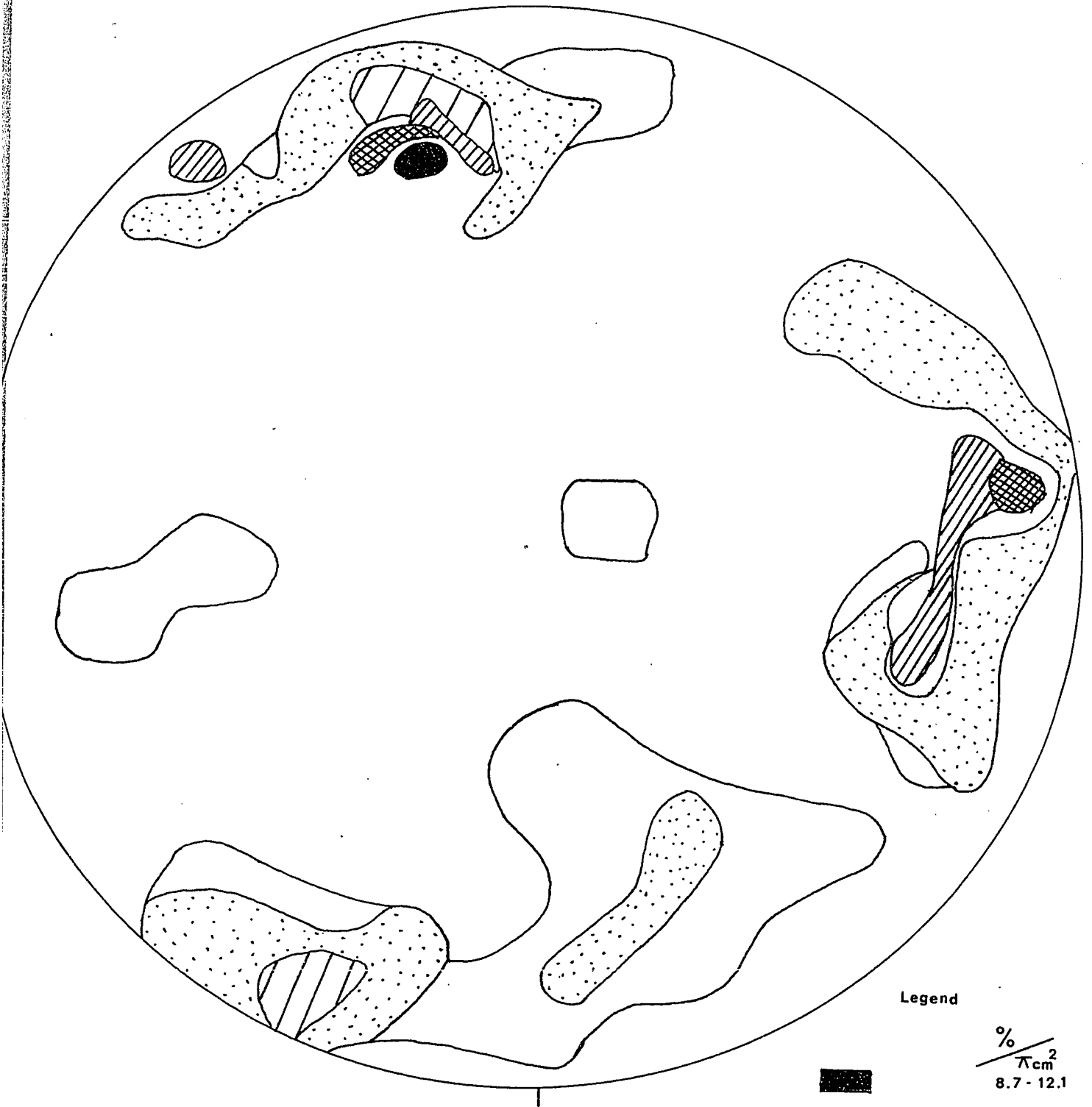
Crystal shape was determined primarily through the use of both colour and black and white photographs of thin sections, as well as looking at individual crystal structure through the universal stage in the cold room.

2.3 Results of Analysis

2.3.1 Crystal Orientation

Figures 3 and 4 show the results of fabric analyses on the ice sample. The diagram reveals four broad maxima occurring around or near the edges of the net. Two of the maxima are located quite close to one another, while the other two are widely separated from each other as well as from the other two maxima. Three of the four maxima represent a fairly high degree of concentration, ranging from 5.3 to 6.9 percent of the total points to a high of 8.7 to 12.1 percent. The fourth maxima is a relatively weak concentration of points at 3.5 to 5.2 percent. This last maxima could conceivably be an extension of one of the other two stronger maxima located in the north west quadrant.

The number of maxima found in this study, (three or possibly four), compares favourably to those found in other ice fabric studies. Rigsby (1951, 1960) found that ice from temperate glaciers showed primarily four strong maxima, lying at the corners of a diamond shaped quadrangle. However the occurrence of three maxima could also be expected. Similar results have been presented for temperate



Legend





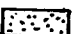

	$\frac{\%}{\pi \text{cm}^2}$
	8.7 - 12.1
	7.0 - 8.6
	5.3 - 6.9
	3.5 - 5.2
	1.8 - 3.4
	0.0 - 1.7

FIG.3 Fabric Diagram Donjek Ice Sample 58 Crystals

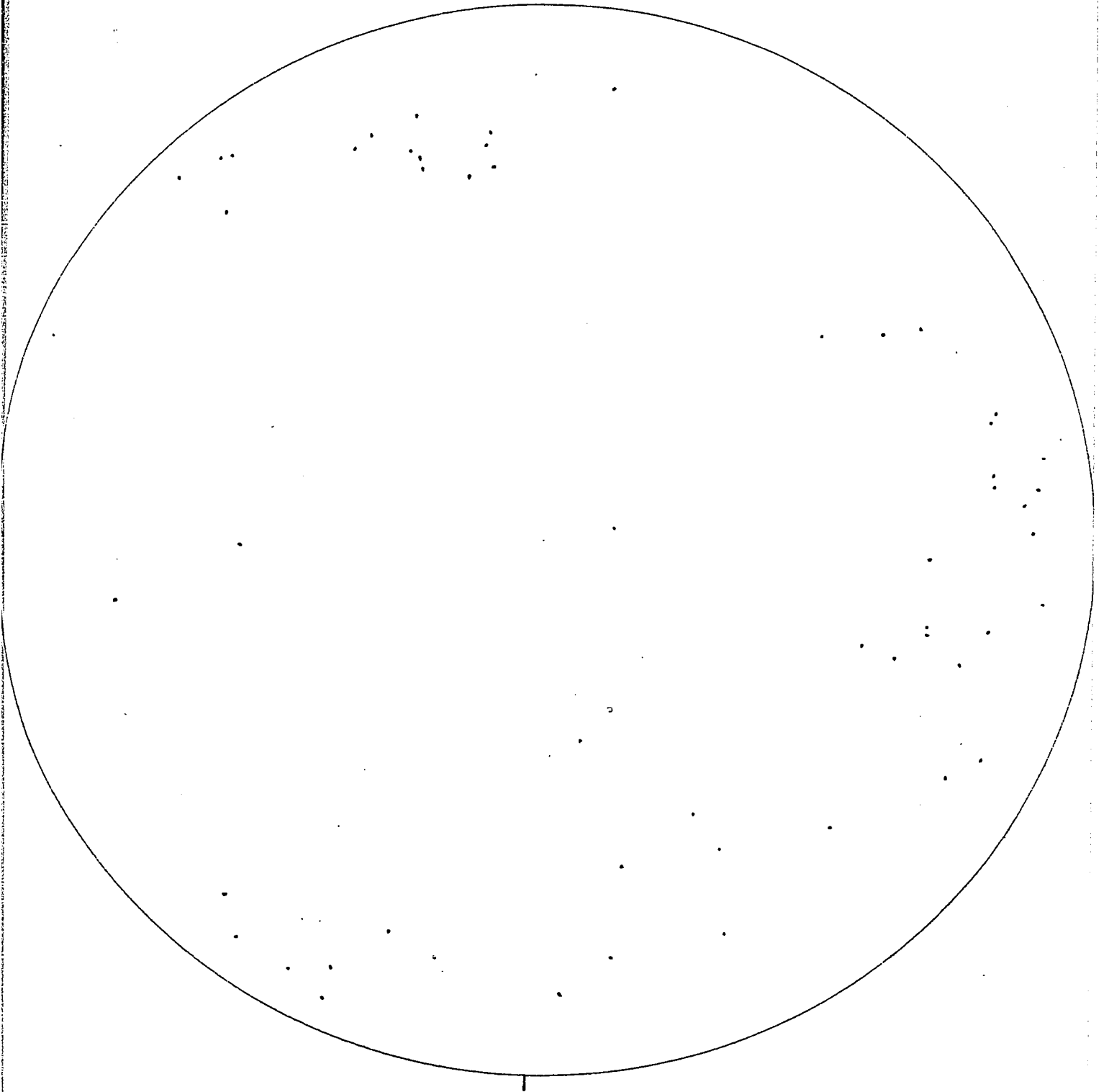


FIG. 4 Fabric Diagram Donjek Ice Sample 58 Crystals

glacier ice (Kamb 1959; Allen, Kamb, Meier, Sharp 1960; Østrem 1963; Taylor 1963; and Anderton 1970).

However many of the samples, obtained by the above mentioned authors, were taken from areas located up glacier from the terminus. Taylor (1963) examined crystals from the terminal area of a valley glacier and found a preferred c axis orientation with a strong three maxima concentration varying in strength from three to eight percent. He showed that the same patterns found in the upper reaches of a valley glacier may be retained as the ice moves down valley, and continue to exist during ablation and recrystallization in the terminal area. Similar results for stagnant ice have been reported by Bader (1951); Rigsby (1960); and Anderton (1970).

A review of the literature shows that both the single and multiple maxima c axis orientation are associated with the same stress fields which are responsible for structural features such as foliation planes, folding and faulting (Kamb 1959; Rigsby 1960; Taylor 1963; Patterson 1969). The changing stress fields not only affect the number of maxima in the ice but also may rotate the affected crystals (Kamb 1959). Such stress patterns may also occur along shear planes which result from differential flow within a glacier such

as that near the bottom, along the sides, or where active ice is overriding stagnant ice as in the terminal area of a valley glacier.

Another factor promoting multiple maxima orientations is recrystallization. This process primarily affects crystals undergoing large stresses such as those which do not have their c axis normal to the shear stress, nor their basal plane properly orientated for crystal glide (Taylor 1963; Anderton 1970). Rigsby (1960), concluded from laboratory experiments that recrystallization is temperature dependent; and that in temperate glaciers, it would occur in ice which is at its pressure-melting point, where molecular flow and ionic bonding occur more easily.

Østrem (1963) and Hooke (1970, 1973) have both shown that multiple maxima may occur as well in snowbank or superimposed ice. This ice type may be subjected to stress by overriding glacier ice which would cause this pattern to occur. However, in general it would appear that both these ice types show a single or double preferred orientation of their c axis. Kizaki (1969); Patterson (1969); and Anderton (1974), have shown that one may find both single and multiple maxima c axis orientation in polar ice, but the most common preferred orientation is that

of a single maxima. Pénner (1961) showed that, in an ice lens developed in leda clay in a laboratory, there was a disorder in the optic axis orientation giving rise to both horizontal and vertical crystal orientations. However, the majority of c axis were primarily located in a vertical direction, displaying a single maxima.

In conclusion, crystal orientation, on an ice core sample taken from the end moraine of the Donjek Glacier, gives results which are comparable to those found by other workers on temperate glacier ice. The results show a better relationship to those studies on stagnant or dead ice than to those on active ice.

Preferred orientations of the c axis and the resultant number of maxima of the c axis are directly related to the shear stress and temperature environment(s) in which the ice crystals either have existed or presently exist, and whether or not the crystals have undergone recrystallization. Also changes in the directions of stress in media may also cause a shift in the orientation of the maxima as well as change the number of maxima present.

The fact that ice within a glacier would be subjected to a variety of strong shear stress conditions as well as

possessing favourable conditions for recrystallization, may lead one to conclude that the Donjek ice sample may represent buried stagnant glacier ice. However, workers performing the same analysis on snowbank ice have shown that similar c axis orientations and multiple maxima may be found. Thus no strong distinction may be made between the various ice types based on fabric analysis alone.

2.3.2. Crystal Size

A total of fifty-eight grains (from horizontal thin sections) were used in determining mean values for crystal area and length of long axis. These results and those presented in the literature are given in Fig.5 (a) and (b), and show that the size of ice crystals from the Donjek end moraine are very similar to those found on other temperate glaciers or stagnant ice. Larger mean area values were reported by Seligman (1949) for ice sampled from the stagnant marginal area of Isfallsglaciaren, Sweden. However he recorded values for only the largest sized ice crystal (area). Similarly, his smallest sized ice crystal was large when compared to that found in the Donjek and to that of Ahlmann and Droessler (1949).

MEAN SIZE OF ICE CRYSTALS

Ice Type	Mean Area (cm ²)
1. Glacier - temperature (terminal area)	
Donjek	4.9
Seligman (1949)	19.6
Ahlmann and Droessler (1949)	3.5
Allen, Kamb, Meier, Sharp (1960)	0.5 to 12
Ekerbon and Palosuo (1963)	2.0 to 8.0
Østrem (1963)	4.0 to 8.0
2. Polar Ice - terminal area	
Østrem (1963)	1.1
Anderton (1974)	0.5
3. Massive Snowbank Ice	
Østrem (1963)	.05 to .38
4. Superimposed Ice	
Østrem (1963)	.1
* Range of crystal area for Donjek ice sample	.04 to 44.0 cm ²

Fig. 5(a)

RANGE OF LENGTH OF LONGEST AXIS

Ice Type	Range (cm)
1. Glacier - temperate (terminal area)	
Donjek	0.3 to 9.7
Taylor (1963)	0.5 to 20.0
Patterson (1969)	up to 10.0
Kamb (1959)	0.05 to 12
Anderton (1970)	0.5 to 4.0
2. Polar Ice Kizaki (1969)	1.0 to 4.0

COMPARISON OF MEANS AND RANGES OF CROSS SECTIONAL
AREAS FOR BLACK AND WHITE AND COLOUR PHOTOGRAPHS
DONJEK ICE CORE SAMPLE

	<u>Black & White</u> (cm ²)	<u>Colour</u> (cm ²)
Mean	4.9	7.5
Median	1.7	2.2
Range in Areas	.04 to 44.0	.04 to 82.6

Fig. 5(b)

The literature indicates that each ice type has its own individual mean grain size which tends to distinguish it from other forms of ice. However, it also revealed that a variety of crystal sizes within each particular ice type could also exist. Crystals from temperate glacier ice (stagnant) have size ranges which are similar to those found in snowbank and polar ice, e.g. compare Donjek range to Østrem (1963) snowbank, Fig. 5(a); and Taylor (1963) to Kizaki (1969) polar, Fig. 5(b).

A discrepancy occurred between the values obtained for ice crystal size for black and white and colour photographs. Figure 5(b) shows a comparison between mean area of ice crystals on both sets of photographs. One factor which may have led to this discrepancy was the difference in the way in which areas of the crystals were calculated. A superimposed grid was used for black and white photographs, while the long and short axis was used for calculating areas from colour photographs.

Østrem (1963) showed a similar discrepancy when calculating mean crystal size on crystals photographed in colour and black and white. However his results showed that mean crystal sizes for black and white prints were greater than for the same crystals photographed in colour.

His reasoning was that black and white photographs do not always show fine grades of colour differences between crystals, and thus may give fewer numbers of crystals and larger mean areas than corresponding colour prints. However there was no large discrepancy recorded in the number of crystals counted on each picture type in this study.

A number of authors have attributed the variation in grain size within ice to three main processes; varying rates of shear stress, recrystallization and annealing over time.

Two trains of thought have developed over the results of increasing shear stress in crystals. The first group feels that increasing shear stress on ice crystals results in a decrease in their size (Rigsby 1958, 1960; Shumsky 1958; Kamb 1959; and Taylor 1963). Both Taylor and Kamb stated that through the process of migratory recrystallization, crystals which are more favourably orientated to stress (those whose c axes are already normal or nearly so to the direction of shear) may actually consume those less favourably orientated, and thus grow at the expense of the more highly stressed crystals.

Gell (1973) considers that crystal size will increase with increasing load and this idea has been supported by other workers in the past (e.g. Bader 1939; Perutz 1940; and Steinman 1959). Steinman's experiments produced a growth in crystal size during recrystallization under load.

Another widely held concept is that crystal growth may occur when a release of the applied load occurs, such as may happen in the terminal area of a glacier. Ice which has been subjected to high stress from deep within the glacier, and which has been brought to the surface in the terminus, consequently has less stress on it as the ice becomes stationary and the overlying ice slowly melts out.

Rigsby (1960) also showed by laboratory experiments, that through the process of annealing ice from -2°C to -0.3°C over time, an increase in the crystal size occurred.

In summary, the ice sample obtained from the Donjek end moraine showed an array of crystal sizes ranging from areas in excess of 44.0 cm^2 (from black and white photographs) down to sizes less than $.04\text{ cm}^2$. Similar ranges have been reported in other types of ice. This range in crystal size within a single ice type is thought

to have been brought about by changes in shear stress rates, recrystallization and annealing over time. However the mean crystal area value places this sample in glacier terminal or stagnant ice type.

Exact measurement of crystal size is made difficult by a number of reasons. Cutting ice samples into thin sections often results in grains being cut through, and matching similar grains up again often becomes difficult. Thus the mean grain size may be underestimated. Crystals which were truncated by the edge of the thin sections also led to underestimation of size. One of the inherent problems in measuring grain sizes is that of taking two dimensional measurements of a three dimensional object. Gow (1969) points out that in general the average particle size obtained from thin section analysis will be less than the true value, simply because a section seldom cuts crystals at their maximum diameter. Also the measurements are of a substance in which crystal growth may not have reached an equilibrium state. Thus the dimensions obtained may not truly represent the final size of the crystal.

A final problem results from the difficulty of trying to measure accurately the dimensions of an object which has an irregular shape, such as ice crystals with

jagged or pointed boundaries. Rigsby (1968) has attempted to measure ice crystals in three dimensions as well as employing an irregularity factor or jaggedness ratio with limited results.

Finally if this ice sample is glacier (dead ice), then one would expect that the crystals would have undergone a release in stress, that they would be near their melting point temperature, and that recrystallization could have occurred in this ice. Migratory recrystallization results in differential grain growth and may in part explain why the ice sample showed a porphyroblastic texture. (Plates I, II, III).

2.3.3 Crystal Shape

The crystals from the sample show a variety of structural features, all of which are primarily the result of deformation of the crystals by external or internal forces.

The most apparent structural feature of the ice crystals is the distortion of the natural grain boundaries. Some of the boundaries have become warped or bent in a more or less arcuate fashion while others have become fragmented or jagged. (Plate I, IV, and Vertical). This

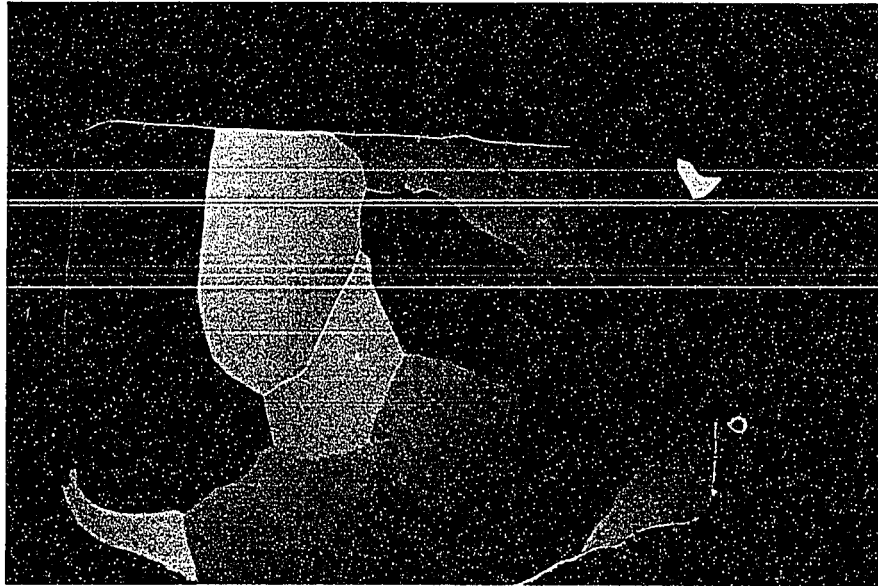


Plate 2.V1 Horizontal view of ice crystals under cross polarization. Ruler in cm^2 . These plates are equivalent to B&W plates 2.1 and 2.11.

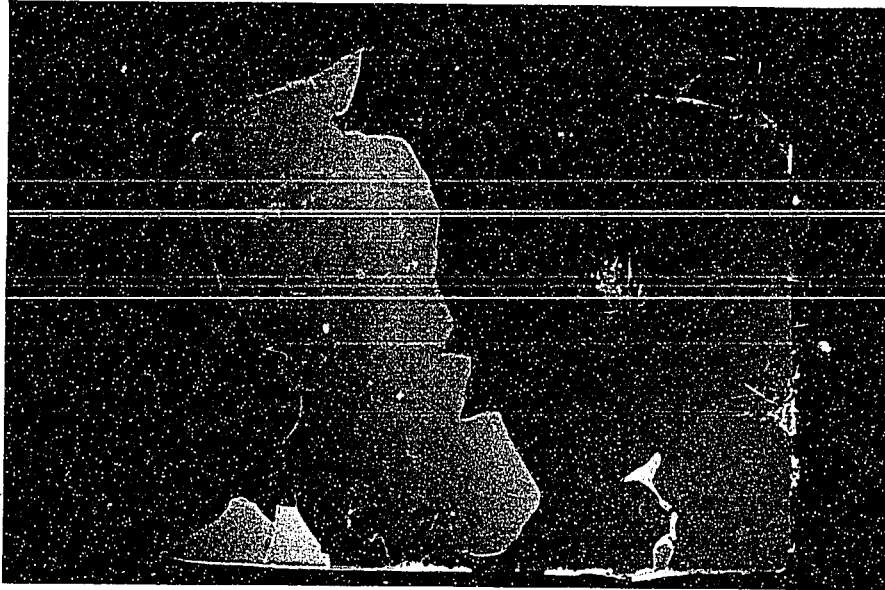


Plate 2.VII Horizontal view of ice crystals under cross polarization. Ruler in cm^2 . These plates are equivalent to B&W plates 2.III and 2.IV.

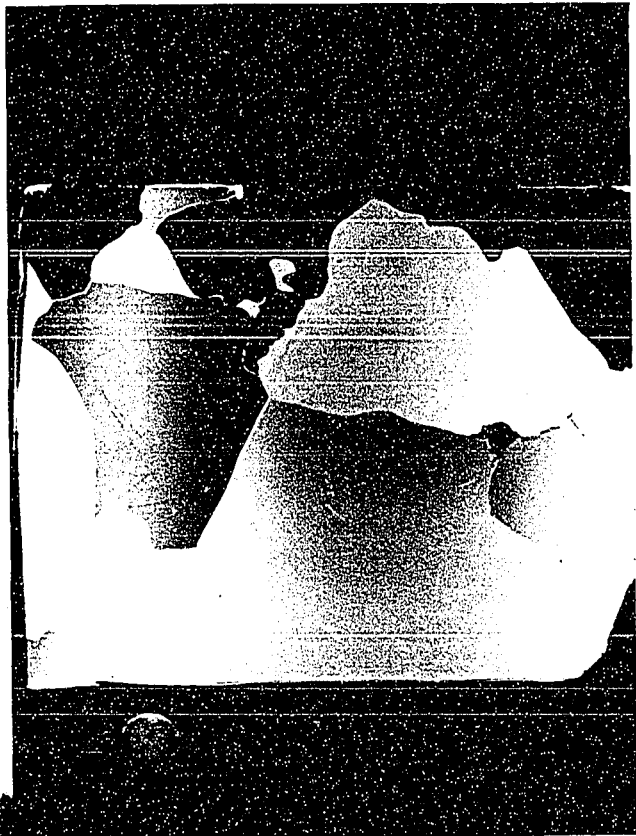


Plate 2.V Vertical view of ice crystals under cross
polorization.

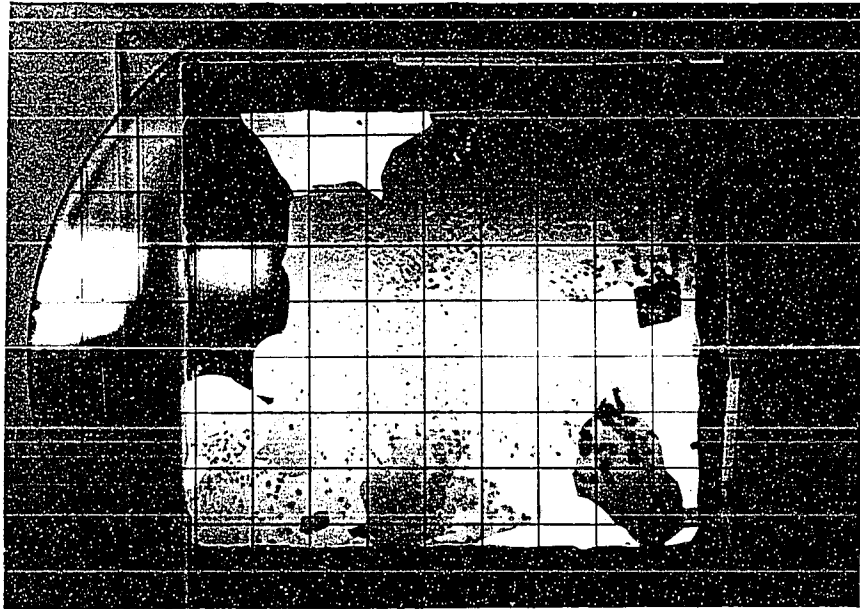
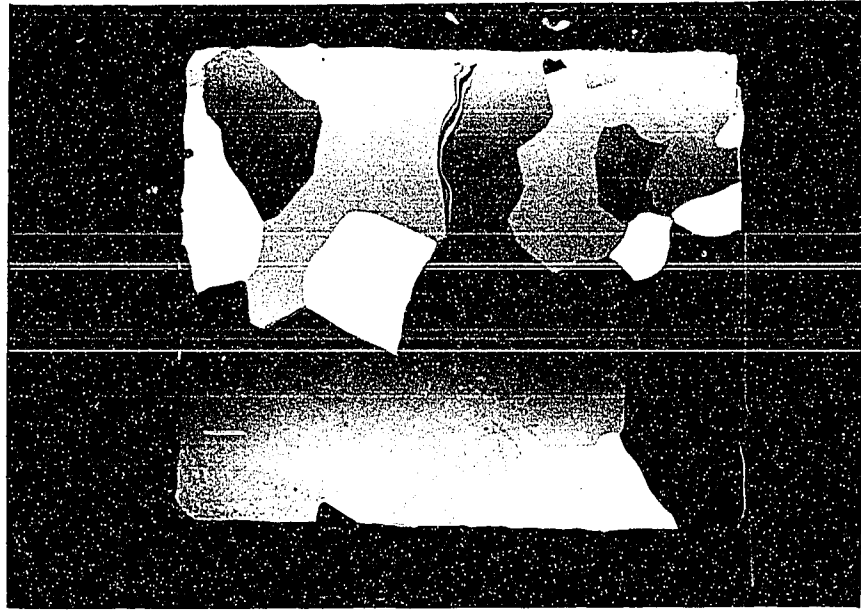


Plate 2.IV Horizontal view of ice crystals under cross polarization. Grid in cm^2 . Lower photograph rotated ninety degrees from upper plate.

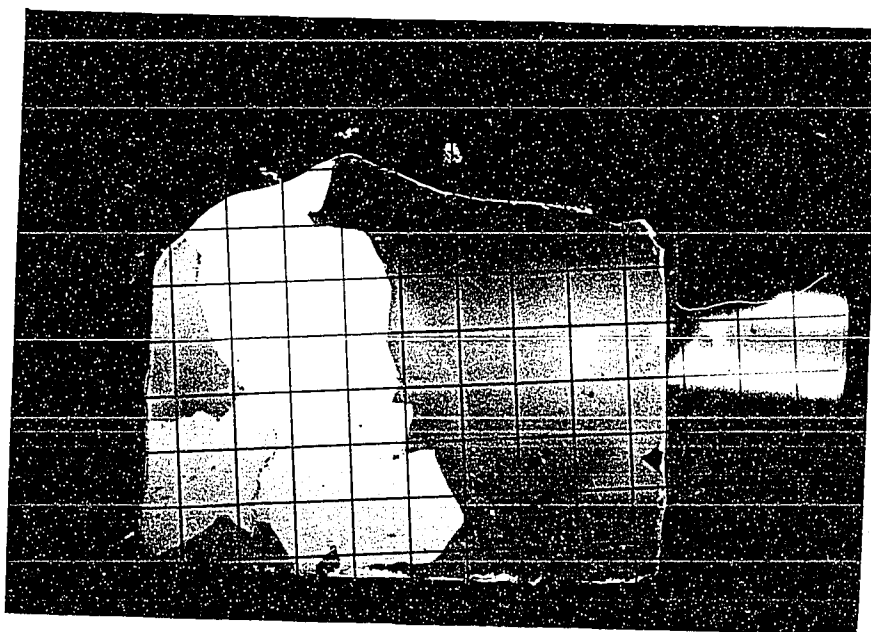
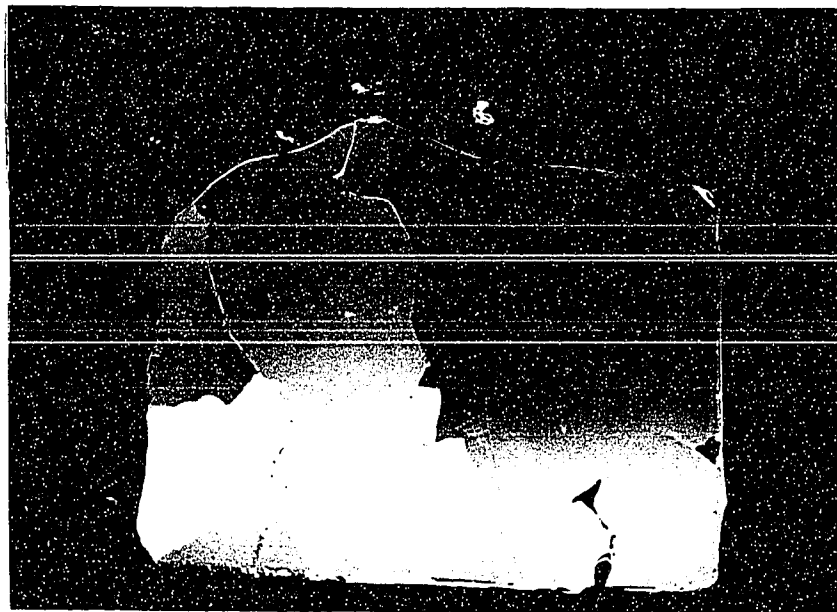


Plate 2.111 Horizontal view of ice crystals under cross polarization. Grid in cm^2 . Lower photograph rotated ninety degrees from upper plate.

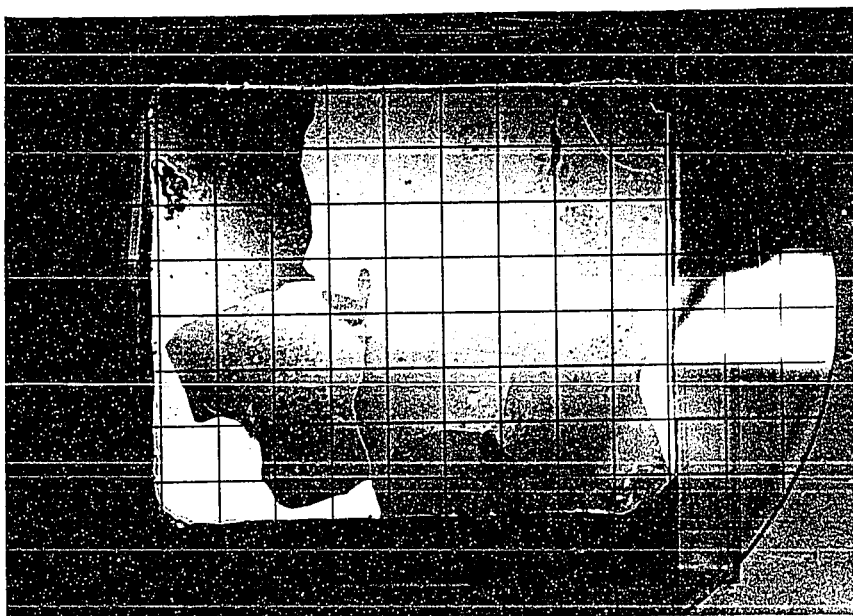
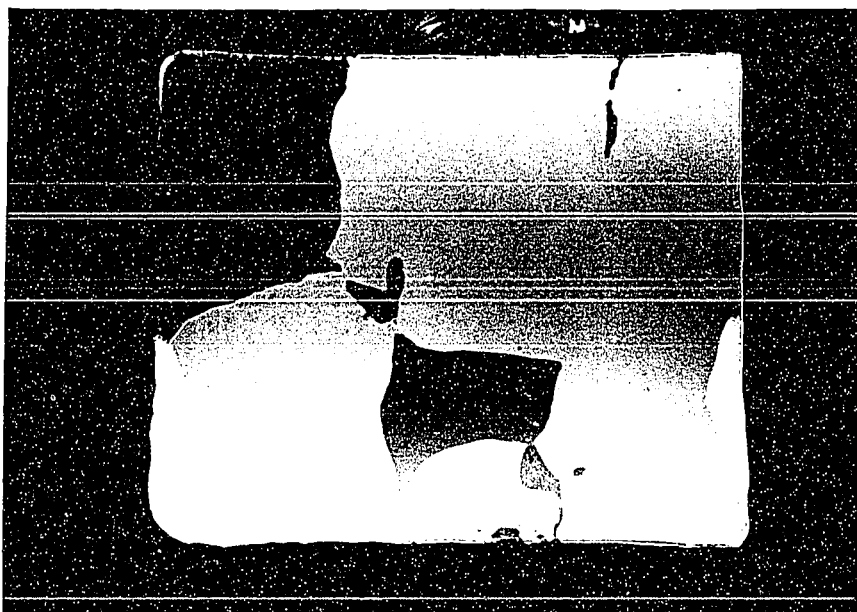


Plate 2.11 Horizontal view of ice crystals under cross polarization. Grid in cm^2 . Lower photograph rotated ninety degrees from upper plate.

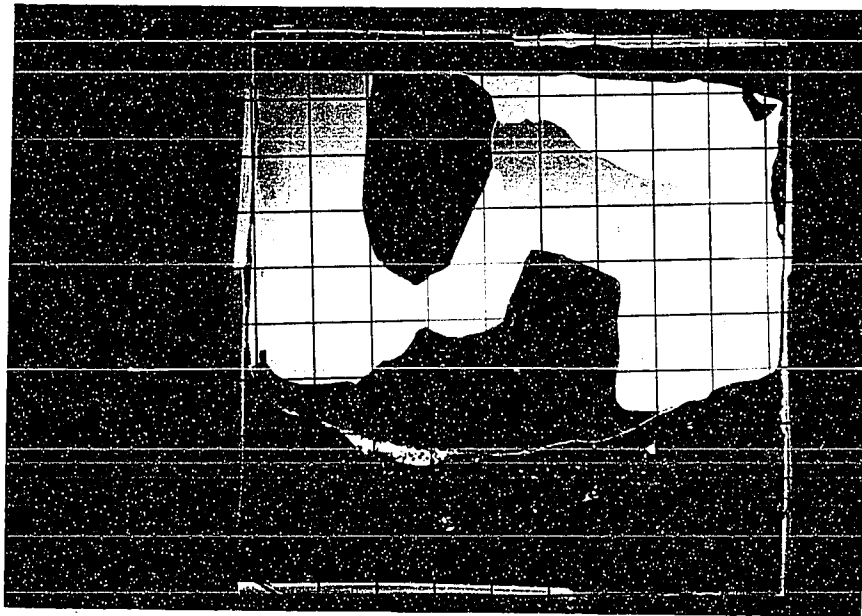


Plate 2.1 Horizontal view of ice crystals under cross polarization. Grid in cm^2 . Lower photograph rotated ninety degrees from upper plate.

particular type of feature is the result of severe deformation (Gold 1963; Gell 1973).

Sub-boundaries (former crystal boundaries) are also apparent, (Plate III). These features may be the result of crystal boundary migration resulting from deformational stresses. Slipbands or striation lines, which result from crystals deforming along planes within each crystal, also occur. Gold (1960) states that "near the melting point single crystals with hexagonal symmetry usually deform by slip on the basal or prismatic planes". These slip planes are usually in the same direction as the basal planes.

Cavities or small holes were found along the grain boundaries or within certain crystals. They are thought to be the result of the coalescence of small holes in the material which may have been there initially or to have occurred during creep. (Plate I). Finally, the grains tended to be interlocked in a similar way to those described by Kamb (1969) and Anderton (1970) for glacier ice, in which the boundaries of one crystal project into those of other crystals and vice versa. This texture, according to Anderton (1970), has resulted from recrystallization under stress.

The above results are similar to those found by Gold (1963) who showed that in laboratory experiments, when an applied load was released, recrystallization occurred with rearrangement of grain boundaries. Irregular grain boundaries and polygonization were associated with this recrystallization. Also, he states that ice has only one effective slip plane and that when a load is applied and does not create a stress in the direction of this slip plane, then local stresses are created within each crystal. These local stresses oppose the main stress and also cause local stresses to occur between grains. When a slow creep rate occurs, then such things as grain-boundary migration, sub-boundaries, cavity formation, polygonization, and bending are sufficient features to absorb the related load or stress occurrence and thus overcome failure.

2.4. Summary

At the outset of this chapter, it was stated that the main purpose would be to determine whether or not textural analysis was a sufficient technique which could be used to distinguish between various ice types. A sample of buried ice from an ice cored end moraine was obtained and subjected to various forms of analysis in a cold room laboratory; and the results were compared to those found in the literature which described similar physical properties from various ice types.

The petrofabric analysis used in this study showed a multiple maxima of c axis orientation common to temperate glacier ice. Most optic axis occupied an equatorial position, having low angles relative to the thin sections. However because of the possibility of similar patterns occurring in other ice types, no firm conclusions can be drawn as to the origin of the ice sample from the petrofabric diagram.

Crystal size measurements, determined by use of the centimeter square grid, long and short axis measurements, and diameter (long axis only) were tabulated. A variety of crystal sizes were found, the majority of which had areas equal to or less than 4.0 cm^2 . (black and white photographs). The fact that some of the crystals had areas greater than those shown on the thin sections resulted in the underestimation of the true area of the crystals involved; and this shows that this ice type has crystal sizes in the same range as those found in glacier terminal ice or dead ice. Thus by crystal size alone the origin of the ice core sample would be temperate glacier ice.

The crystal shapes found in this study are those of ice which have been severely strained and in which recrystallization has been occurring. It would seem

unlikely that the weight of the overlying ice was able to create the variety of stresses required to produce these features. However, Hooke (1970, 1973) and Gell (1973) have shown that buried ice may become incorporated into and/or undergo severe deformation by advancing glacier ice. Thus, buried ice may display similar structural relations to that of glacier ice. This makes it extremely difficult to differentiate ice types on structure alone. A much more detailed analysis of the history of ice crystal deformation would be required before more definite results could be stated.

Various forms of buried ice such as glacier (temperate, polar), snowbank or superimposed snowbank, and segregated ice may all reveal similar textural properties under individual sets of conditions. Thus one cannot use textural analysis alone to differentiate between various ice types. Possibly a more rigorous textural analysis, used in conjunction with other means of revealing ice properties such as chemical analysis, would allow a more definite statement to be made concerning origins of buried ice types.

Also a more complete sampling method would have allowed comparisons to be made, i.e. by using such properties as those revealed through textural and chemical

analysis, on the distribution of the ice type under investigation. For example, samples taken at intervals along the maximum extent of the ice core would have revealed if any strong similarities in the above mentioned properties existed, and thus allow one to speculate on the extent of the uniformity of the ice type., i.e. whether or not the ice core consists all of one ice type or in fact is made up of several types. Similarly one could sample the terminus of the glacier and compare the properties thus revealed to those found in the buried ice.

As well, a larger number of crystals from each sample should be used to increase the statistical significance of the fabric analysis unless strong patterns emerge early in the plottings.



Plate 3.1 View of proximal side of western portion of terminal moraine looking up valley. Note ice core exposure and mud flow near center of picture.

3. MORPHOLOGY OF THE DONJEK END MORaine

3.1 General Form

Plate 3.1, shows the general morphology of the Donjek moraines. From a distance the end moraine appears as a large ridge rising sharply above the relatively flat outwash plain. The height of the moraine above the valley floor varies from 18 meters up valley to heights exceeding 45 meters further down valley. The width of the moraine is not continuous but is cut by a number of melt water channels formed by the draining of proglacial lakes and by erosion by glacial melt water streams such as the Donjek River.

The moraine is asymmetrical in shape with the distal side being steeper than the proximal side which has more of a long gently sloping ramp like appearance. Similar moraine asymmetry has been reported by Price (1970) for ice cored Neoglacial moraines in the Yukon, Canada and by Andersen and Sollid (1971) for Neoglacial moraines in South Norway. The proximal sides of the moraines were gently convex and the distal side appeared straight or slightly concave. Price (1970), and others before him, stated that this shape results from the way in which the

moraine was originally formed, i.e. by morainic material being pressed out from beneath the glacier.

One of the most prominent features on the moraine are melt water ponds, giving the surface a pronounced pitted appearance. They are primarily oval in shape but vary considerably in size. Denton and Stuiver (1966) have shown from a comparison of air photographs starting in 1935, that the lakes or ponds on the western portion of the moraine have been slowly increasing in size; and they feel that this may be the result of ice core melting. Many former lake beds are also present on the moraine.

Other prominent features located on the moraine are distinct ridge patterns. Denton and Stuiver (1966) noted a number of small ridges, approximately 2.5 meters high, 9 meters wide, 125 meters in length, and with well rounded crests, located on the western portion of the end moraine.

Johnson (1971) recognized the complex morphology of the ice cored end moraine; and noted that

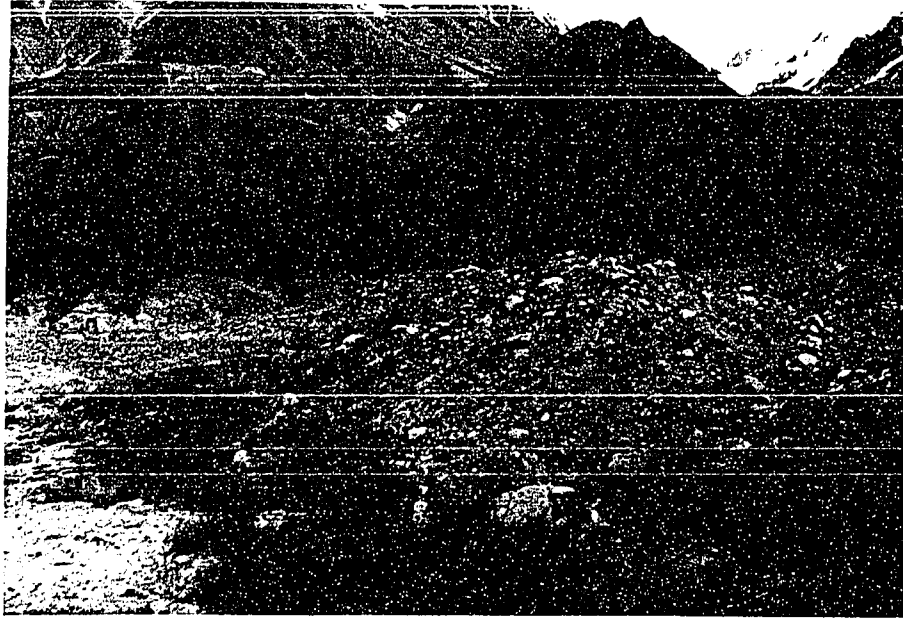


Plate 3.11 Small ridge separating well vegetated drift A from sparsely vegetated drift B.

large areas of the moraine consisted of parallel ridges with heights similar to those described by Denton and Stuiver and having slopes up to 45 degrees. These ridge profiles are broken by a series of cracks which are generally parallel to the axes of the ridges, and are thought to be due to downslope slipping of the till along the ice-till interface. (More quantitative data on these cracks is presented in Chapter 6).

A distinct ridge, up to 0.7 meters in height, occurs on the northern and eastern section of the moraine and separates the well vegetated part of the moraine from the less well vegetated areas (Plate 3.11) Denton and Stuiver (1966) differentiated these two areas into Drifts A and B.

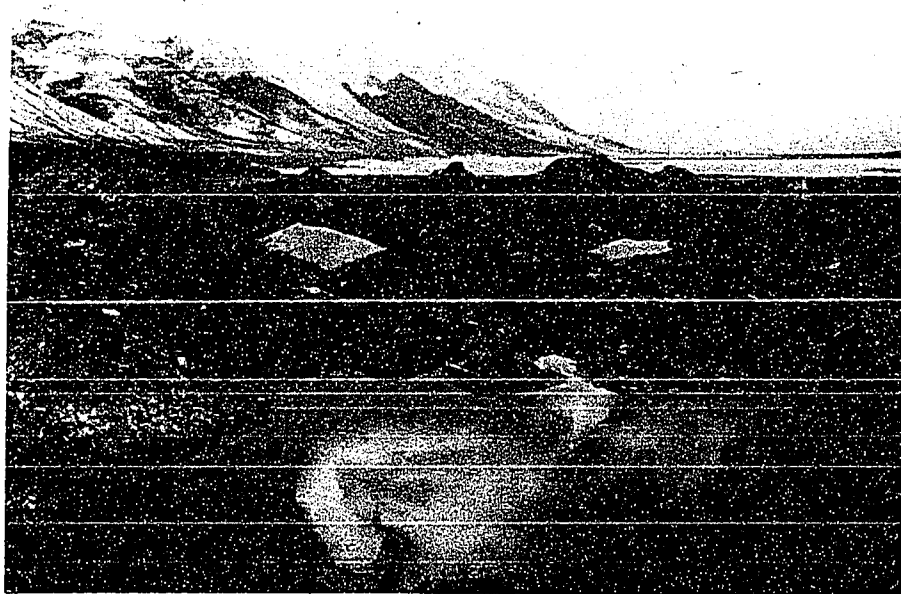
Drift A, the older of the two, supports a heavy vegetation cover; has slopes and ridges which are stable and well rounded; and melt ponds which are deeply inset into the moraine as shown by the high slope angles surrounding these features. Aerial photographs show that in general the ponds are much larger in area than those located on Drift B.

Drift B consists of end moraine sediments which have been deposited on the inside or proximal side of the moraine. Mechanical analysis did not show a significant variation in grain size between the two drifts; however mean slope angles were less here than those on the distal side. Melt ponds had not been as deeply inset into the moraine and, during part of the study season, several were seen to be overflowing their banks and draining down the proximal back slope. Ridges were more peaked than those on Drift A and cracking was apparent, reflecting greater denudation and greater slope instability. This area was actively being modified by melt water streams, mudflows, and ice core exposures with resulting slumping and mudflow activity. The lack of vegetation cover could be expected to enhance the activity of such geomorphic processes as rill and sheet wash, deflation, creep, and rain splash resulting in further modification to the surface morphology.

The distal portion of the moraine contained the highest percentage of vegetation cover ranging from 80 percent coverage on the outer edge to less than 30 percent on the inner portion. The most frequently



A



B

Plate 3.111 A conical hill (A) and melt water ponds (B) located along the terminal moraine.

occurring vegetation types here were lichen, mosses, and small sedge. Trees were found growing only on Drift A, and coring of the largest trees revealed similar results to those of Denton and Stuiver (1966), with maximum ages for spruce trees (*Picea Clauca*) 90 to 94 years while those of poplar (*Populus Balsamefera*) were 30-50 years. The oldest trees were located along the flanks of the distal side of the moraine beside the heavily vegetated valley walls, while trees growing along the distal portion facing north were much younger, reflecting the greater distance and thus the longer time period required for germination. Drift B had a very sparse vegetation cover consisting of a smattering of very young poplar trees and tufts of sedge.

Scars from both active and fossil slumps and mudflows are present over much of the moraine, as well as abandoned melt water channels, mounds or hillocks, and kames.

3.2 Slope Analysis

3.2.1 Introduction

Until quite recently, little or no quantitative data had been published on slopes of ice cored moraines. Sharp (1949) described the terminal area of valley glaciers covered with superglacial debris as being chaotic in appearance having ridges and hillocks with steepest slopes ranging between 30 and 45 degrees. Rampton (1970) measured mean slope angles on the Neoglacial moraines fronting the Kutlan Glacier, (St. Elias Mountains), but his values represented certain segments on the moraine sides rather than transects across the whole of the feature. Loomis (1970) measured slope angles on an ice cored medial moraine located on a presently active glacier in the St. Elias Mountains, while Johnson (1971) mentioned the maximum slope angles obtained on ridges of the Donjek end moraine.

In this study it is proposed to analyze slope data recorded from transects around the entire ice cored end moraine in the Donjek Valley. Simple statistical analysis, in the form of mean slope angle, standard deviation and frequency distribution, was performed on the slope data collected.

3.2.2 Methodology

Slope angles were measured by use of an abney level and graduated pole. A number of traverses across the moraine were measured so that equal representation could be given to every morphological zone on the moraine. Each traverse was taken from the proximal to distal side, and passed through areas which revealed certain geomorphological processes and distinct landform types. Proximal and distal sides of the moraine were defined arbitrarily from the highest point on each traverse. A thirty foot sample length was chosen because of the length of the profiles (up to 2500 feet or 760 meters) and any changes within each segment were noted.

Basic statistical parameters were determined for the following divisions on the moraine:

1. Individual traverses
 - proximal to distal sides
 - slope orientation (west and east, north and south facing slopes)

2. Integrating slope values around the moraine
 - proximal and distal sides
 - slope orientation

3. Climatic divisions
 - the end moraine was divided into two areas based on exposure to valley winds (see chapter 4).
 - (a) Lee area comprising the entire western portion of the moraine.
 - (b) An area directly exposed to valley winds (including both northern and eastern sections of the moraine).

3.2.3 Data Analysis

Figures 6 and 7 show values obtained for the various statistical parameters. The complexity of the moraine surface is seen by both the very high range of slope angles, and the relatively high standard deviations obtained for the whole of the moraine and for the climatic divisions.

INDIVIDUAL PROFILES

Profile	Distal		Proximal		Slope Orientation				Max	Min
	\bar{X}	M	\bar{X}	M	\bar{X}	M	\bar{X}	M		
					W		E			
Q	25 (4)	28	16 (14)	14	20 (6)	20	17 (12)	14	33	4
H	18 (7)	17	14 (8)	12	17 (8)	14	14 (7)	12	36	2
I	15 (17)	17	14 (22)	12	17 (14)	17	13 (24)	11	38	1
M	14 (26)	11	15 (70)	11	15 (35)	11	15 (54)	12	43	0
N	14 (13)	12	9 (64)	8	15 (15)	13	10 (53)	8	38	0
P	10 (35)	5	13 (31)	9	10 (37)	6	14 (29)	11	34	0
D	16 (20)	15	6 (76)	4	7 (49)		10 (41)		37	0
E					13.2		10.6			
B	19 (22)	16	11 (50)	9	12 (36)	9	16 (34)	14	45	0
C	14 (36)	13	6 (50)	6	7 (44)	6	12 (40)	12	36	1
K	9 (32)	9	7 (55)	4	$\frac{N}{10}$ (35)	9	$\frac{S}{9}$ (34)	6	29	0
G	11 (25)	6	8 (19)	8	10 (22)	7	9 (19)	8	33	0
A	13 (14)	12	9 (22)	8	10 (21)	8	12 (15)	12	30	1
F	10 (22)	7	8 (34)	7	9 (25)	7	9 (29)	7	30	0

FIG. 6

\bar{X} = Mean Slope Angle
M = Median Slope Angle
Max = Maximum Slope Angle
Min = Minimum Slope Angle
() = No. of Segments in each transect

INTEGRATED RESULTS

	Proximal	Distal	West	East	North	South
* \bar{X}	11.0	15.0	14.1	13.5	9.8	9.8
S.D.	7.5	7.9	6.7	8.0	9.3	7.2

CLIMATIC DIVISIONS

	Lee				Windy			
	Proximal	Distal	West	East	Proximal	Distal	West	East
\bar{X}	14.6	16.2	16.8	14.0	9.0	12.3	9.1	12.8
S.D.	5.0	10.7	9.1	5.8	7.5	10.0	6.8	9.5

* \bar{X} = Mean Slope Angle
 S.D. = Standard Deviation

All values are presented in degrees

FIG. 7

Proximal-Distal Sides

Mean Slope Angles

Slope angles along the distal flanks of the moraine were between 20 and 30 degrees on individual profiles, while those on the proximal flanks were between 1 and 12 degrees. The highest distal and proximal angles occurred at the two extreme up valley positions on the arcuate shaped moraine, while between these two areas the values were lower but no distinct pattern emerged. Maximum and minimum slope angles on each individual profile were noted (FIG. 6) but again no distinct pattern was apparent. The maximum slope angle recorded was 45 degrees while the lowest angle was 0 degrees. Similar ranges were reported for ice cored features by Loomis (1970) and Rampton (1970).

In all three cases, i.e. individual, integrated, and climatic, the distal portion of the moraine showed higher mean slope angles than the proximal side. As well, within the climatic divisions, the lee area had greater mean slope angles on both of its sides than had the exposed area.

Frequency Distributions

Frequency distribution diagrams for both integrated and climatic divisions showed similar results in that the most frequently occurring class interval on their distal sides was 8-11 degrees. On their proximal sides, both the integrated and climatic (exposed) divisions showed similar but lower class intervals at 0-3 degrees, while the lee area had a higher interval ranging from 8-11 degrees.

Slope Orientation

Mean Slope Angles

For individual slope profiles on the western portion of the moraine, west facing slopes were generally greater than east facing slopes; while for the eastern section of the moraine east facing slopes, on each transect, were greater than their corresponding west facing slopes. Here both west facing slopes on the western section of the moraine and east facing slopes on the eastern portion represent the distal slopes of each ridge. On the northern section, the north facing slopes were generally greater than south facing slopes;

but the difference between their means was only one or two degrees while high standard deviations were recorded for each.

Summing all values for west and east facing slopes around the moraine revealed that those which were west facing had only a slightly higher mean value than east facing, (FIG. 7), and that both had high standard deviations. Within the climatic division, west and east facing slopes in the lee area had higher mean slope angles than those on the exposed area; but each division revealed high standard deviations. Both north and south facing slopes had similar mean slope angles and high standard deviations.

Frequency Distributions

Frequency distribution diagrams for individual transects showed that both west and east facing slopes, on the western and eastern portion of the moraine, had similar modes occurring in the range of 3-15 degrees. Integrated values for the whole of the moraine and the climatic divisions showed the most commonly occurring

class interval to be 4-7 degrees for both west and east facing slopes. Individual transects on the northern portion of the moraine showed the most common interval for north facing slopes to be 4-7 degrees with a minor peak at 27-31 degrees, while south facing slopes had a broader interval between 0-3 and 4-7 degrees. Integrating the slope angles for this section of the moraine showed a slightly wider range of the most commonly occurring interval for north facing slopes at 4-7 and 8-11 degrees, while that for south facing slopes was 0-3 degrees.

A typical slope profile taken over the western portion of the moraine (see FIG. 2 for exact location) is presented in the appendix.

3.2.4 Summary

The complexity of the morphology of the ice cored end moraine is shown by the high range of slope angles encountered on individual traverses, and the high standard deviations obtained for all mean slope angles around the moraine. The least angular differences occurred

along the flanks of the moraine, whereas the greatest differences occurred in the area between these two portions.

The overall shape of the end moraine is asymmetrical with higher slope angles on the distal than the proximal side. The ridges on the proximal side showed sharper crests than those on the distal side, which in turn showed more minor peaks on the percent frequency distribution of slope angles. This difference may be partly explained by the subjective nature by which the division between the proximal and distal side was made.

West and east facing slopes, in general, had higher mean slope angles than north or south facing slopes. Integrating mean slope angles around the moraine for slope orientations showed that both west and east facing slopes had similar overall means. However, the integrated mean value for west and east slopes was greater than that for north and south slopes.

Finally, mean slope angles for both proximal and distal and slope orientations on the lee area were greater than those for the exposed section of the moraine.

The mean slope angles presented here are somewhat lower than those reported by Rampton (1970) for the Neoglacial moraines of the Klutlan glacier. Rampton reported proximal and distal angles to be 20.2 and 24.4 degrees respectively for Klutlan moraine IV whereas those for the Donjek moraine are 11 and 14 degrees. This difference may partially be explained by the fact that Rampton did not sample directly across the moraine but from the flank portion of the moraine, on areas which were carefully chosen and were relatively free from external drainage. The inclusion of the moraine between these two sampling areas may well have led to a difference in his mean slope angles. However, both moraines are asymmetrical with steeper distal sides and a concave form, as compared to a gentle more convex shaped proximal side.

The variation in the number of modes displayed on the histograms for the Donjek glacier moraines is

very similar to those obtained by Rampton for the Klutlan Neoglacial moraines. This polymodal character of the diagrams attests to the complexity of the mean slope angles on ice cored moraine surfaces.

3.3 Summary on Form of End Moraine

The general form of the Donjek end moraine is a large massive ice cored feature, both asymmetrical and arcuate shaped, possessing a complex morphology.

The fact that the end moraine is underlain by ice is known from several outcrops of the ice core. A detailed account of these exposures together with their distribution and influence on the moraine morphology is presented in chapters 5 and 6. Briefly the following points can be made with respect to the ice core.

(a) It gives the impression that the moraine is a massive accumulation of debris. However sections on the Donjek moraine show that the overlying debris may represent only a small proportion of the total thickness with the ice making up the remainder.

(b) There is a high degree of correspondence between surface topography and that of the underlying ice.

(c) Ablation of the ice core results in various degradational processes on the moraine which modify the morphology of the moraine over time.

From aerial photographs the end moraine seems to be relatively smooth in appearance; but a closer examination in the field shows that the surface is highly complex, consisting of a variety of features which vary in size, extent, and number from one side of the moraine to the other. In general the distal side of the moraine contains higher mean angle slopes, a denser and older vegetation cover, larger lakes, more rounded ridges, and gives the appearance of being more stable than the proximal side.

The diversity of features which have been produced on the moraine surface reflects the variety of environments to which the moraine has been subjected since its formation. For example, such features as scars from former or presently active forms of mass movement, old lake beds, abandoned melt water channels, hills, depressions, gaps, and the lack of any discernible soil structure together with the variation

in the composition of the morainic material over relatively short distances, all reveal the diversity of both past and present environments.

4. CLIMATIC AND GLACIAL SURGE INPUT FACTORS AND GROUND TEMPERATURES

In order to more fully assess the impact of certain degradational processes on the morphology of the end moraine, it is necessary to determine both the factors and the intensity of these factors involved in producing these processes. The most important factors thought to be controlling processes are the results of local climatic conditions and glacial surge action. The activity of certain processes was not measured for the whole of the summer thaw period, so care was necessary in the extension of the conclusions to the total summer season. A summary of the climatic parameters is presented in this chapter together with a short discussion on glacial surge action.

The interaction of the climatic parameters with the ground surface results in the transmission of energy (heat) through the soil. This energy may be used to promote degradational processes where the depth of penetration is greater than the thickness of material over the ice core of the moraine. Variations in the soil temperatures were correlated with variations in the micro climatic parameters. (Chapters 5 and 6).

4.1 Climatic Inputs

4.1.1 Introduction

A brief account of the regional weather pattern was presented in Chapter 1, in which it was shown that the study area is

located in a continental type climate due to its location on the lee side of the St. Elias Mountains. During the winter, which lasts approximately seven months, the area is predominantly under the influence of an interior high pressure system which is located near the McKenzie delta. Total precipitation at the government run meteorological station at Burwash Landing during the 1972 field season was 129.0 mm. The summer period (months in which mean monthly temperatures are above 0°C) extends for a period of five months, usually May through to September, during which time the region is under the influence of a series of low pressure systems; and total precipitation during this period at Burwash Landing is approximately 218.0 mm. Within this regional pattern many local variations can be expected to occur especially in the valley of the St. Elias Mountains area.

4.1.2 Micro Climatic Trends At Moraine Stations

Air Temperature

Mean daily air temperature for both the moraine meteorological stations over the study period are presented in (FIG. 8) and mean; monthly values (FIG. 9) show that A station, during the study period, was warmer than B. Both stations show similar mean maximum monthly temperatures for the study period, but A station had higher mean minimum monthly temperatures resulting in a higher range of air temperatures and thus a lower mean daily temperature at B station.

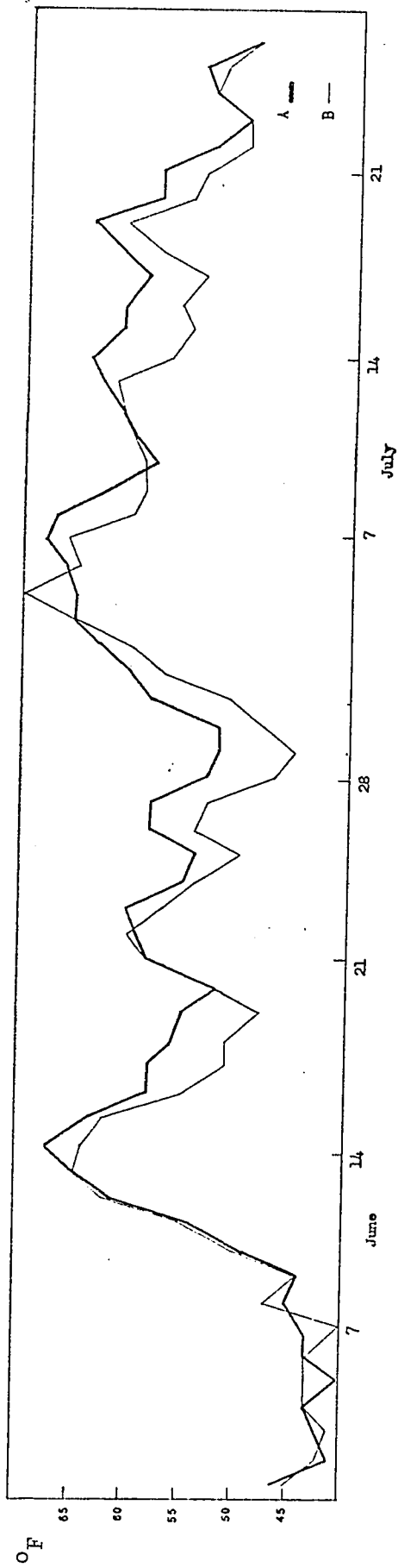


FIG. 8 MEAN DAILY AIR TEMPERATURES

MEAN MONTHLY AIR TEMPERATURE

	A	B
June	(11.7)	(10.6)
July	(15.6)	(13.9)
* \bar{X}	(13.9)	(12.2)

MEAN MAXIMUM AND MINIMUM MONTHLY AIR TEMPERATURE

	A		B	
	Max	Min	Max	Min
June	(14.4)	(8.9)	(15.6)	(7.2)
July	(17.8)	(13.9)	(16.7)	(11.1)
** \bar{X}	(16.1)	(11.7)	(16.1)	(9.4)

* \bar{X} mean value for each month

** \bar{X} mean value for total study time

The same relationship occurs if one compares the number of days, in the study period, when one station's air temperature equaled or exceeded that of the other. Of the total number of days in the study (54), both A and B stations had daily maximum temperatures equalling or exceeding one another 50 percent of the time each, i.e. 50 percent of the time $A \geq B$, and 50 percent of the time $B \geq A$ for maximum temperatures. However in 83 percent of the study time, the minimum daily temperatures at B were lower than those at A station.

The mean air temperature was calculated for the total study time, (FIG. 10), together with the number of times the temperature at each station exceeded the other at each interval. A station exceeded B station the least at 1800 hours and the most between 0900 and 1200 hours. There was no difference in the time of occurrence of maximum and minimum temperatures.

Cloud Cover

The percentage of time and the amount of cloud in tenths at the moraine for the study period is shown below. The most cloudy conditions occurred during the month of June, in which sixty-nine percent of the time the cloud cover was eight tenths to complete.

DISTRIBUTION OF MEAN DAILY AIR TEMPERATURE
FOR THREE HOUR INTERVALS

	0300	0600	0900	1200	1500	1800	2100	2400
A	(12.8)	(11.7)	(12.2)	(14.4)	(15.6)	(15.6)	(14.4)	(13.3)

B	(11.1)	(10.0)	(10.6)	(12.2)	(14.4)	(15.0)	(13.9)	(12.2)
---	--------	--------	--------	--------	--------	--------	--------	--------

* Temperature given in °C

PERCENTAGE OF TOTAL STUDY TIME AIR TEMPERATURE
AT A EXCEEDED THAT AT B OVER THREE HOUR INTERVALS

	0300	0600	0900	1200	1500	1800	2100	2400
A > B	83	83	90	79	59	51	61	73

* Values expressed as a percentage

FIG. 10

Cloud Cover at A and B

<u>Tenths</u>	<u>Percent of Total Time</u>
0 - 3	27
4 - 7	33
8 - 10	40

Relative Humidity

The mean daily relative humidity for each station is given in FIG. 11 . A comparison of mean maximum and minimum values for the season showed that B station had a higher relative humidity than A;and in terms of number of days, B station was higher than A 57 percent of the time.

This difference between stations may be partly accounted for by the fact that B station is surrounded by kettle lakes, (Chapter 3); and even though the mean monthly air temperature is slightly higher at A, the potential for atmospheric moisture is greater at B.

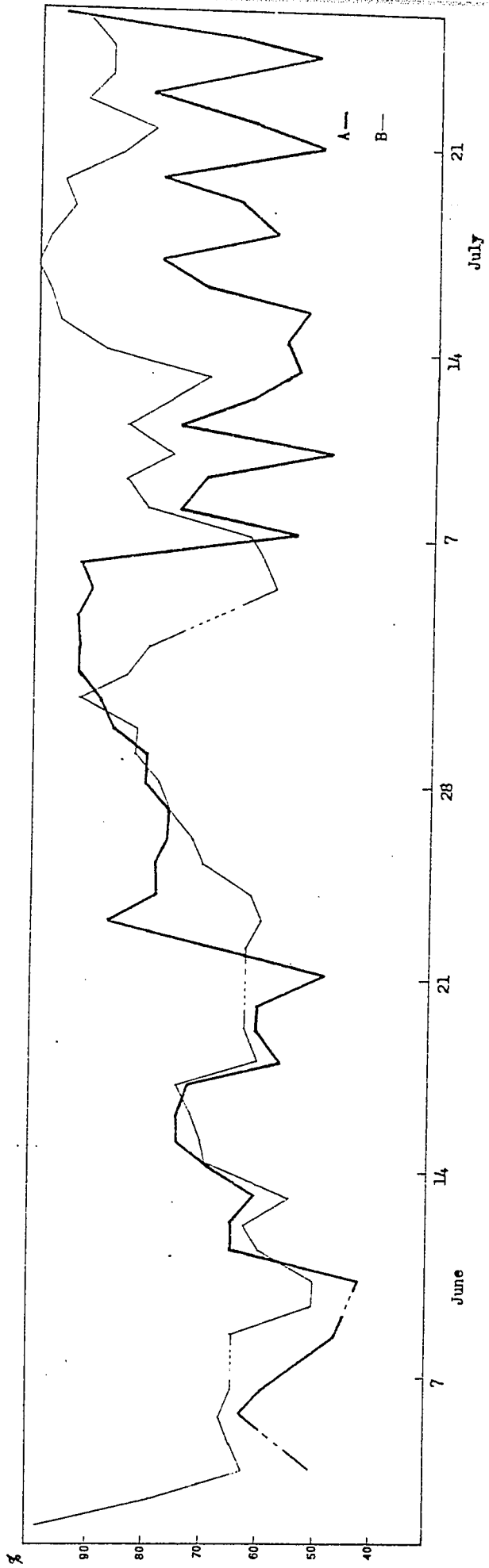


FIG. 11 MEAN DAILY RELATIVE HUMIDITY

A comparison of FIG. 8 and FIG.11 shows that the humidity at A and B does not reflect their respective ambient air temperatures, as was found by Taylor-Barge (1969). Results for the Donjek show an inverse relationship between times of occurrence for maximum and minimum relative humidity and corresponding air temperatures.

Solar Radiation

Mean daily amounts of total incoming radiation were calculated for both stations (FIG. 12). Mean daily and mean daily maximum amounts (FIG.13) showed that both stations received equal amounts. However the number of days one station exceeded the other, (i.e. for mean daily amounts), showed that A was greater than B for 78% of the total time.

Calculation of the times when either A or B stations exceeded one another at 3 hour intervals per 24 hours over the entire study time are also shown in (FIG.13). The results show expected values for a valley orientated in a nearly north-south direction, in which the mountains on the western side are at a higher altitude than the mountains on the eastern side. B station is in shadow for a longer period of time than A station. This was shown on graphs on which quantity of radiation received at 3 hour intervals per 24 hours was plotted. A station received greater amounts of solar radiation around 2100 hours, whereas the difference between the two stations was much less at 0600 hours. This shadow

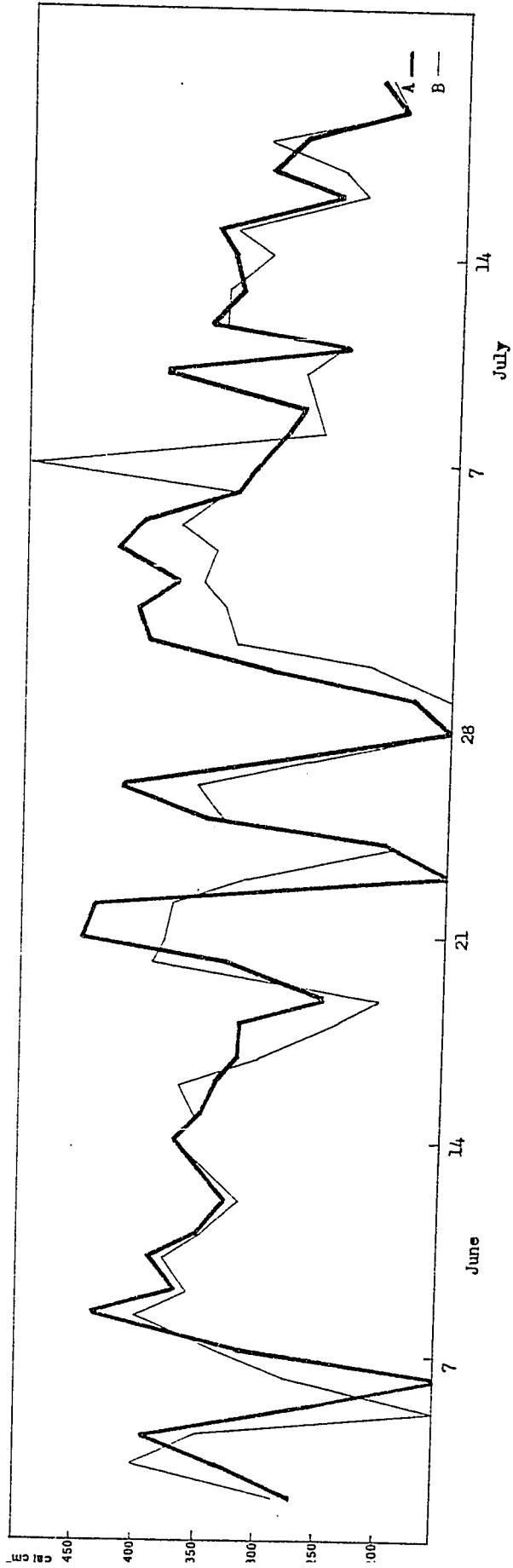


FIG. 12 MEAN DAILY SHORT WAVE RADIATION

MEAN DAILY AND MEAN MAXIMUM DAILY AMOUNT OF
SHORTWAVE RADIATION RECEIVED AT A AND B

	A	B
* Mean Daily	306	307
** Mean Maximum Daily	3.0	3.1

* Values given in cal/cm²/day

** Values given in cal/cm²/sec.

PERCENTAGE OF TIME WHEN A EXCEEDED B AT 3
HOURLY INTERVALS PER 24 HOURS (SOLAR RADIATION)

	0300	0600	0900	1200	1500	1800	2100	2400
A > B	91	55	61	52	57	61	72	92

FIG. 13

effect of the surrounding topography helps to explain why the radiation values recorded on the moraine are somewhat less than those from Whitehorse over the same time period (Monthly Records - Environment Canada 1972). Wendler and Ishkawa (1974), working on the McCall Glacier, have reported a 15 per-cent loss of direct solar radiation as a result of the effect of surrounding mountains.

Wind Speed

Wind speed was calculated for the 1972 field season, while wind direction and wind speed were recorded in 1973. The trends which were found in the 1973 data are assumed to be indicative of the normal Donjek Valley situation.

MEAN DAILY WIND SPEED FOR 1972 SEASON

A	B
* 2.7	1.7

* meters/sec.

Over the total study period, A was greater than B 91.5 per-cent of the time. This was the expected pattern, as B was located close to the western side of the valley which is protected from

winds moving down the Donjek Glacier into the Donjek Valley. The cool down valley winds are initiated over the Donjek Glacier which has its main trunk orientated in a west-east direction (Chapter 1, FIG.2). These winds meet the Donjek Valley winds, which originate over the Kluane Glacier located at the head of the Donjek Valley (FIG.1), over the terminus of the Donjek Glacier. The winds from the Donjek Glacier deflect the Donjek Valley winds towards the eastern side of the Valley. This results in the down valley winds at A station to be from a south south east direction with B station in the lee of down valley winds. The lack of any topographical barrier means both stations are equally affected by up valley winds, and thus the only time A and B differ in wind conditions is when it is predominantly down valley.

Mean daily wind variations for A station during 1973 are shown in FIG.14, and a comparison of means for a similar time period in the previous season showed that higher winds were recorded in 1973. ($1973 \bar{x} = 5.0\text{m/sec.}$; $1972 \bar{x} = 3.6 \text{ m/sec.}$). Wind velocities were calculated at 3 hour intervals over a 24 hour period for the total study time, (FIG.15); and the resultant distribution, together with the times when maximum and minimum wind velocities occurred, corresponded with times when similar variables for air temperature occurred. This is probably a local condition due to strong heating over bare fluvioglacial materials in the valley bottom during the day, which is supplemented by colder air moving down glacier later in the evening. Early morning hours had lowest wind speeds.

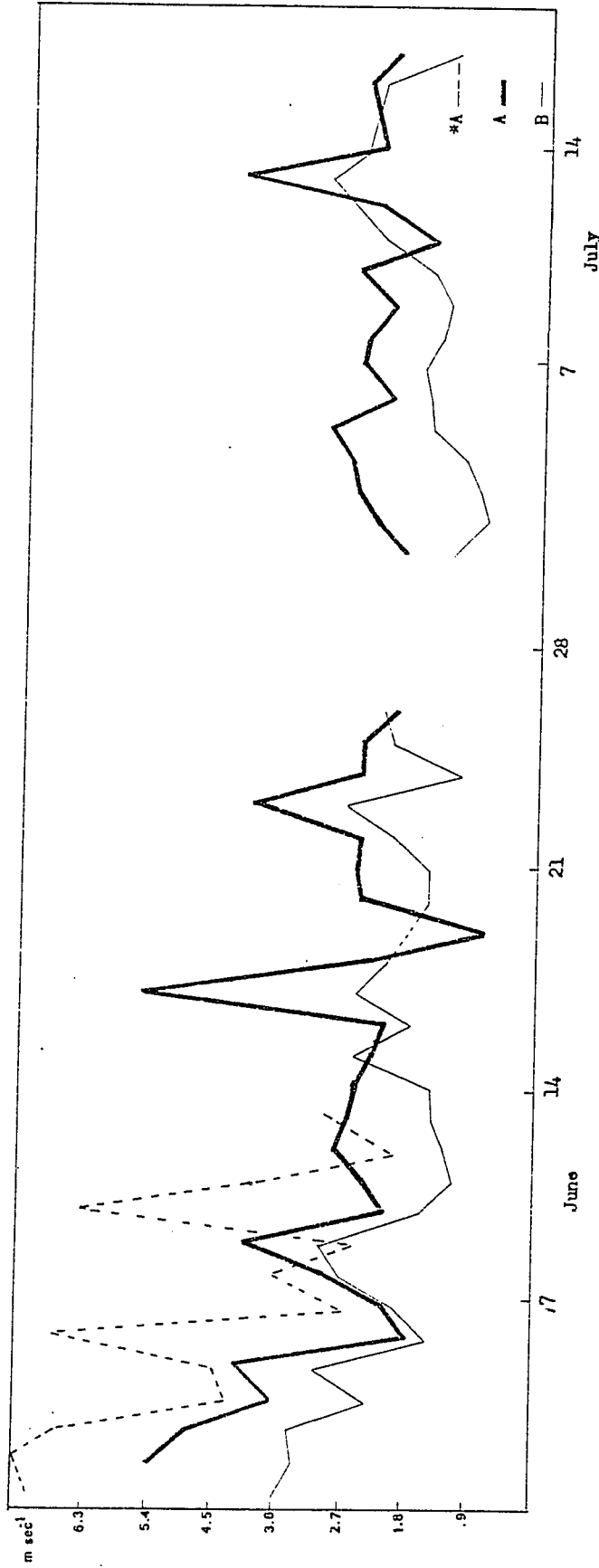


FIG. 14 MEAN DAILY WIND SPEED

* 1973 results taken 3 meters above moraine surface (shown as dotted line).

Higher wind values at A may also help explain why warmer minimum daily air temperatures occurred here than at B station. The turbulent mixing of the air at A tended to prevent the cooling effect which occurs in areas which have little or no wind in the evening hours (Geiger, 1966).

Wind Direction

The results of the wind direction measurements show that down valley winds occurred 76 percent of the total time, up valley approximately 20 percent of the time, and the remainder as cross valley winds.

MEAN WIND SPEED FOR 3 HOUR INTERVALS
PER 24 HOURS 1973

0300	0600	0900	1200	1500	1800	2100	2400
4.5	3.2	3.6	4.1	6.3	5.8	5.8	5.4

* Values are given in meters per second

FIG. 15

There was very little change in wind direction over 24 hour periods. Winds seldom gusted from one direction to another, but blew consistently from the same direction. For example, from May 29, 0600 to May 20, 2400 the wind blew consistently from the north north west. From May 31 to June 4, winds occurred consistently from the south south east; June 4 to June 5, 0900 winds blew continuously from the north north west. This strong predominance of direction occurred with relatively strong wind speed; and whenever the wind dropped below approximately 2.9 m/sec., wind direction would begin to change (from down valley to up valley or vice versa) or become erratic. This reduction of speed and directional change would occur in periods of 6 hours or less.

Up valley winds seem to occur as the result of regional rather than local conditions. Heavy cloud cover and precipitation were associated with the occurrence of these winds. Thus it would appear that the low pressure systems associated with this weather cause the prominent up valley wind conditions.

Present data clearly indicates that wind direction in the Donjek Valley is primarily a result of the surrounding topography, with the valley funnelling winds either up or down valley. Within the valley system there seems to be little micro variation in wind direction, and the winds do not conform to simple glacier wind or katabatic wind models.

Evaporation

Daily values of potential evaporation at each station are presented in FIG. 16, and show that A generally had the highest values. The mean value for the study period was 62 percent higher at A; and of the total number of days in the study, A was higher than B for 90 percent of the time. The area in the vicinity of B station did, however, have greater surface moisture available for evaporation.

Evaporation follows the expected pattern of relationships to other parameters. The daily evaporation curve correlates closely with the ambient air temperature curve, but shows a subdued form for B station. (Compare FIG. 8 to FIG. 16). During the two major warming trends (June 11-15 and July 3-8), evaporation values were high; while during the cooler trends (June 1-10, June 16-20 and July 10 and on), values tended to be lower. A similar pattern was also found to exist with mean daily soil temperatures.

Wind speed affects not only ambient air temperatures but also to a degree, evaporation rates, as high wind speeds and high evaporation rates occurred simultaneously (FIG. 17). However, relative increases in the amount of evaporation were also recorded on days when wind speed was low, but the amounts were generally not as high as those given in this figure.

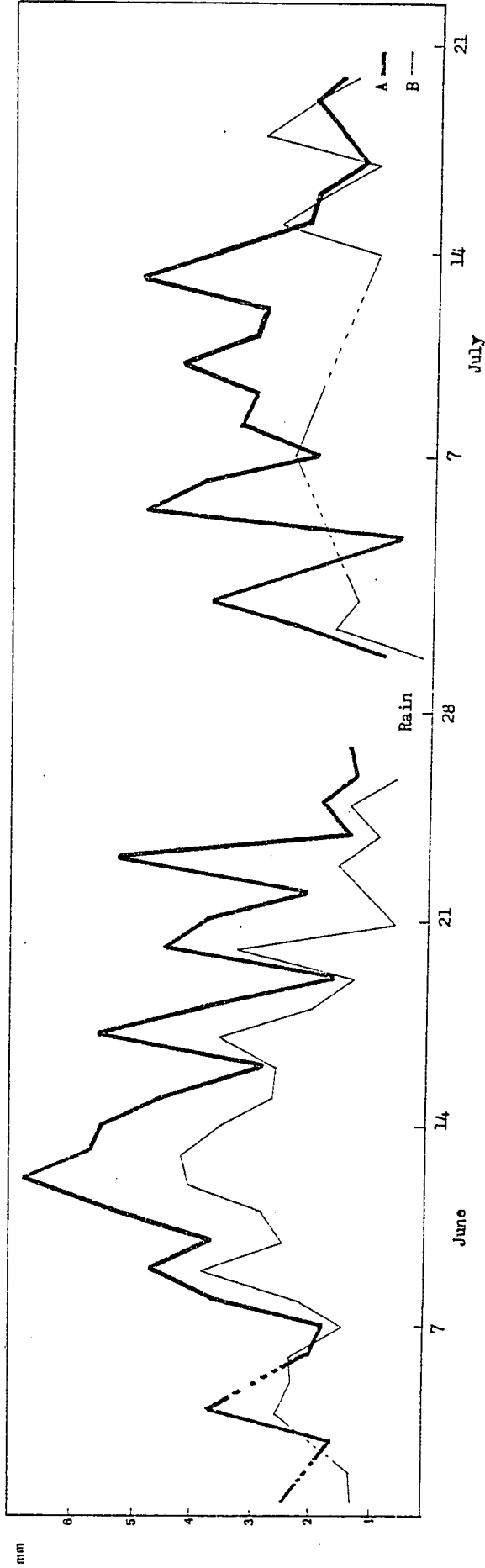


FIG. 16 TOTAL POTENTIAL DAILY EVAPORATION

DAYS OF HIGH WIND SPEED AND CORRESPONDING
AMOUNTS OF EVAPORATION

Date	Wind Speed (m/sec)		Evaporation (mm)	
	<u>A</u>	<u>B</u>	<u>A</u>	<u>B</u>
June 9	4.2	3.1	4.6	3.8
17	5.6	2.5	5.5	3.5
23	4.7	2.8	5.2	1.6
July 13	4.2	3.1	4.9	3.9

* Mean daily evaporation A = 3.0, B = 1.9 mm

FIG. 17

Precipitation

The amount of precipitation received on any one day varied between stations, (FIG. 18), but total for the study period showed A was higher (see figure below). A exceeded B for 52 percent of the time that precipitation occurred; while B exceeded A for 28 percent of the time; and both received equal amounts 20 percent of the total time.

TOTAL PRECIPITATION JUNE 1 TO JULY 26

	A	B
June	48.0 mm	48.0 mm
July	18.0 mm	11.0 mm
Total	66.0 mm	59.0 mm

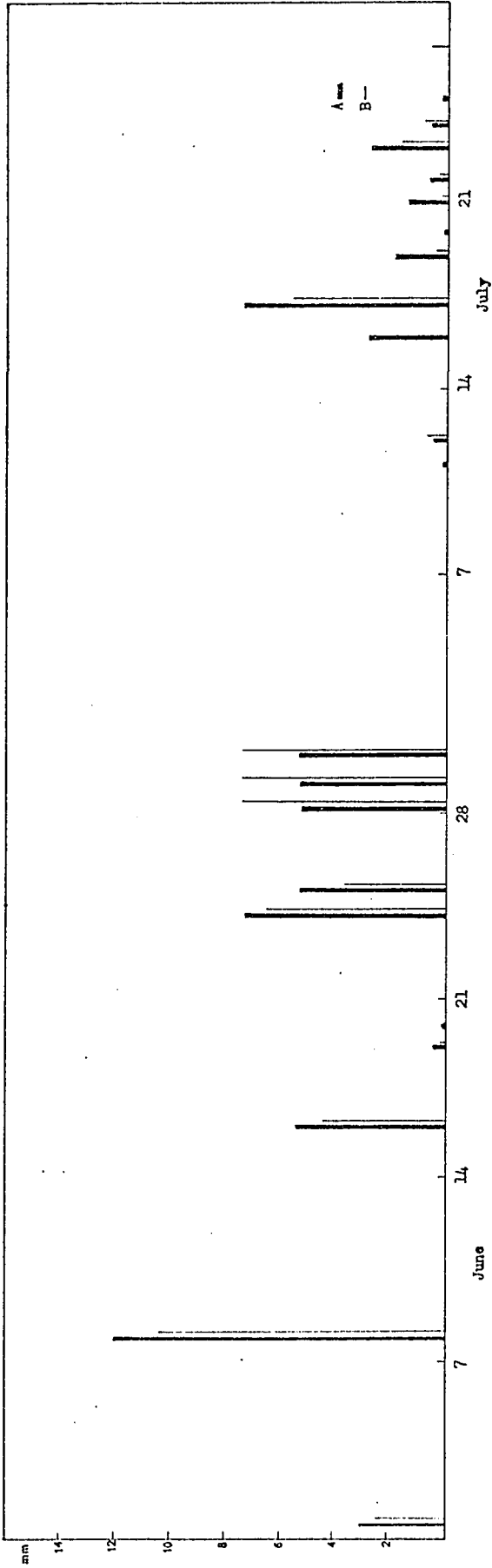


FIG. 18 TOTAL DAILY PRECIPITATION

4.2 Soil Temperatures

Climatic inputs operating on or near the surface of the moraine cause an energy exchange at the air-ground boundary resulting in heat input to the ground, which subsequently is transmitted through the material.

An analysis of the soil temperatures at A and B stations over the study period show that generally B had higher temperatures at each depth. A similar relationship was shown to exist for the number of days when one station exceeded the other at each depth. Mean daily temperatures, mean daily maximum and minimum temperatures, and the number of days one station exceeded the other for the entire study period are shown in Fig. 19 through Fig. 23. The greatest range of temperatures existed between the maximum and minimum daily temperatures at A station, in which maximum temperatures were similar to those at B but minimum temperatures were well below those at B. These lower minimum temperatures resulted in A having lower mean daily temperatures over the study period.

Variations in the time when maximum and minimum temperatures occurred at each depth were recorded both at and between stations; but over the study period, A generally recorded these values several hours before B.

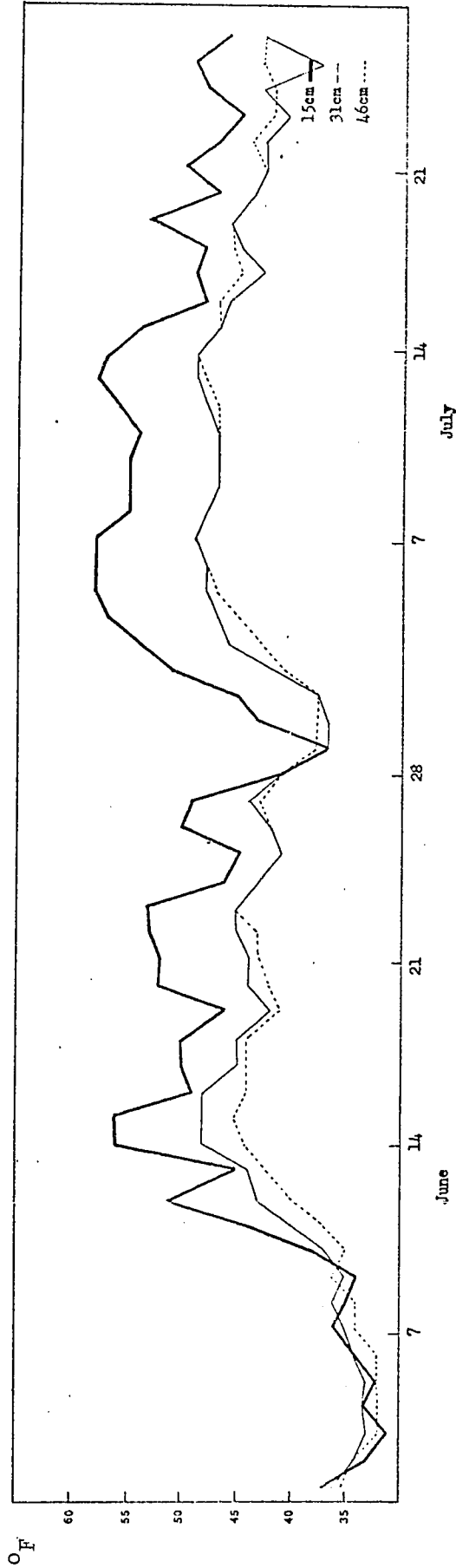


FIG. 19 MEAN DAILY SOIL TEMPERATURE AT A STATION

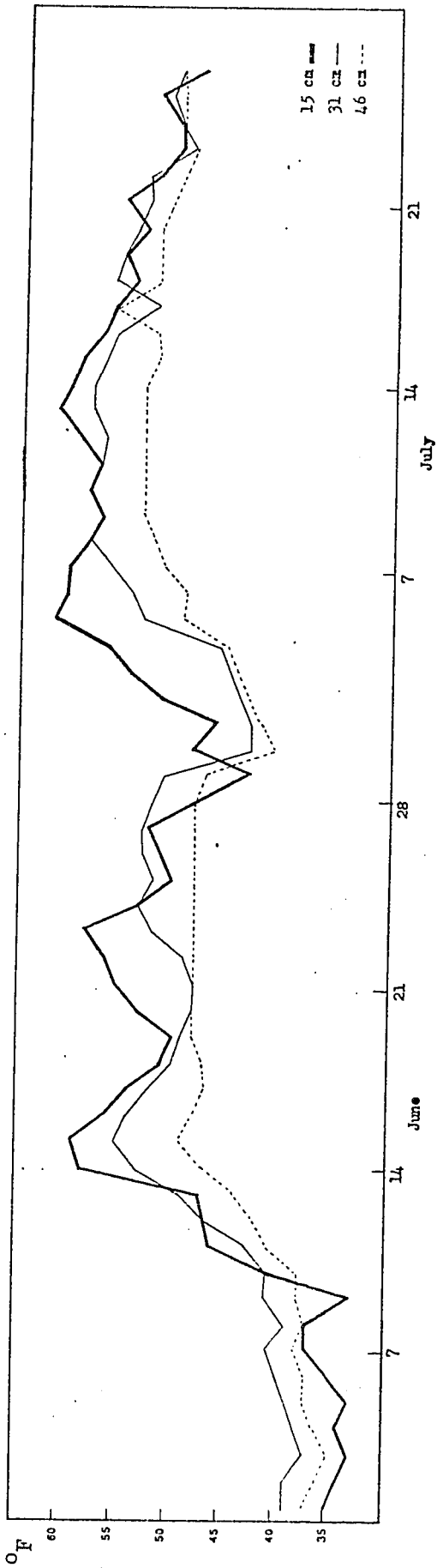


FIG. 20 MEAN DAILY SOIL TEMPERATURES AT B STATION

MEAN DAILY SOIL TEMPERATURE FOR STUDY PERIOD

	A	B
Depth		
15	9.4	11.1
31	6.1	10.6
46	6.1	8.3

* Depth in centimeters

** Temperatures in Centigrade

FIG. 21

MEAN DAILY MAXIMUM SOIL TEMPERATURE

	A	B
Depth Surface	33.9	37.8
15	12.8	12.8
31	7.8	10.6
46	6.1	8.3

MEAN DAILY MINIMUM SOIL TEMPERATURE

	A	B
Depth Surface	-	-
15	5.6	8.9
30	5.0	10.0
46	5.6	7.8

* Depth in centimeters

** Temperatures in Centigrade

FIG. 22

PERCENT OF TOTAL TIME ONE STATION EXCEEDS THE OTHER AT
EACH DEPTH (BASED ON MAXIMUM AND MINIMUM DAILY VALUES)

Maximum Temperatures

15 cm: A exceeds B, 56 percent of the time
31 cm: B exceeds A, 96 percent of the time
46 cm: B exceeds A, 98 percent of the time

Minimum Temperatures

15 cm: B was warmer than A, 98 percent of the time
31 cm: B was warmer than A, 100 percent of the time
46 cm: B was warmer than A, 100 percent of the time

FIG. 23

4.3 Glacial Surge Input

Evidence that ice core exposure may result from the pushing and eroding action of a glacier advance into an ice cored feature is poorly reported. Johnson (1971) observed that the Donjek Glacier surge, which commenced in 1969, resulted in the push of the active ice into the moraine. This in turn caused shearing of the stagnant glacier ice core towards the surface, and in certain cases resulted in this ice being exposed. Bayrock (1967) observed this same phenomena during the Steele Glacier surge in 1966. Similar action may have exposed sections of the underlying ice core on the western side of the end moraine on its proximal side.

Glacial surges have been hypothesized for the Donjek Glacier during and after formation of the Neoglacial moraine, some 300 years B.P. (Denton and Stuiver 1966). More recent surges, 1935, 1956-61, and 1969 have been reported by Denton and Stuiver (1966), Meier and Post (1969), Johnson (1971); and are well documented in a series of air photographs by W. A. Wood. It is conceivable that during the surge which occurred in 1969, in which the glacier advanced .8 km, that the glacier pushed into the side of the end moraine, up valley from B station, eroded the overlying material and exposed the ice beneath. Aerial photographs,

taken by W. A. Wood during this time, show the glacier in contact with this portion of the moraine. As a result of this glacial action, two very large exposures have occurred.

4.4 Summary

An analysis of glacial surge and micro climatic inputs on the moraine shows that there is a variation in the intensity of these inputs at the two sites. Recent glacial surges have been shown to have affected predominantly the western portion of the moraine near B station, resulting in removal of a portion of the overlying debris exposing the ice core beneath.

Higher average ambient air temperatures occurred at A as a result of higher minimum temperatures together with higher rainfall, evaporation, and wind values; while B had slightly higher quantities of relative humidity. Both stations had similar amounts of radiation input over the study period.

As was expected, a strong resemblance occurred between the shape of the curves on the graphs showing mean daily air and soil temperatures, with the exception of the lag time between the periods when air temperatures recorded their highest or lowest values and when soil temperatures recorded their corresponding high and low values. Soil temperatures at B were higher than those at A at all monitored depths throughout most of the study period. The influence that these various climatic parameters and soil temperatures have had on the distribution and initiation of various degradational processes will be discussed in Chapter 6.

5. DEPTH OF FREEZE-THAW OCCURRING ON THE
MORaine AND ICE CORE ABLATION

5.1 Introduction

Chapter 6 gives a detailed account of additional degradational processes which were investigated in this study and it shows that the processes were either directly or indirectly influenced by ablation of the buried ice. Ablation of debris covered ice depends upon the temperature gradient through the ground. It is the purpose of this chapter to determine the depth to which heat (energy) is being transmitted through the debris and to determine the amount of ablation that could be expected to occur within that depth. The amount of ablation of the ice which could result from geothermal heat flow at this latitude will be determined together with the amount of ablation which results when the overburden has been removed by glacial surge action exposing the ice beneath. Finally calculation of the minimum length of time which would be required to completely melt out the ice core under 'ideal' conditions was attempted. These results are used to help explain both the initiation and distribution of

certain degradational processes around the end moraine in conjunction with the climatic and glacial surge inputs previously discussed (Chapter 4).

Another factor upon which the transfer of heat through the soil depends is the lithology of the soil. In an attempt to determine any variation in the type of material of which the moraine consists, grain size analyses were performed on samples taken on traverses across the moraine, as well as where prominent features such as fossil or active forms of mass movements, prominent ridges, cracking, and other distinct changes in slope occurred.

5.2 Grain Size Analysis

Methodology

Mechanical analyses of the samples was performed by the use of sieves at 1/2 phi intervals, and a ro-tap shaker. Weights were measured to the nearest one tenth of a gram. The samples were divided into a coarse fraction -1.0 phi and lower, a sand fraction between -1.0 phi and 4.0 phi, and a fine fraction 4.0 phi and greater (Folk 1968).

Statistical parameters such as mean grain size, sorting, skewness, and kurtosis were derived from the mechanical analysis and cumulative curves were plotted on arithmetic probability paper for the size fraction -1.0 phi to 4.0 phi. No analysis was performed on the coarser or finer fraction as the main purpose of this study was to determine any broad changes in the soil type around the moraine. A detailed analysis of this work is presented in the appendix while a brief summary of the results follows.

Results of Analysis

No discernible trends or patterns were found between individual traverses which were sampled. However broader divisions of the moraine, (see Chapter 3), showed that the western section (lee area) of the moraine contained the highest percentage of fines, was the least well sorted and was skewed towards the finer size range; and was apparently effected by a more erratically fluctuating medium of transport than elsewhere on the moraine. The eastern section, by contrast, contained the

highest percentage of coarse material, was best sorted and skewed towards the coarser fraction; and was affected predominantly by a less variable medium of transport. The northern section of the moraine appeared as a transition zone between the other two in that all statistical values fell between them.

The broad variations which were found to exist between profiles attests to the complexity of the character of the material; and this coupled with the occurrence of old fluvial and lake deposits, mudflows, kames and kettles, shows the variety of environments of deposition which occurred on the moraine and the resultant reworking that the material has been subjected to. No significant variations between A and B stations at depth were found from this analysis, but variations with depth did occur within each site. Much of the statistical data found in this study on grain size conforms to that which Landim and Frakes (1968) used in their description of till, i.e. till samples show the poorest sorting, near symmetrical skewness around zero, have small mean size values, and are mesokurtic.

5.3 General Conditions And Assumptions For Calculation Of Freeze-Thaw Depths

In order to understand the amount of ablation which may occur in an area underlain by buried ice and the resulting reshaping of the topography, the effect of climate on the temperature distributions within the soil must be investigated. The most commonly used equations in calculating this relationship are those employing the mean monthly or annual air temperatures. This climatic parameter, when measured in a given location, depends upon the degree of reaction between the climatic factors and the resulting energy exchange occurring at the ground-atmosphere boundary. According to Williams and Nickling (1971), "At any given time and place, air temperatures are affected by the vagaries of weather and specific surface conditions, but are nevertheless usefully represented by mean values, which in turn can with some approximation be represented by a sinusoidal wave".

Mean annual air temperatures for the study site are not available so values were used from the nearest

government operated weather station, Burwash Landing, located some 48 km downvalley (FIG. 24). Although values for the winter months are not available, data for the summer months on the moraine showed greater mean daily air temperatures there than at Burwash Landing. Thus the depth of thaw may be underestimated on the moraine. An approximate sine wave was drawn for the mean monthly air temperatures 1972 (FIG. 25). It must be remembered, however, that the instruments at the moraine stations were not at standard meteorological height.

A general discussion of heat flow through the ground showing both its dependence on certain soil parameters as well as the more commonly used variables employed in heat transfer equations, has been presented in the appendix. The following gives the results of these general considerations as applied in the field.

5.3.1 Depth of Penetration of a Periodic Wave

According to Williams and Nickling (1971), the depth to which a periodic variation (sine wave), extends may be defined by the equation

$$Z_i = 2 \sqrt{\pi a T}$$

where Z_i = depth at which the delay is a whole period

T = period of wave

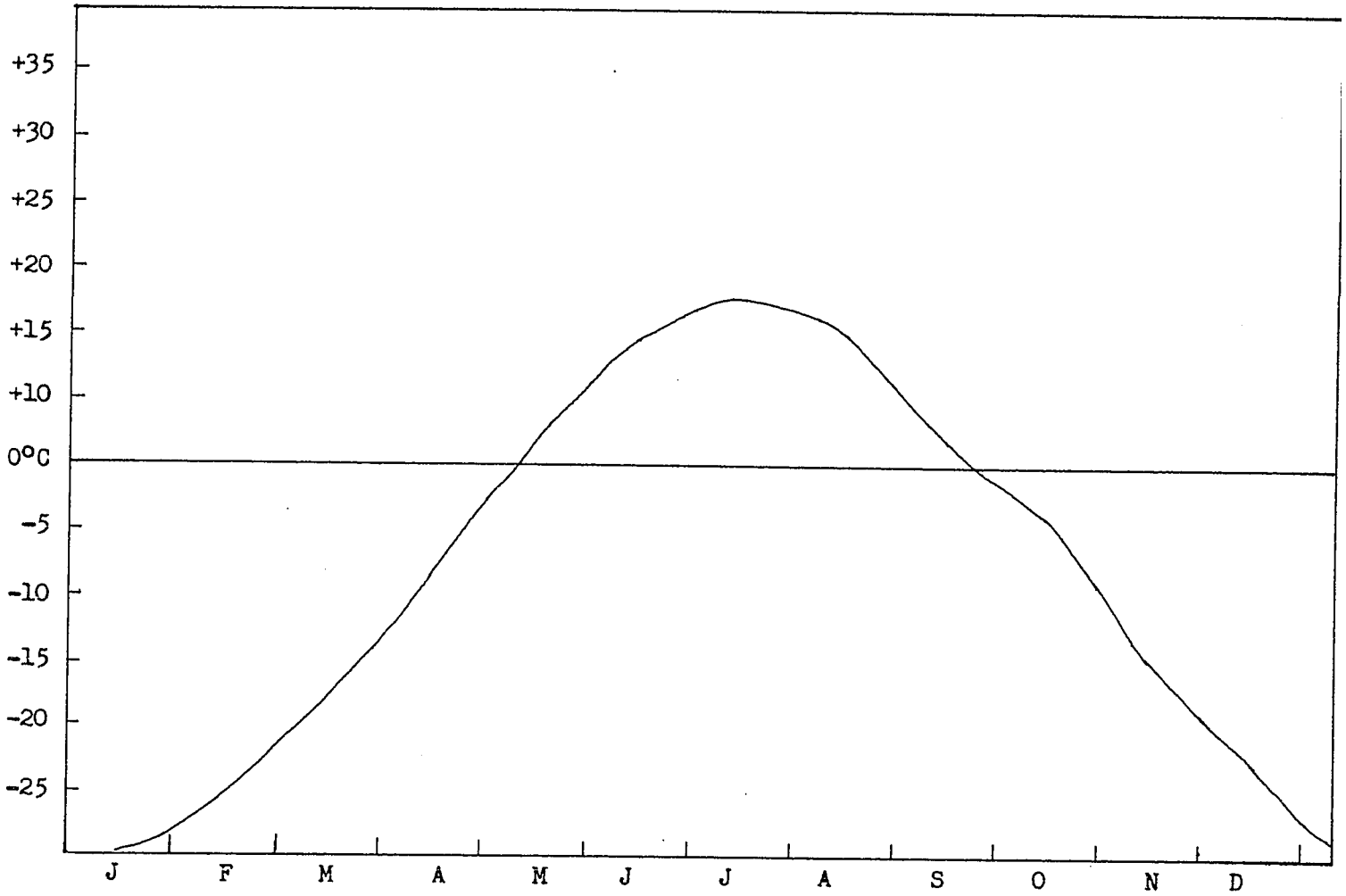


FIG. 24 MEAN MONTHLY AIR TEMPERATURES 1972 BURWASH LANDING

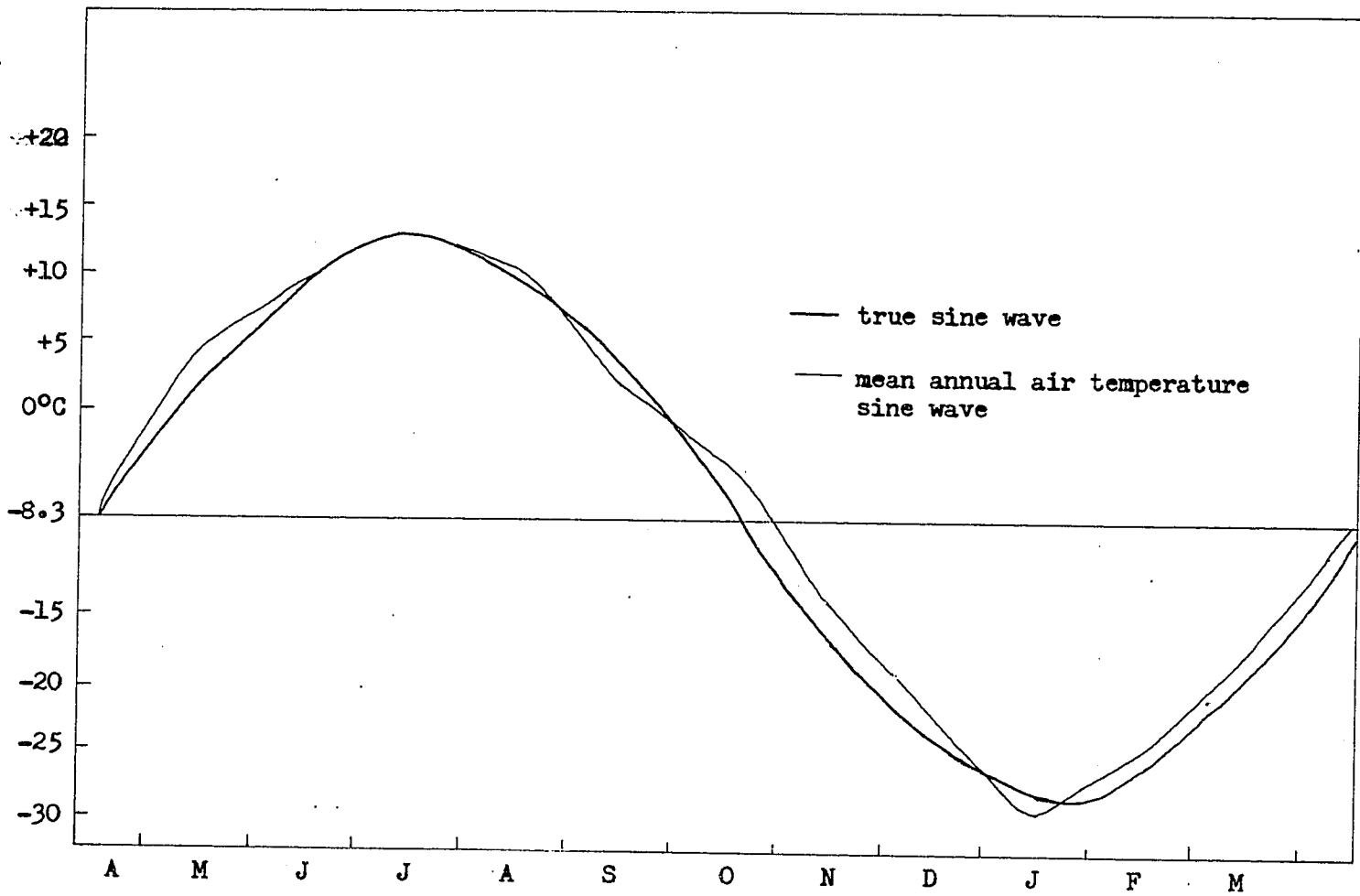


FIG. 25 MEAN AIR TEMPERATURES BURWASH LANDING

$$a = \text{diffusivity} = \frac{\text{thermal conductivity}}{\text{columnetric heat capacity}}$$

$$\sqrt{\lambda} = 3.14 \text{ radius}$$

On a daily basis (when T = 24 hours) this depth on the moraine was

$$Z_i = 2 \sqrt{3.14 \times .014 \times 86,400}$$

$$Z_i = 122 \text{ cm or 1.2 meters}$$

On an annual basis

$$Z_i = 2 \sqrt{3.14 \times .014 \times 31,536,000}$$

$$Z_i = 2354 \text{ cm or 23.5 meters}$$

These values represent an ideal thermal regime i.e. heat transfer by conduction only, no change in soil moisture content over the period, homogeneous soil conditions, no snow cover, no change of state i.e. water-ice, frozen ground, etc.

Thus on the Donjek end moraine, calculations of quantities of heat flux through the moraine material, using the properties of a sinusoidal wave, show a minimum depth of 1.2 meters on a daily basis and 23.5 meters on an annual basis. A more realistic approach in

studying heat transfer through a soil which is located in a zone of discontinuous permafrost and which at least in part, is known to be underlain by an ice core, would be to determine the depth to which the soil freezes and thaws during the year. By calculating the depth of thaw in the soil, one can determine the critical depth of overlying material required to protect the ice core from possible melting.

Two methods of determining the depth of soil freezing and thawing have been employed here:

- 1) the simplified Stefan method (1943), and
- 2) the modified Berggren method (1956). A third method, taken from Terzaghi (1952), was used only in calculating the depth of thaw in the soil.

5.3.2 Depth of Freeze

(1) Simplified Stefan Method:

This method of determining the depth of frost penetration or soil freezing makes certain initial assumptions:

- a. The soil is homogeneous

- b. The volumetric latent heat of fusion, L , is the only heat that must be removed when the soil freezes (i.e. the volumetric heat of unfrozen and frozen soil are neglected).
- c. The temperature gradient in the frozen material is linear.
- d. The pore water is not moving.

The idealized conditions assumed for this formulae are shown in FIG. 26. This diagram assumes that the continuity equation for diffusion is satisfied, i.e.

$$\frac{ad^2T}{dz^2} = \frac{dT}{dt}$$

in which $a = \frac{\lambda}{c} =$ diffusivity

$T =$ soil temperature

$Z =$ depth of soil

$t =$ time

This implies that the latent heat supplied by the pore water as it freezes to a depth Z in time t equals the rate at which the heat is conducted to the ground surface.

The freezing period (in months) for Burwash Landing meteorological station is shown in FIG. 27, and the Stefan formulae and depth of freezing is given below.

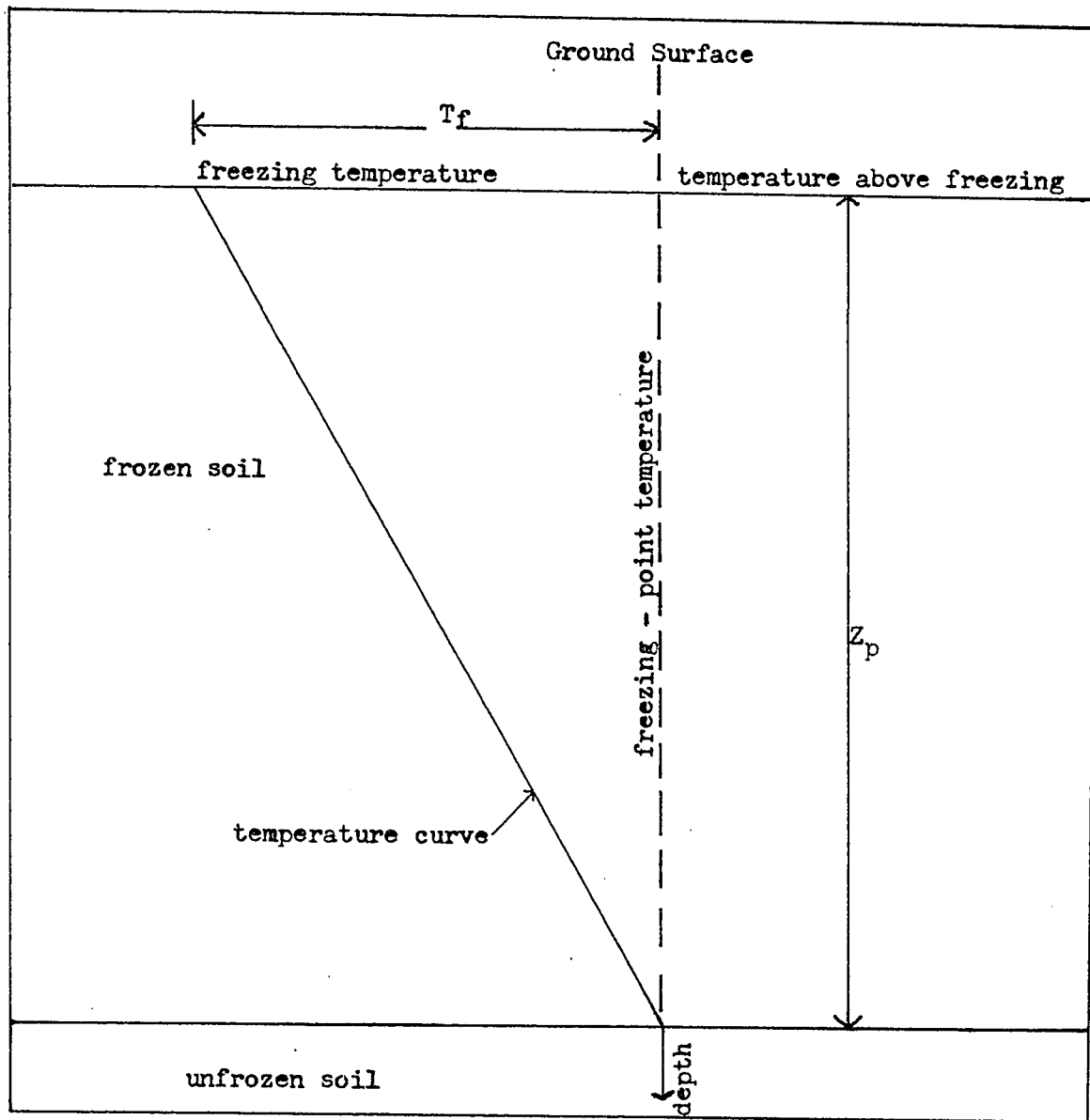


FIG.26 SIMPLIFIED STEFAN MODEL (from Tuma & Abdel-Hady, 1973, p.293)

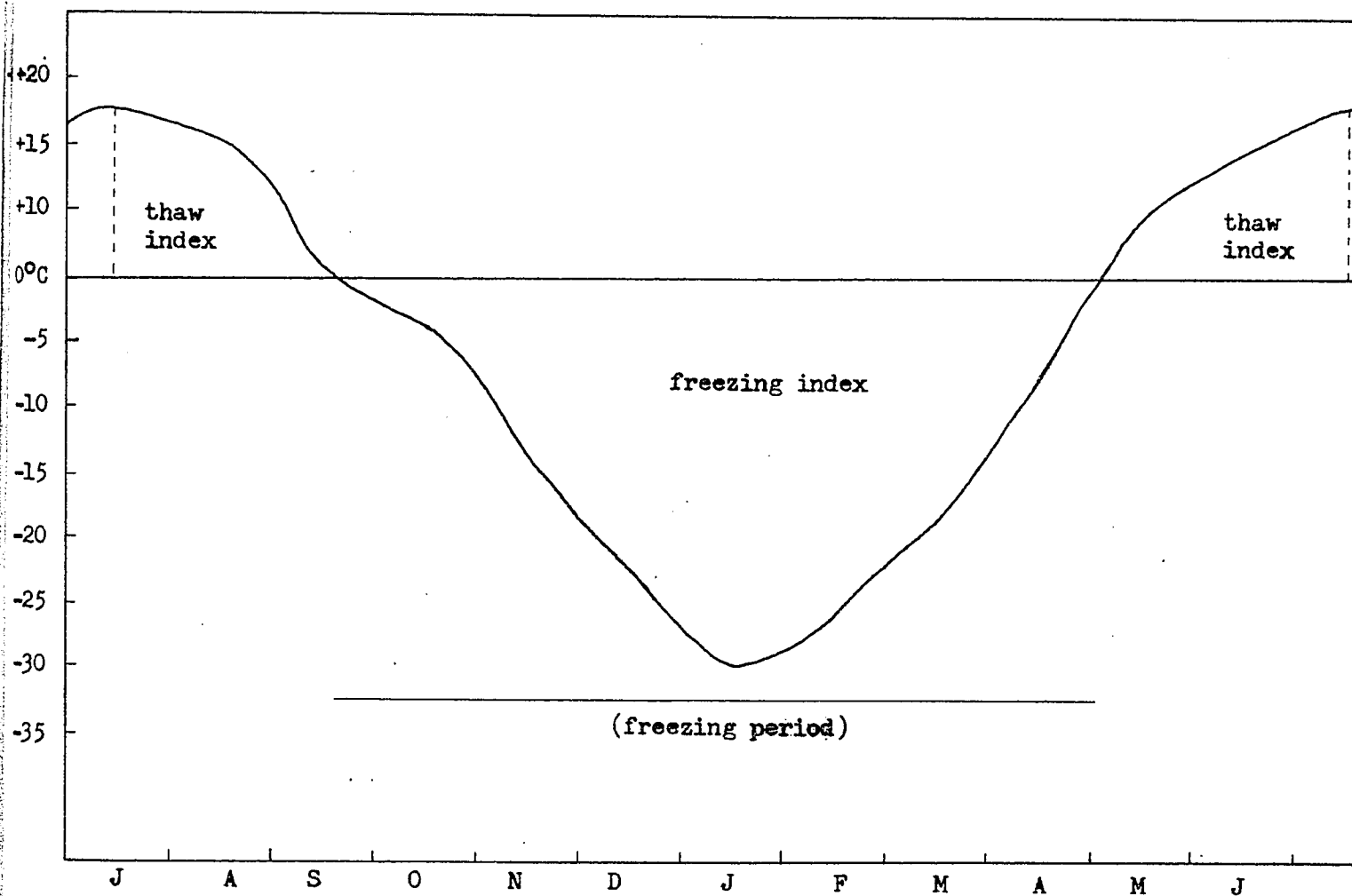


FIG. 27 ANNUAL VARIATION IN AIR TEMPERATURE 1972, BURWASH LANDING

$$Z_p = \sqrt{\frac{48K_f F}{L}}$$

where

- Z_p = frost-penetration depth (feet)
- F = freezing index-chart (degree days)
- K_f = heat conductivity of frozen soil
(1) BTU/inch/sec/°F
- L = latent heat of fusion (2) (BTU/ft³)

(1) From charts of thermal conductivity
H.P. Aldrich 1956

(2) $L = (1,434 \quad)wy_d \text{ BTU/ft}^3$

Tuma & Abdel-Hady p290

$d =$ dry density (BTU/ft³)

$w =$ % water content

$$Z_p = \sqrt{\frac{48 \times 2.8 \times 6721}{2269}}$$

$$Z_p = \underline{20 \text{ ft or } (6.1 \text{ meters})}$$

The frost penetration depth on the Neoglacial moraine may be expected to approximate 6.1 meters.

This value represents a maximum depth of frost penetration. The moisture content of the soil here is at

a maximum. Also the freezing degree index may be slightly underestimated as the values were worked out in months instead of days.

(2) Modified Berggren Method:

The solution to this method is also based on the diffusion equation, as given for the Stefan method, as well as on a number of other conditions (FIG. 28). It is assumed that the soil is homogeneous but that the temperature gradient throughout the soil (in both frozen and unfrozen states) varies in a non-linear fashion. Also soil thermal properties such as thermal diffusivity and thermal conductivity of both frozen and unfrozen soil, and the volumetric heat capacity of the frozen soil and the latent heat of fusion are employed in this equation.

$$Z_P = \lambda \sqrt{\frac{48K_f F}{L}}$$

in which K_f = thermal conductivity of frozen soil

F = freezing degree index

λ = dimensions correction factor always less than unity. *

L = latent heat of fusion

* The correction factor depends on the thermal

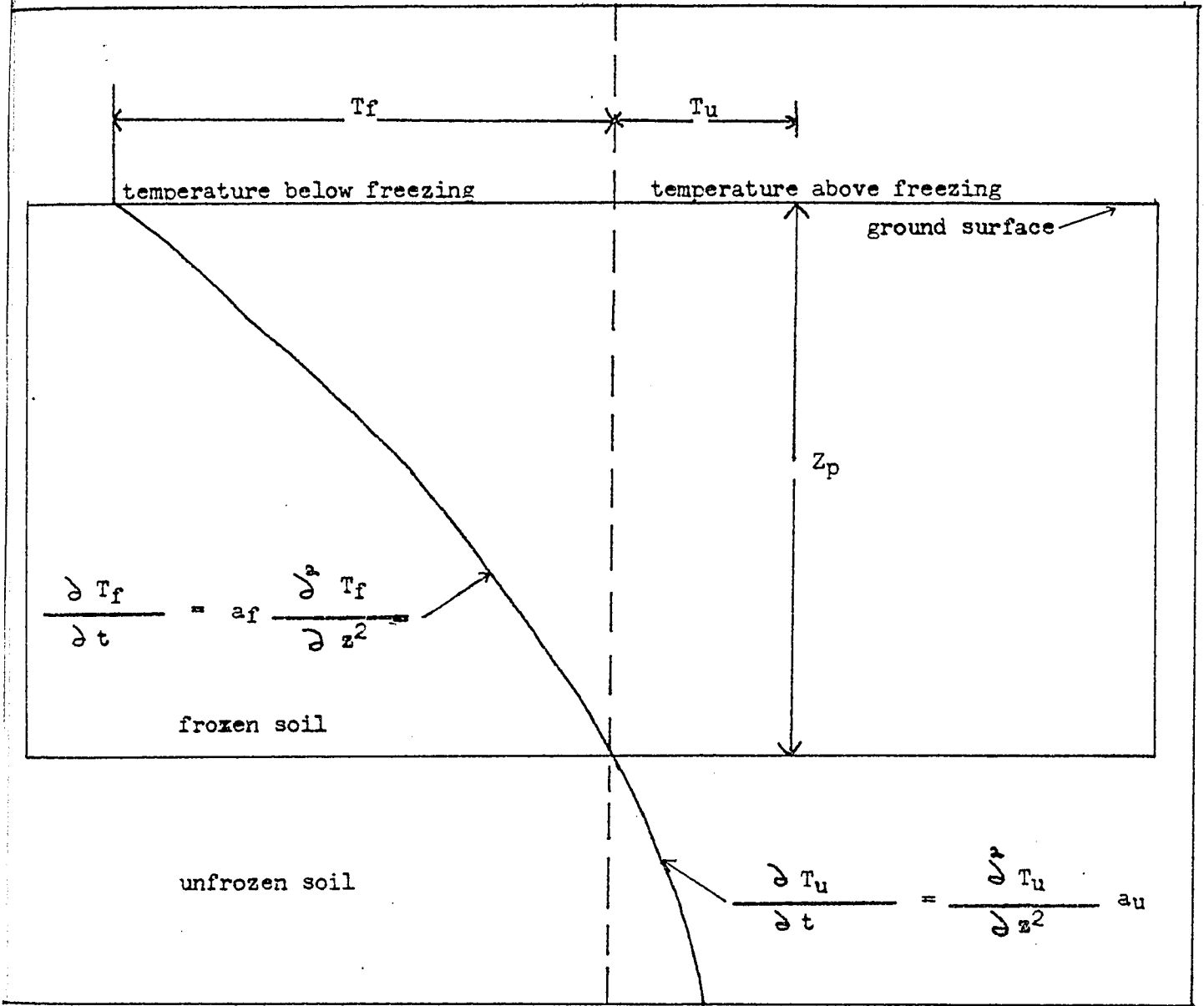


FIG.28 MODIFIED BERGGREN MODEL (from Tuma & Abdel-Hady, 1973,p.294)

properties of the frozen and unfrozen soils and is a function of two parameters, the thermal ratio and the fusion parameter. It is derived in the following manner,

$$\alpha = \frac{T_u}{T_f} = \frac{T_u t}{F} \quad \text{where } \alpha = \text{thermal ratio}$$

as an approximation T_f may be taken to equal $\frac{F}{t}$

(Yong & Warkentin 1966)

where T_u = mean temperature of unfrozen soil
 T_f = mean temperature of the frozen soil
 F = freezing degree index
 t = freezing period

Both T_u and T_f are absolute values and may also be measured in terms of temperature difference from the freezing temperature 32°F (0°C).

$$\text{e.g. } T_u - 32 = x$$

$$32 - T_f = y$$

The fusion parameter u is derived as below :

$$u = \frac{C_f T_f}{L} \approx \frac{C_f F}{L t}$$

where C_f = heat capacity of frozen soil. Here a value was obtained from Scott (1964).

Employing Berggren's equation

$$Z_p = .92 \sqrt{\frac{48 \times 2.6 \times 6721}{2269}}$$

$$Z_p = 17.7 \text{ ft or } 5.4 \text{ meters}$$

Thus the depth to which frost penetration occurs is 5.4 meters. This value is somewhat smaller than that obtained by Stefan's formulae and this may be partly the result of employing more specific soil thermal parameters as mentioned above. Both of the above methods may closely approximate each other when the correction coefficient approaches unity.

This may occur when:

- 1) the soil under investigation has a high moisture content.
- 2) in areas where the mean annual surface temperature equals that of the freezing temperature of the soil-water system.

The above results give only an approximate freezing depth which may occur in the end moraine, as certain parameters such as the thermal conductivity and heat capacity were calculated from charts showing values for finer grain size soils than that for the moraine.

According to Tuma and Abdel-Hady (1973), the frost penetration in coarser soils (gravel-sand) will be greater than that for finer soils because of the generally greater thermal conductivity of coarser soils.

5.3.3 Depth of Thaw

(1) Simplified Stefan Method:

Stefan's formulae may also be used to calculate the depth of thaw which is occurring in the Donjek end moraine. The only parameters which are altered from those used in calculating frost penetration are the thermal conductivity which was recalculated for unfrozen soil and the freezing degree index which was recalculated and became the thaw degree index. Thus

$$Z_p = \sqrt{\frac{48Ku F}{L}}$$

where Ku = thermal conductivity of unfrozen soil

F = thaw degree index

L = latent heat of fusion = (1.434---) wyd

$$Z_p = \sqrt{\frac{48 \times 2.4 \times 2211}{2269}}$$

$$Z_p = 10.6 \text{ ft or } 3.2 \text{ meters}$$

The depth of thaw that one could expect by use of Stefan's formulae is 3.2 meters.

(2) Modified Berggren Method:

$$Z_p = \sqrt[3]{\frac{48Ku F}{L}}$$
$$Z_p = .96 \sqrt{\frac{48 \times 2.6 \times 2211}{2269}}$$
$$Z_p = 10.4 \text{ ft or } 3.1 \text{ meters}$$

Both Stefan and Berggren equations yield similar thaw depths of approximately 3.2 meters and this may stem from the fact that the soil under investigation was assumed to be at its field capacity.

(3) Terzaghi:

Another method of calculating the depth of thaw in areas subjected to a freeze-thaw cycle is that given by Terzaghi (1952), employing Washburn's equation in which the mean temperature of the thaw season is employed as approximating the mean surface temperature of the soil, as well as employing a soil porosity value.

$$Z = \sqrt{\frac{2t TKh}{72n + \frac{T}{2(0.53 + .47n)}}$$

where Z = depth of thaw (cm)

T = mean temperature of thaw season ($^{\circ}\text{C}$)

t = thaw period (Sec)

Kh = thermal conductivity ($\text{cal}/\text{cm}^{-1}\text{Sec}^{-1} \text{ }^{\circ}\text{C}^{-1}$)

* n = soil porosity $n = 1 - \frac{\lambda d}{Gs\lambda_o}$

where d = dry density of soil

Gs = specific gravity of solid

o = unit weight of distilled water at 4°C

* Tuma and Abdel-Hady 1973, P. 13

$$Z = \sqrt{\frac{2 \times 13132800 \times .009 \times 8.0}{72 \times .307 + \frac{8.0}{2(0.53 + 0.47 \times .307)}}$$

Z = 260 cm or 2.6 meters

According to Terzaghi, the depth of thaw in the morainic material is 2.6 meters, which is approximately 0.6 meters less than that given by both the Stefan and Berggren methods. A possible source of error in Terzaghi's equation could be the result of taking all the mean monthly air temperatures (thaw period) as being representative of the air-ground interface.

The above results are similar to those given by Boulton (1967), and Østrem (1965) for till, in which it was found that melting was occurring in an ice core which was covered by 2.8 meters and 2.5 meters of material respectively, at a similar latitude as the Donjek end moraine.

5.3.4 Summary

The depth to which one can expect a periodic heat fluctuation in the morainic material on a daily basis is 1.2 meters while on an annual basis it is 23.5 meters. These values were calculated on the basis that heat transfer through the soil at a given depth, as well as the mean monthly ambient air temperatures in the area, assume the form of a sinusoidal wave from which certain soil characteristics such as thermal conductivity, diffusivity, lag times, and general temperature fluctuations can be calculated. These values in turn can be used with mean annual air temperatures to give depth of freeze and thaw in a given soil type. However certain basic assumptions such as a homogeneous soil in which heat transfer occurs vertically only by conduction, no transfer of energy by pore water motion or by changes of state e.g. condensation,

must be made before one can use equations giving these depths. Further generalizations were made in this work in that the mean annual air temperature was not that of the study area but was from a government station located some distance downvalley. The effect of this was an underestimation of the depth of thaw as temperatures at the study area were warmer than those used. Bulk density values, thermal conductivity and volumetric heat capacity values were taken from charts for frozen soils which in general represented finer soils than those found on the moraine. As moisture conditions for the soil could be expected to vary considerably both over time and with depth, the value employed here represented a maximum value for this soil type and thus leads to high values for certain soil thermal parameters and higher depth results. However the results do show trends which may be expected to occur in the study area. Obviously these trends will vary as each soil thermal parameter or air temperature changes, and it is expected that any changes in the ablation process will be reflected in corresponding changes in the rates of degradational processes which themselves are caused primarily by ablation.

5.4 Ablation of Debris Covered Ice

5.4.1 Calculations

The amount of ablation that would occur on ice that was covered by a mantle of debris, equal in thickness to the depth of thaw, was calculated over the study period at both stations. The formulae used was that of McKenzie (1969) which assumes heat transfer in the soil is by conduction only and that the soil is both homogeneous and contains an equal amount of moisture throughout.

$$S = \lambda \frac{dT}{dZ}$$

where S = soil heat flux

λ = soil thermal conductivity

$\frac{dT}{dZ}$ = vertical temperature gradient existing at that level

where $\lambda = .009 \text{ cal (cm/sec/}^{\circ}\text{C)}$

$$\frac{dT}{dZ} = \frac{6.1^{\circ}\text{C}}{272 \text{ cm}} = .022 \text{ deg/cm}$$

The vertical temperature gradient, which existed from the deepest measured soil temperature (46 cm) down to the ice-till interface at 3.1 meters, was determined for both stations for this period. Thus at B station

$$S = .009 \times .022$$

$$S = .0002 \text{ cal/cm}^2/\text{sec}$$

$$S = \underline{1071.4 \text{ cal/cm}^2/2 \text{ months}}$$

According to McKenzie (1969), 0.90 grams of ice occupy 1 cm³ and the latent heat of fusion is 80 cal/gm. Therefore the ice surface at B would be lowered approximately 14.9 cm over the study period.

Similarly at A station

$$S = \lambda \frac{dT}{dZ}$$

$$\text{where } \lambda = .009 \text{ cal/cm/sec/}^\circ\text{C}$$

$$\frac{dT}{dZ} = .015 \text{ }^\circ\text{C/cm}$$

$$S = .009 \times .015$$

$$S = .00014 \text{ cal/cm}^2/\text{sec}$$

$$S = \underline{750 \text{ cal/cm}^2/2 \text{ months}}$$

This quantity of heat is sufficient to lower the surface of the ice at A by 10.4 cm over the study period.

The difference in the amount of ablation at the two stations is primarily the result of their differing temperature gradients which in turn may be partly explained

through the difference in micro climate (Chapter 4), as soil characteristics - both mechanical and thermal parameters - were the same at both stations. The relationship between micro climatic parameters and degradational processes is dealt with in detail in Chapter 6.

5.4.2 Summary

The amount of melting that would occur at the two stations over the study period was determined through heat transfer by conduction only, assuming a homogeneous soil, equal distribution of soil moisture, and that the average amount of heat transfer to the surface of the stagnant ice block during June and July was 1071 cal/cm^2 at B and 750 cal/cm^2 at A. This difference may partly be explained by the varying micro climatic parameters at each station as soil characteristics were found to be similar.

Exposures of the ice core on the moraine revealed that the depth of the overlying till was in places equal to or less than the thaw depth of approximately 3.2 meters, and that depending on the location of these areas one could expect a minimum lowering of the moraine between 10.4 and 14.9 cm for the study period in 1972. Differential ablation on the moraine may partly be explained through both

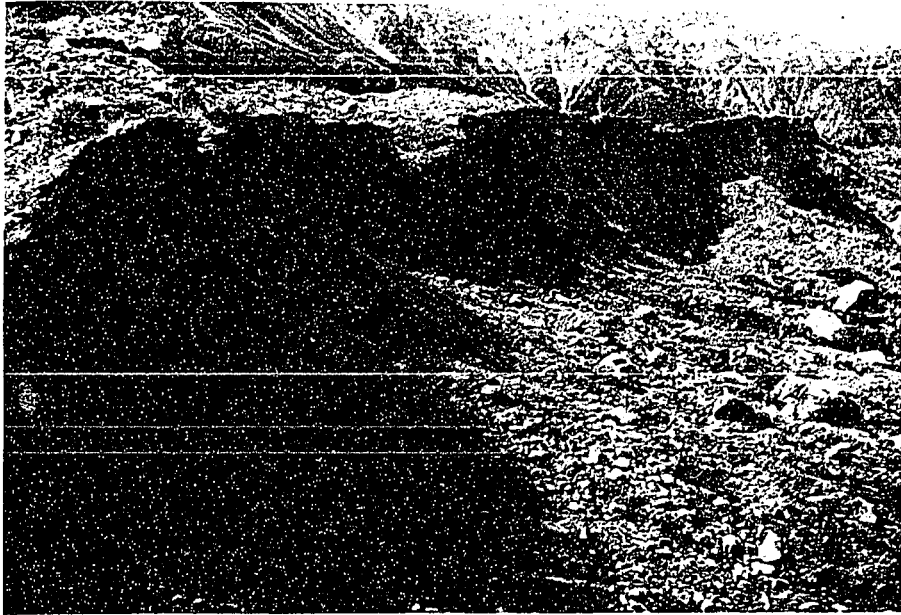


Plate 5.1 View of headwall of exposure 11 showing exposed ice core and overlying till with slumped material at base.

variations in the vertical temperature gradients and variations in the depth of the overlying debris around the moraine.

5.5 Ablation of Exposed Ice

5.5.1 Direct and Diffuse Radiation

Two ice faces located on the proximal side of the western portion of the moraine, remained exposed to direct solar radiation effects throughout the field season. Although the exposures face east at an angle of up to 60 degrees from the horizontal, radiation values were recorded for a horizontal surface only. A table given by Scott (1964) for average amounts of total direct daily solar radiation at latitude 60°N , on a vertical surface facing an easterly direction during the month of June, showed that these values were far less than those on a horizontal surface. However his value obtained for an east facing slope was larger than the individual averages recorded at the two moraine stations for direct radiation on horizontal surfaces for June. The difference may be explained by the effect of the surrounding mountains which act as barriers to the reception of the sun's energy in early morning and the earlier part of the evening (Chapter 4), thus cutting down on the total amount of solar radiation which may be

received. As a result, radiation values recorded at B station were used in calculating melt on the ice exposures even though they are an overestimate of the amount which would be received on an east face on the moraine.

The average amount of short wave solar radiation, received at B for the month of June was 306 cal/cm^2 per day, while the latent heat of fusion is 80 cal/gm . Thus 306 cal/cm^2 would melt approximately 3.8 gms of ice. According to McKenzie (1969), 0.90 gms of ice would be equivalent to 1 cm^3 by volume. Then 3.8 gms of ice would be equivalent to 4.2 cm^3 by volume. Thus, the average rate of ablation on the two exposures would be 4.2 cm per day or approximately 126 cm for the month of June and 263 cm for the total study time. This daily value is similar to that found by Østrem (1959) and Loomis (1970) (Fig. 29) for uncovered ice on which ablation was occurring at 5.4 cm/day and 4.5 cm/day respectively in areas of similar latitude. These values will be compared to rates of headwall retreat presented in Chapter 6. The amount of melt may be overestimated for the study period on the basis of the above calculation, but it may be underestimated by the fact that long wave radiation could not be measured. It does give, therefore, some indication as to the amount of melt which would occur as a result of direct ice exposure to both

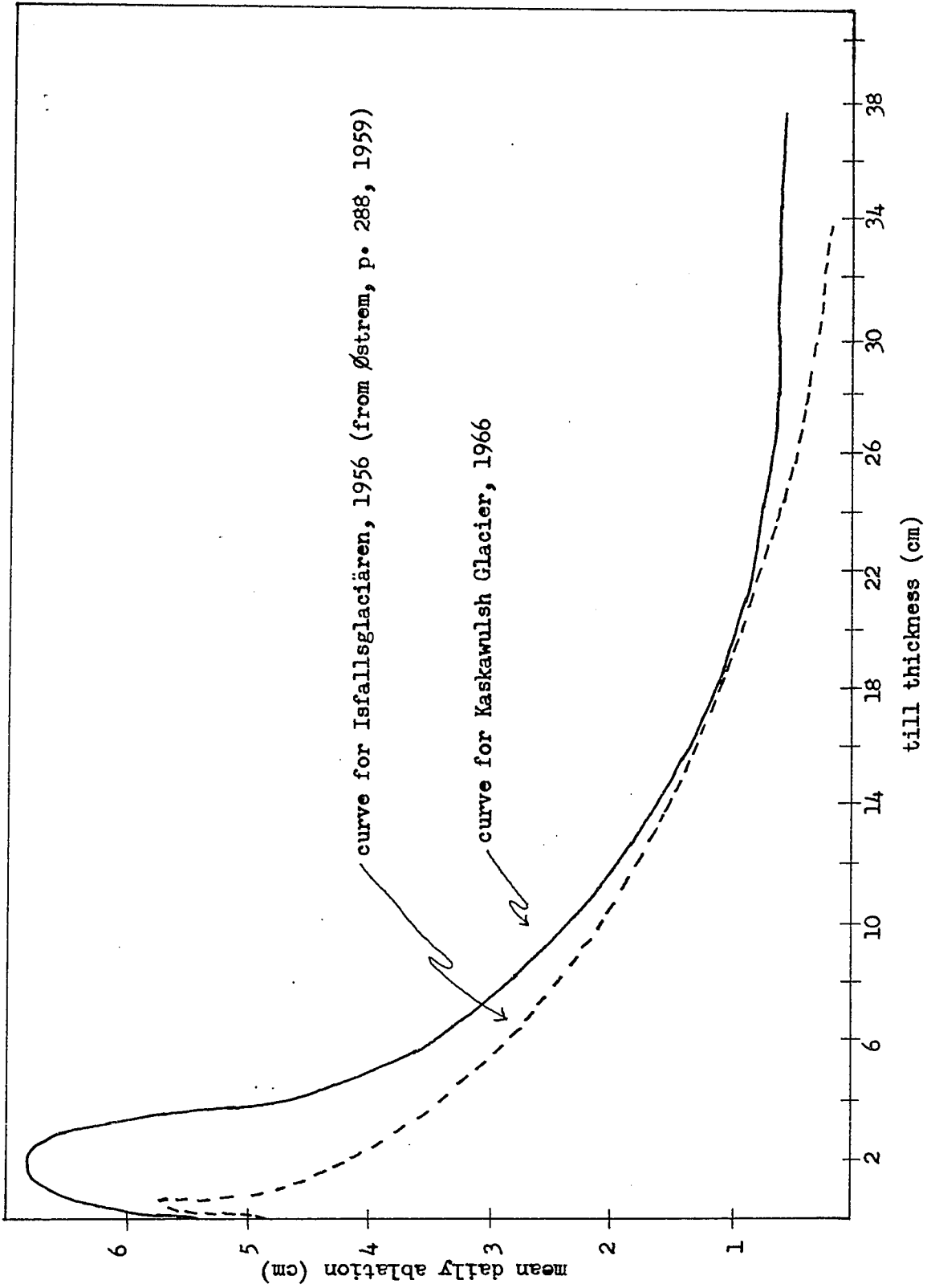


FIG. 29 RELATION OF MEAN DAILY ABLATION TO TILL COVER THICKNESS ON ISFALLSGLACIÄREN (1956) AND KASKAWULSH GLACIER (1966).

direct and diffuse radiation.

5.5.2 Evaporation on Exposed Ice Faces

The amount of ablation due to evaporation from the ice faces has been calculated by use of Kuzmin's formulae for snow evaporation, which, according to Bruce and Clark (1969), is capable of producing reasonable estimates as the surface area is small and thus may be subjected to a mass transfer formulae. According to Kuzmin;

E = evaporation from ice (mm/day)

U_{10} = average daily wind speed at height
10 m (m/sec)

e_2 = vapour pressure at 2 m (m/s)

e_0 = saturated vapour pressure at snow surface
temperature (m/s)

$$E = (0.18 + 0.098 U_{10}) (e_0 - e_2)$$

As the major ice exposures occurred on the west side of the valley, and south of B station, wind values of B station were employed. These values were obtained from 1 meter above the ground. Vapour pressure e_2 was taken from the closest government monitored station in the area - Burwash Landing. Although this value may not give a true representation of that found in the valley (see ambient air temperature comparisons), it may serve as an indicator in

showing the approximate importance of this process in degrading ice exposures.

During the month of June the amount of evaporation taking place was approximately,

$$E = (0.18 + 0.098 \times 2.25 \text{ m/sec}) (6.11 - 6.72)$$

$$E = .015 \text{ mm/day}$$

During the month of July,

$$E = (0.18 + 0.098 \times 1.55 \text{ m/sec}) (3.86)$$

$$E = 1.66 \text{ mm/day}$$

Total amounts for the months of June and July,

June total 0.450 mm

July total 51.460 mm

Total 51.910 mm

The effect of wind speed in promoting evaporation is overshadowed by the importance of the vapour pressure gradient existing between the evaporating body and the overlying air. That the total amount of ablation due to evaporation is small when compared to that by melting may be the result of the large quantity of heat required to cause a solid mass (ice) to sublime (675-680 cal/gm) as compared to the heat of fusion (80 cal/gm).

There are certain potential errors in this estimate caused by substitution of parameters in parts of the equation which either have not been measured at the study site or have not been measured exactly as asked for in the equation, i.e. vapour pressure at 2 meters, and wind speed height. Also the unusually high vapour pressure reported by Burwash Landing is a rather doubtful value. However the results are thought to allow a reasonable estimation of trends which are occurring on the moraine.

5.6 Ablation of Ice Core as a Result of Terrestrial Heat Flow

Another source of heat which may be transferred to a buried ice mass is from terrestrial heat flow. Lee and MacDonald (1963) have produced tables giving average amounts of this type of heat transfer that can be expected in various parts of North America, and in the Yukon this is estimated at 6.49×10^{-6} J/cm²/sec. This would be sufficient to melt approximately 0.61 cm of ice per year assuming the area is not underlain by continuous permafrost.

5.7 Summary

This discussion of a procedure to determine the

amount of ablation that occurs on debris covered stagnant ice, as a result of the interaction between climatic and soil thermal parameters as well as that from terrestrial heat flow, shows that the potential amount of subsidence on the moraine as a result of ice melting under a layer of debris over the study period, was 10.0 cm at A station and 15.0 cm at B, and the total amount per year was 55.0 cm and 77.5 cm respectively. However many broad assumptions had to be made before these equations could be employed:

- mean monthly air temperatures for 1972 formed a sinusoidal wave together with the soil temperatures measured - so phase equations could be used.
- the morainic material was homogeneous down to the ice surface.
- heat transfer was by conduction only and occurred only in a vertical direction.
- moisture content of the soil was at field capacity throughout together with no movement of pore water.
- effect of snow cover was disregarded.

It is quite apparent that the majority of these are generalized assumptions in this study. Grain size analysis showed that the debris varied considerably over the moraine and it is reasonable to assume that the till

would do so with depth. Heat transfer may occur by condensation, evaporation, sublimation and rain water percolation together with movement of ground water. Heat transfer may also occur in a horizontal direction. It is doubtful that the soil was continually at field capacity and the percentage of moisture would change continually in response to many other factors. Thermal conductivity values had to be substituted from charts for frozen soil and radiation and evaporation parameters adjusted to allow use of their respective equations. The end result was to produce values which could only be used to predict trends of ablation on the moraine.

Melting on ice faces exposed to direct and diffuse solar radiation were estimated to be 263 cm for the study period while that due to terrestrial heat flow was 0.61 cm/yr.

The length of time that would be required to completely melt the underlying ice core, given present climatic conditions for the study period, was estimated on the basis of certain assumptions:

- the average amount of heat input for the study period may be extended over the total

thaw period giving an average rate of ablation of 0.7 m/yr.

- the underlying ice core extends only down to the valley floor. However Johnson (1971) has reported an ice core existing beneath the mantle of the floor which became exposed as a result of shearing by the advancing glacier during its 1969 surge.

The height of an ice core exposure above the valley floor was determined in the field to be approximately 42 meters and this together with a yearly ablation rate of 0.7 m/yr gives a minimum length of time of 60 years for complete melting out of the core, given that the above idealized climatic and soil conditions will continue to exist over this period of time.

5.8 Summary of the Depth of Freeze-Thaw and Ice Core Ablation on the Moraine

Both the quantity and depth of penetration of the energy transmitted into the soil, from the exchange at the air-ground boundary, were found to depend on certain soil parameters such as thermal conductivity and diffusivity, moisture content, and the lithology of the

soil (see Appendix). Grain size analysis showed that there was considerable variation in the size distribution over short distances and around the entire moraine, with the finest material occurring on the western portion of the moraine while the coarsest fractions were located on the east. Statistical tests showed that the material was till consisting of boulders, cobbles, sands, and a clay-silt fraction.

Depth of freeze-thaw on the moraine were calculated giving results of 5.4 to 6.1 meters for freeze and 2.6 to 3.2 meters for thaw. However many assumptions were made so the results give only a rough indication of what could be expected in this material. Individual results of ablation of debris covered ice showed that B possessed greater ablation rates than A even though the two soils had similar physical characteristics down to the 46 cm level (maximum depth to which soil temperatures were measured). The variation between the two stations will be correlated with the variations in micro climatic parameters (Chapter 6).

The amount of melting due to incoming radiation on an exposed ice surface and the amount of loss due to evaporation from this same face was estimated to be 263 cm and 5.2 cm over the study period respectively. The

loss due to terrestrial heat flow was 0.61 cm per year. Complete melting of the ice core, under certain assumptions, would take a minimum of 60 years, given that the existence of the climatic and soil conditions for 1972 will remain the same over this time period.

6. DEGRADATIONAL PROCESSES

6.1 Introduction

A variety of degradational processes such as rill and sheet wash, stream erosion and transportation, deflation, weathering, fast and slow moving forms of mass movements, and ice core ablation occur in varying degrees of intensity on the end moraine. Two groups of degradational processes were investigated;

- a) Processes due to Ice Core Ablation, i.e. mass movements - slumps slides
- b) Processes due to Melt Water Stream and Pond Action

It is the purpose of this section to investigate the occurrence of these degradational processes in terms of the variation in climatic inputs operating on the moraine, (chapter 4), as well as to describe topographical features associated with these processes.

6.2 Ablation

Ablation of both debris covered and exposed ice was considered in Chapter 5, in which it was shown that a difference existed between the amount of ablation which would occur at the thaw depth at both stations. This

difference was directly related to variations in the quantity of heat received at each site, which in turn is related to climatic variations rather than to changes in soil types and thermal parameters.

The ablation process enhances other forms of degradational processes such as mass movements, and melt water streams and pond action. In order to determine the influence that the micro climatic parameters have on the distribution of these processes around the moraine and their resultant topographical changes, one process (mass movement) together with its initiation and rates of retreat was investigated along with the climatic parameters operating near each site over the same time period. Trends rather than specific values were noted.

6.3 Mass Movements and the Action of Melt Water Streams and Ponds

The types of mass movements which were studied on the moraine are what Leopold and Wolman (1964) have classified as falls and slides, which in turn, became a form of flow at the base of their headwalls. The occurrence of

these mass wasting processes is thought to be a direct result of the variation in both glacial surge and micro climatic inputs operating on and within the end moraine. Glacial surge action (discussed in Chapter 4) in 1969 showed that the advancing glacier eroded the overlying debris exposing the ice beneath. The exposed ice wastes back (as a result of influence of various climatic parameters on it, i.e. radiation, wind, evaporation, rain), and undermines the headwall causing the overlying material to fall to the base of the cliff. As well as receiving direct heat energy on the exposed face, the ice may receive additional energy transmitted through the overlying material; and provided the debris thickness is equal to or less than the depth of thaw (3.2 meters), additional melting will occur at the ice-till interface. The melt water formed at the interface may saturate the lower layer of the till and this, combined with the assumed convex form of the ice core, can result in the production of a slip plane along which the overlying material may slide or slump. Loomis (1970) has suggested that a slope angle of 39-43 degrees is the critical angle at which till becomes unstable at the ice-till interface, but this angle may vary according to the fines content of the till. All sites on the moraine, in which slumping of material along the ice-till interface was occurring, had slope angles within this range.



Plate 6.1 Melt water stream incision into morainic material
(foreground) exposing ice core beneath (background).

Other methods, by which the overlying debris on slopes could be removed, was through the action of melt water streams and ponds. Both processes result primarily from the ablation of the underlying ice core and to a lesser degree from precipitation. During the summer, small kettles, on the lee proximal side of the moraine, were observed to be overflowing their sides; and this overflow formed melt water streams which flowed down the side of the moraine joining one kettle to the next. Where the slope was great enough, the stream incised itself into the moraine exposing the ice beneath (Plate 6-1).

As well as eroding the material, the stream transported debris which had slumped off the ice face, and thus helped to increase the rate of headwall retreat. Similar processes of hollow formation have been described in the high Arctic by Lamonthé and St. Onge (1961).

Melt ponds helped to initiate mass movement through the processes of basal sapping, and saturation of material along their sides. Both processes result in slope instability; and where the till depth is equal to or less than the thaw depth, a slip plane may form



Plate 6.11 Ice core exposure on side of melt water pond.

along which large masses of morainic material may slide down into the pond. Johnson (1971) has also reported the close correlation between till slipping along rotational slip planes, and mudflow activity, and the occurrence of lakes on the Donjek end moraine.

Finally, there were some mass movements which seemed completely unrelated to any obvious initiating mechanism. The explanation put forward here is that these slumps were initiated by a combination of ablation due to climatic inputs, and a high water table which was occurring at this time of the season due to heavy rains, followed by a period of high radiation and warm air temperatures. The intensity of these climatic parameters and mass movements is dealt with in a later section.

All forms of mass movements and resulting ice exposures were ephemeral in nature, with the exception of the two ice exposures which were caused by glacial surge action. The key to sustaining these processes once they have been initiated, is to have the material removed so that it will not cover the exposed ice. In the initial stages, the melt water from the ablating ice

is sufficient to cause the slumped material to flow in the form of a mudflow. However, in all cases except the surge initiated forms, accumulation of debris at the base of the ice face exceeded the amount being removed by mudflow activity; and eventually the hollow and ice core became completely infilled, resulting in stabilized slumps. In the case of those slumps which were initiated by melt water stream action, the overflow from the ponds ceases within a matter of several weeks; and as a result, the slumps quickly infill. The ice faces, caused by glacial surging, continued to be exposed throughout most of the study period, as the mudflow material was removed continually by lateral melt water stream action of the Donjek Glacier.

Although fossil mudflows and scars were found on the proximal and distal sides of all sections of the moraine, presently active forms of mass movements were located, with the exception of an exposure which was on the distal side of the Lee area, only on the proximal side of the western or lee portion. Exposures III, IV, V, VI, VII, (FIG.30), were all ephemeral exposures occurring on north facing slopes at

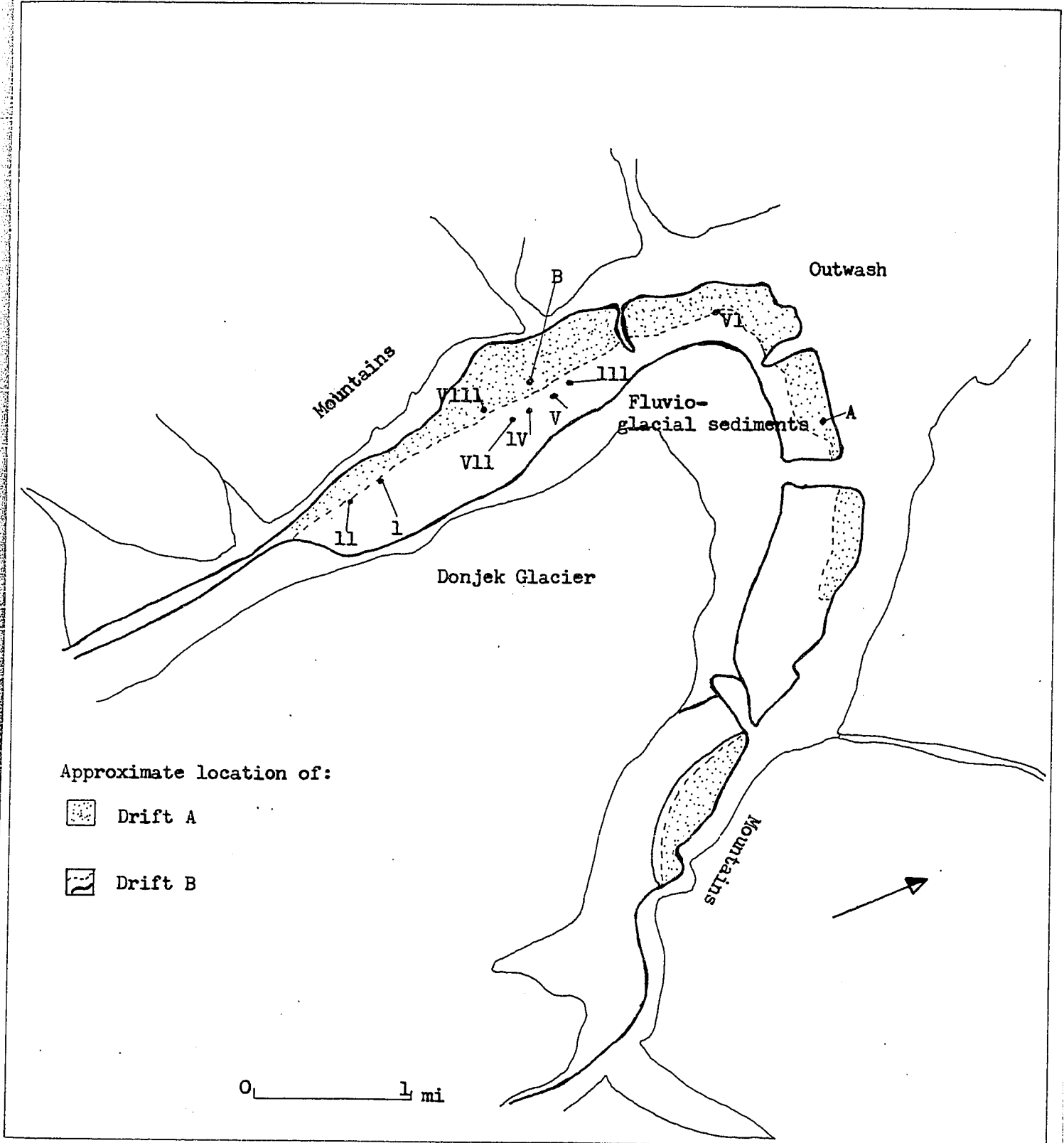


FIG. 30 DISTRIBUTION OF ICE EXPOSURES JUNE - JULY 1972

various heights on the proximal side of the moraine. Exposures III and VII were initiated by melt water stream action; while exposure VIII, which occurred on a west facing slope, was initiated by a combination of basal sapping, till saturation by lake water, and melting of the core as a result of heat flow through the soil. All the above exposures were located on slopes which approximated the critical angle for which detritus can maintain a continuous cover over an ice surface. As well, exposures IV, V, VI, VII, and VIII, had till thicknesses which were less than the thaw depth; and this, combined with the higher amount of ablation that occurs in the lee area (Station B), may explain the occurrence of these exposures. Grain size analysis showed that the western portion of the moraine contained a higher percentage of fines than that on the north or east side. According to Tuma and Sharp (1949), and Abdel-Hady (1973), coarser material enhances ablation because of the greater ease with which air and water may circulate through. The occurrence of less ablation in the coarser areas may be the result of the ice core having ablated more in the past; therefore, a sufficient soil cover now protects it from further melt (slope angles are less steep here than those in the lee area and fossil mudflows, parallel cracking, and active and fossil melt ponds are also present here).

6.4 Rates of Headwall Retreat

6.4.1 Results of Analysis

Figure 31 shows rates of retreat for ice exposures I-VI from June 25 - July 14, 1972. These were calculated by averaging the rate of retreat at individual markers at each exposure per week, and then calculating the rate per day for that period. The results show higher values than those reported from Arctic areas, (St. Onge 1961, Mackay 1966, French 1973), and this may be due to the high energy input which resulted from micro climatic conditions which occurred over this relatively short period. This relationship is discussed in detail in the next section. In some of the above cases, the marking stakes were completely removed during a week, and thus the recorded values represent minimum rates of retreat. Exposures I and II existed throughout the total study time, whereas the remaining exposures were ephemeral in nature lasting up to 21 days. The average rates of retreat for June and July for I and II were 8.0 and 13.0 cm/day. These results are higher than potential values calculated for the same ice faces as a result of only incoming short-wave radiation (Chapter 5, 5.5.1).

RATES OF RETREAT OF ICE EXPOSURES 1972

Exposure	I	II	III	IV	V	VI
Date of Measurement						
25/6-2/7	10.0	16.0	23.0	4.0	26.0	
2/7 -7/7	8.0	6.0	25.0	12.0	32.0	17.0
8/7-14/7	17.0	50.0	18.0		29.0	8.0
Mean for Study Period	13.0	26.0	19.0	8.0	29.0	14.0

* Values given in cm/day

FIG. 31

The lower ablation values due to direct radiation may be explained by a number of factors, such as not taking into account the amount of ice melt due to heat transfer through the soil from ground-atmosphere exchange, terrestrial heat flow, and evaporation. However, combining these events with the radiation values still gives lower results, so further explanation is required. One possible explanation lies in the method by which the debris is moved over the ice. On an exposed ice face in which the overlying till depth is equal to or less than the thaw depth, melting and till saturation occur along the ice-till interface promoting mass movement along a slip plane. As well, ice melt on the exposed face undermines overlying debris; and a combination of these two methods results in large masses of debris slowly moving over the ice face. As the main mass of debris slides over the surface of the ice, the lower portion falls over the exposed ice and is slowly removed as a slurry or mudflow (FIG.32). Thus, while ice melt is occurring as a result of incoming radiation, large masses of overlying debris may be moving slowly down slope resulting in large rates of headwall retreat. Occasionally the slump covers the exposed ice face completely, resulting in quiescent periods in which no

headwall retreat occurs. However, further ablation may again result in the slumped debris being removed as a slurry, exposing the ice core beneath. This was directly observed in the field; and accounts for the large rates of regression occurring between July 8 and 14 on exposure II (FIG.31), and July 20-27 on exposure I in which 12.3 meters of material were removed.

Markers placed around the perimeter of each exposure showed that differential melting was taking place, with the highest amounts occurring directly at the apex of each short lived exposure, i.e. on the north facing slope, while the next highest rate was that on west facing slopes. Both exposures I and II, which were essentially facing in an easterly direction, also had their highest rates on north facing sections; while lower rates occurred on south and east facing slopes respectively. One would expect that the greatest amount of incoming radiation would occur on west and south facing slopes, and that the greatest ablation rates would also occur on these slopes (Bishop 1957, Lamont and

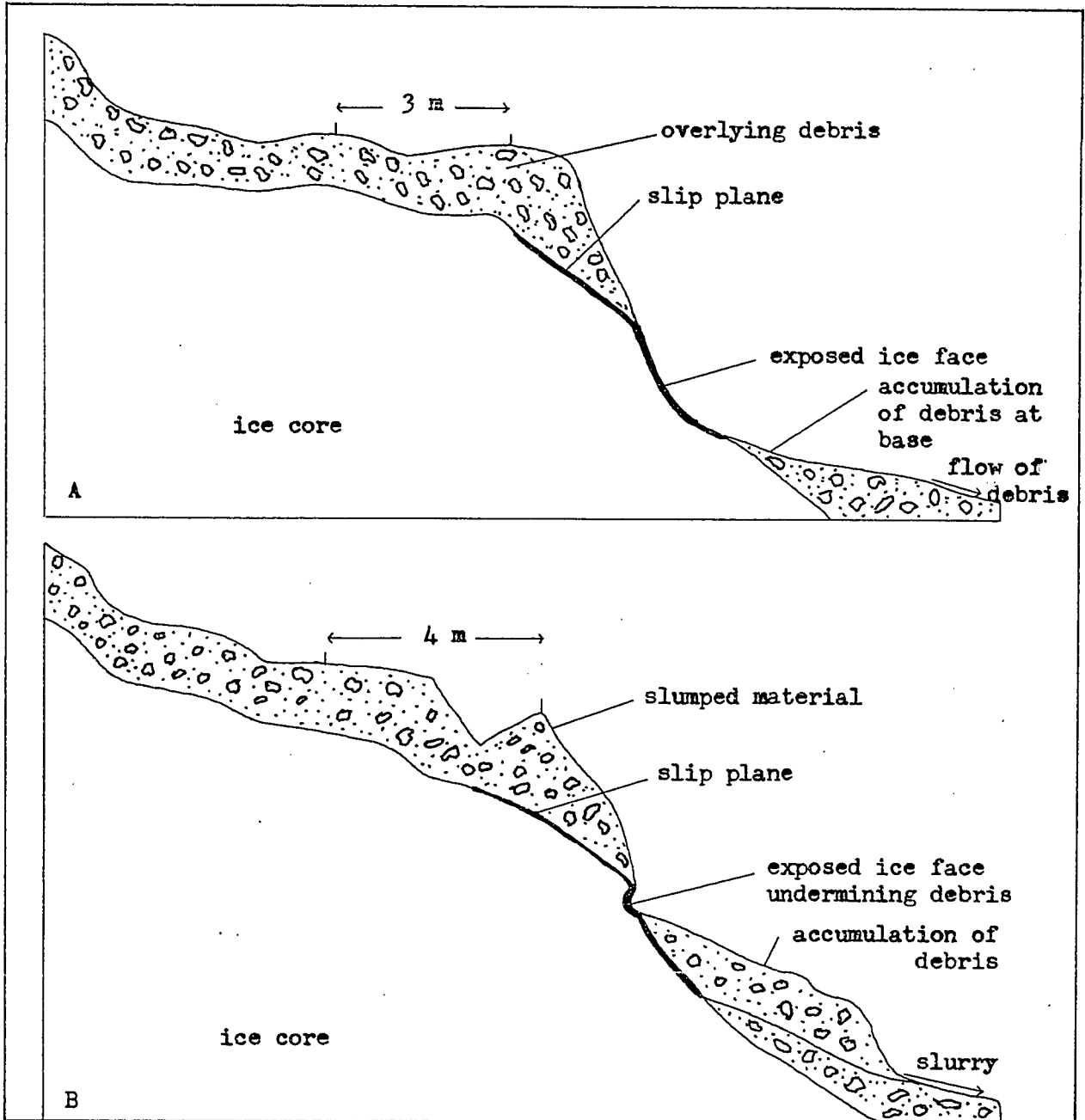


FIG. 32 SLUMPING OF DEBRIS ALONG THE ICE-TILL INTERFACE AT AN ICE CORE EXPOSURE

St. Onge 1961, Loomis 1970). However, as previously shown, radiation on west facing slopes is diminished as a result of the high mountains on the western side of the valley. It seems more probable that the variation was due to a difference in depth of overlying till, in which north facing slopes had the least amount of cover, and thus the greatest amount of ablation.

6.4.2 Summary

Rates of retreat on exposures which existed throughout the total study period, i.e. June and July 1972, gave results which are similar to those reported by St. Onge (1961), Mackay (1966), and French (1973). Higher rates of retreat were recorded during the season following periods of major climatic changes. The relationship between these rates and climatic changes is dealt with in the following section.

The rates of headwall retreat were higher than the combined amounts of wastage calculated for ice faces exposed directly to incoming radiation, evaporation, and melting due to heat flow through the soil. This difference was accounted for by the combined effect of the exposed ice

face undermining the material above, as well as by the formation of a slip plane at the ice-till interface over which large masses of debris may slide.

Preferential headwall retreat occurred on north facing sections within each exposure for two primary reasons: differential debris cover in which the least amount occurs at the apex promoting increased ablation there, and reduced insulation on west facing slopes as a result of mountain screening.

6.5 Headwall Retreat and Micro Climate

6.5.1 Results of Analysis

Most of the exposures measured in 1972 occurred between June 25 and July 21, and by July 24, all but exposures I and II had infilled and become inactive. Within this time period, the two major periods of initiation of exposures and high rates of headwall retreat were June 25 - July 1 and July 8 - 14. It is the purpose of this section to try and determine what individual climatic parameters and/or sequence of climatic events may have been responsible for these occurrences.

A synopsis of the micro climate is presented in FIG. 33 in which mean values for individual climatic parameters calculated over weekly periods are given, as well as mean values for soil thermal data. Figure 34 gives the percentage of individual total amounts of retreat for each exposure over the same time period as the synopsis.

Two very similar trends occurred in the climate, both prior to the initiation or recording of high rates of headwall retreat. Both maximum and minimum ambient air temperatures increased substantially together with above average incoming radiation, high evaporation rates, and little cloud cover. Wind values were decreasing during these periods; and were below the seasonal average during the week where most exposures first occurred, and prior to the week when large rates of retreat again occurred. Higher wind values tended to hinder the transfer of heat to lower depths in the soil; so that during or prior to slumping, low wind values allowed

greater heat transfer in the soil. Although the relative humidity decreased prior to June 25 - July 1, during this period and before and during July 8-14, the humidity increased in value. Increases in humidity together with low air temperatures are thought to increase soil temperatures by increasing mass transfer through condensation. Low evaporation rates were recorded during the critical weeks, while precipitation both preceded and occurred during these weeks. Precipitation may have a twofold effect on soil conditions, both of which lead to instability on the ice cored moraine.

The first effect occurs if enough rain falls and percolates into the soil so that the liquid limits of the soil are reached or superseded; and this, combined with any slope, causes the soil to flow as a liquid mass. Alternatively, the water may increase the mass of the soil in such a way as to cause the material on high angle slopes to exceed the cohesive force, and cause the material to slump or slide down.

SYNOPSIS OF MICRO CLIMATE AND SOIL TEMPERATURES JUNE 10 - JULY 24

Date	June 10-17	June 18-25	June-July 26-2	July 3-9	July 10-16	July 17-24	Seasonal Averages
------	------------	------------	----------------	----------	------------	------------	-------------------

Climatic Parameters

Air Temperatures - °C

- Means	18.3	11.7	10.6	17.8	15.0	12.2	12.2
- Mean Max.	21.7	14.4	12.2	20.6	17.2	15.0	16.1
- Mean Min.	8.9	8.9	8.3	15.0	11.7	10.6	9.4
Range	12.8	5.5	3.9	5.6	5.5	4.4	

Rain - % of total

	8.5	19.5	38.0	rain	10.0	17.0	
--	-----	------	------	------	------	------	--

Wind - m/s

	2.7	1.8	1.4	1.3	2.0	-	1.8
--	-----	-----	-----	-----	-----	---	-----

Radiation - cal/cm²

	355	307	256	352	302	284	307
--	-----	-----	-----	-----	-----	-----	-----

Evaporation - mm

	3.5	2.4	1.0	2.3	2.4	1.6	1.9
--	-----	-----	-----	-----	-----	-----	-----

Humidity - %

	92	81	93	85	92	96	92
--	----	----	----	----	----	----	----

Cloud Cover

	Low	Medium	High	Low	High	High	
--	-----	--------	------	-----	------	------	--

Soil Temperatures - °C

Max. Surface Temperatures	40.6	36.7	34.4	43.9	38.9	31.7	37.8
Max. 15 cm	14.4	13.9	10.6	16.7	16.2	12.8	12.3
Max. 31 cm	10.0	10.6	9.4	11.7	14.1	12.3	10.1
Max. 46 cm	7.2	8.9	7.2	9.4	11.6	10.6	8.0

Min. 15 cm

	8.3	9.4	7.7	12.2	12.9	9.7	8.3
--	-----	-----	-----	------	------	-----	-----

Min. 31 cm

	8.9	9.3	8.8	11.0	13.3	11.1	9.4
--	-----	-----	-----	------	------	------	-----

Min. 46 cm

	6.7	8.8	7.1	8.9	11.1	10.5	7.2
--	-----	-----	-----	-----	------	------	-----

Range 15 cm

	6.1	4.5	2.9	4.5	3.3	3.1	
--	-----	-----	-----	-----	-----	-----	--

Range 31 cm

	1.1	1.3	.6	.7	.8	1.2	
--	-----	-----	----	----	----	-----	--

Range 46 cm

	.5	.1	.1	.5	.5	.1	
--	----	----	----	----	----	----	--

* All values represent mean weekly results

RATES OF HEADWALL RETREAT JUNE 10 - JULY 21

Exposure	I	II	III	IV	V	VI
	%	%	%	%	%	%
<hr/>						
Date 1972						
June 10 - 17	8.7	9.2				
18 - 24	6.1	12.6				
25 - July 1	10.3	13.8	30.8	11.0	50	
July 2 - 7	9.0	5.6	25.1	20.5	50	51
8 - 14	23.5	51.3	44.2	68.5	-	28
15 - 21	42.4	7.6				28

* Values expressed as a percentage of individual total amounts.

FIG. 34

The second effect enhances mass transfer of heat through the soil, as the result of rain water obtaining heat energy by conduction from the upper surfaces of the warm soil. As the water percolates down through the soil, it may transfer some of its heat to the cooler surface below. This heat energy in turn may be used to melt the underlying ice, which in turn saturates the soil directly overlying the ice, forming a slip plane along which overlying debris may move. This latter event was shown to occur by McKenzie (1960) on an ice cored kame terrace in South East Alaska, in which the most significant soil temperature rise at depth occurred during periods of heavy precipitation. Soil temperatures at 15, 30 and 46 cm depths, at both A and B station before and during rainfall, showed that soil temperatures decreased during the rain period, and increased after the rain had ceased (FIG. 35). Similarly, relatively large amounts of precipitation occurred just prior to the week of June 10 - 17, with the highest amounts of rainfall of the season occurring on June 24, 25, 28, 29, and 30. Smaller amounts of rain also occurred prior to and during the week of June 26 - July 2.

Mean maximum and minimum soil temperatures, averaged over each week, also increased substantially during the period before June 25-July 1 and during the week of July 8-14. Although surface and 15 cm depths recorded increases concomitant with ambient air temperatures, the lower depths lagged behind; and did not reach their maximum temperatures until one week later, i.e. one week prior to June 24 - July 1 and during the week of July 8 - 14.

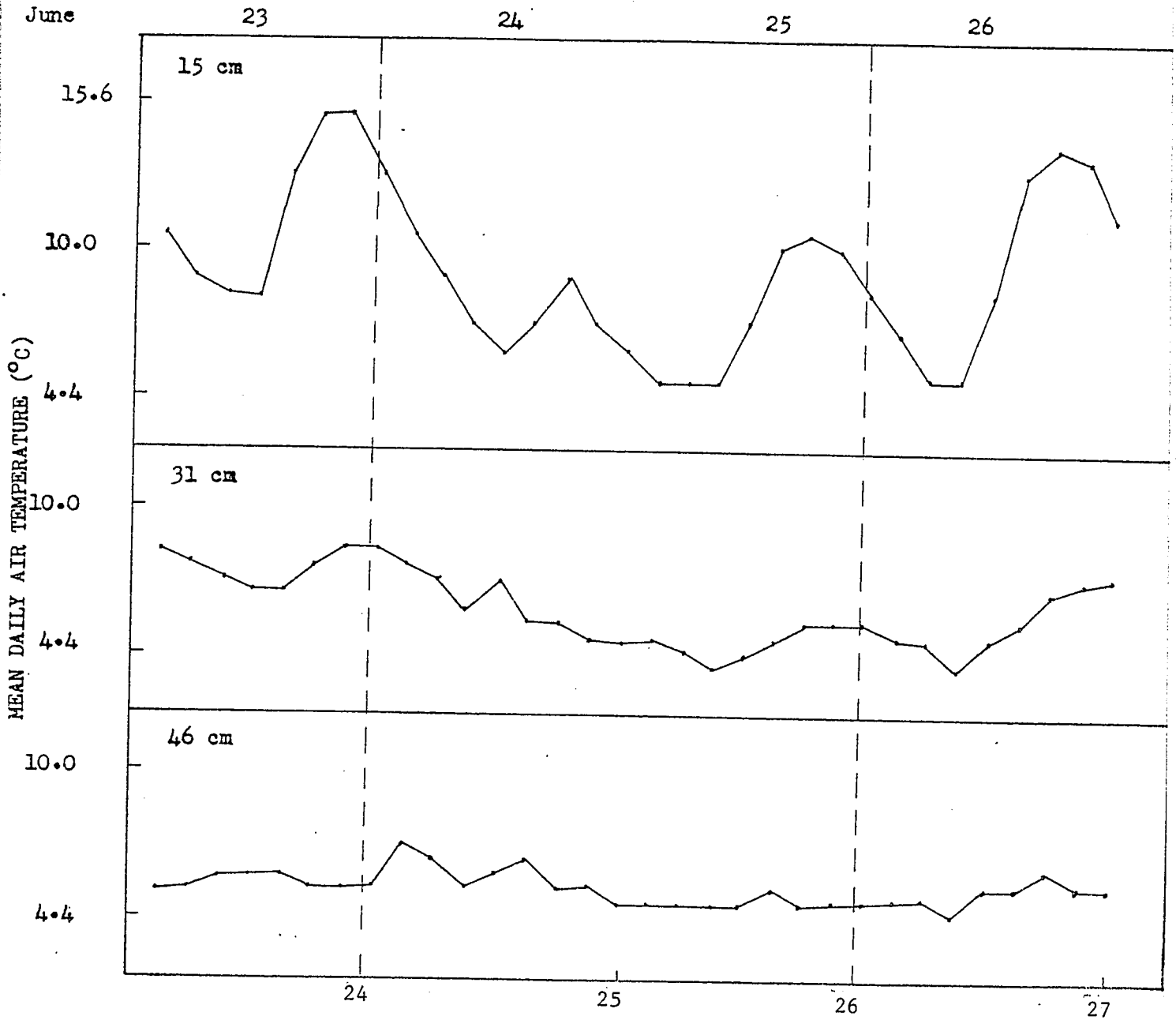


FIG.35 DAILY SOIL TEMPERATURES AT A STATION DURING JUNE. PRECIPITATION OCCURRED ON THE 24th AND 25th AS SHOWN BY DOTTED LINES.

6.5.2 Summary

Results show that increases in mean ambient weekly air temperatures of between 5.0 and 12.0°C, together with both above average amounts of incoming radiation and relative humidity, and rainfall before and during the critical time, and low wind and evaporation values, are the micro climatic parameters which could be responsible for both the initiation of certain slumps and relatively high rates of headwall retreat of the Donjek end moraine.

6.6 Variations Around the Moraine

Although A station reported higher maximum and minimum ambient air temperatures and rainfall with equal amounts of mean radiation as B, soil temperatures were less here with correspondingly lower quantities of heat being transmitted through the soil. As previously shown, it was these same variables which enhanced ablation at the various exposures. However, certain other climatic variables operating at A such as high wind values, lower relative humidity, and evaporation values tended to dampen this effect.

Stronger winds at A station seemed to result in a faster cooling of the soil there than at B station where

winds are lower. Graphs showing soil temperature variations with depth at certain times each day show that A cools more quickly than B after attaining its maximum temperature; and it is at this same time that winds are strongest. Thus, a smaller amount of heat was being transmitted through the soil at A than at B. During the evening hours, the stronger winds at A again tended to promote further cooling of the ground due to air turbulence. Higher minimum air temperatures at A than at B, together with lower humidity values, would also reduce the possibility of mass transfer of heat through condensation and vapour diffusion through the soil.

B station, on the other hand, was not only transmitting larger amounts of heat through the soil during the day, as a result of lower wind values; but was also conducting less heat energy back to the air during the evening because of less air turbulence. Thus, B had higher minimum soil temperatures and lower minimum ambient air temperatures than did A. The higher humidity values combined with lower air temperatures would induce mass transfer of heat through condensation and vapour diffusion in the soil. Also, smaller amounts of heat would be lost from the soil through evaporation because of the lower values here.

Finally in Chapter 1, 1.3, reference was made to the soil colour differences at each station, in which it was

shown that A was located on a lighter grey toned soil than B. This would result in A having a higher albedo and correspondingly lower absorption coefficient than B, again resulting in A having smaller quantities of heat transmitted through its soil.

Thus the micro climate existing at B station, together with its soil colour property, renders it more conducive to initiating and influencing the rates of certain degradational processes occurring on the moraine than that at A station.

6.7 Resultant Topographic Forms

The same processes, which occur on the debris-covered terminal section of a glacier, continue to operate on the mass when it has completely detached itself from the main trunk of the glacier, with the main difference being the intensity with which they occur. In most cases, the processes do not occur as frequently as they did when part of the glacial system; but the magnitude of the results of these processes has increased. This change has been brought about by both an increase in the depth debris cover over the ice, and changes in the micro climate over the debris surface. The resulting topographic forms occurring on the ice cored end moraine are therefore similar to those found on the glacier, but in certain cases are larger.

The single most important degradational process,

affecting the occurrence of other processes as well as directly causing changes in the morphology of the moraine, has been that of ablation. Differential thickness of the material, together with variations in the micro climate over the surface, have continued to give a hummocky appearance to the moraine. Areas with less till cover, higher intensity of climatic inputs, or possessing soil thermal parameters which enhance heat transfer, tend to be lowered at a faster rate than areas which do not have these characteristics. Inversion of relief may occur as a result of the debris slumping, sliding, and falling to lower areas where it further insulates the ice beneath. The debris around this accumulation may melt out, leaving the initial slumped material as a distinct mound or hill.

Large scale movements of material, promoted by ablation on the moraine, have resulted in large masses of material slowly moving down slope producing long linear cracks which run parallel to the moraine ridges. These masses have, in some cases, caused cracks to form, which are 155 or more meters in length, 0.6 to 0.9 meters in depth and have been displaced laterally 0.5 to 0.6 meters. The resulting appearance is crevasse like in some cases, while in others the cracks appear as terrace like forms. In areas where ablation continues to expose an ice face and where material

at the base is continually being removed as a slurry or by stream action, such as occurs at exposure I and II, large amphitheater like depressions appear. These cover up to 836 square meters in area, and have reduced the relief from over 46 meters to less than 23 meters.

Melt ponds are another feature produced by melting ice, and they in turn lead to a variety of forms. As the ice melts out beneath the lake or pond subsidence occurs, it results in some ponds becoming more deeply entrenched into the moraine and increasing the length and steepness of their slopes. Shallower ponds may dry up, leaving a hollow containing sand, silt, and clays. These former lake bottoms may become plateau moraines as a result of material around the beds being lowered by ablation of the ice core (Goldthwait 1951, Gravenor and Kupsch 1959).

Some lakes or ponds overflowed as a result of an inflow of water from a high water table, caused primarily by melting ice and precipitation. The resulting stream action incised both steep and shallow valleys on the moraine, as well as crudely sorting and washing the material over which it flowed, by eroding

and transporting the finer debris to the lower slopes, while leaving larger stones and boulders higher up on the moraine. Also stream action in some cases drained ponds and lakes, leaving dry lake and pond floors on the moraine, or formed melt water gaps across the moraine.

6.8 Summary

The occurrence of ice exposures and slumps in the lee area of the moraine, rather than on other sections of the moraine, were found to be influenced more by the depth of overlying material than by the variations of micro climatic parameters around the moraine. The ablation process enhances other forms of degradational processes such as mass movement, and melt water stream and pond action, all of which promote ice core exposure and further degradation on the moraine. Also, most ephemeral exposures occurred on north facing slopes; while within almost all exposures studied, the fastest rates of backwall retreat occurred on north and west slopes, i.e. on east facing exposures, rates were faster on north and west slopes within each hollow, while on north facing exposures the apex retreated the fastest.

Rates of headwall retreat for slumps active throughout the study period averaged 10.5 cm/day for June and July, whereas

the rates for ephemeral slumps and slides were 17.5 cm/day during their existence. The climatic triggering mechanism thought to be responsible for initiating these slides was an increase in mean ambient air temperatures of 5.0 to 12.0°C per week, together with above average incoming radiation, relative humidity, and rainfall (before and during the critical weeks that initiation or high rates were recorded), and low wind and evaporation rates.

The topographic features such as the hummocky appearance of the moraine, inversion of relief, linear cracks, hollows around the shores of certain melt ponds, moraine plateaus, dried up depressions filled with sand, silt and clay, steep walls around certain ponds, steep shallow valleys on the moraine as well as coarser material on the upper sections of the valley, are the results of these processes operating on the moraine; and would therefore appear to be controlled to a degree by the local climatic conditions, but more so by the depth of material overlying the ice.

7. CONCLUSIONS

The variation in microclimatic inputs on an ice cored end moraine does not fully explain the occurrence, i.e. geographic location, of certain types of degradational processes which are presently operating on it. However the initiation and increases in rates of these processes (ablation, slumps and slides, stream and pond action) may be explained to a degree by corresponding increases in certain microclimatic parameters such as ambient air temperature, precipitation, relative humidity, incoming radiation, and decreases in the intensity of others, such as evaporation and wind. Thus values showing fluctuations of these climatic parameters, over intervals within the thaw period, are better indicators of the degree of activity of these processes than are mean values for these parameters over the thaw season. Due to the nature of the study no specific values were assigned to these factors; only trends were noted.

On ice which has been directly exposed to the atmosphere, radiation seems to play the major role in promoting ablation, more so than other climatic variables such as evaporation, humidity, ambient air temperature or wind. Variation around the moraine of the above mentioned climatic variables also accounts primarily for the variation in the quantity of heat being transmitted through the soil at the two meteorological stations, resulting in differential

ablation rates.

Rates of headwall retreat for slumps which were active throughout the study period are similar to those reported for comparable features in the Arctic. These results are primarily thought to reflect the micro climate which exists in the mountainous environment rather than being indicative of the Yukon in general.

That an ice core does exist at least in part of the end moraine, i.e. specifically the lee area, is known from a number of exposures which were observed in the field located at various heights on its surface. The fact that ground ice has existed or may still exist in the remainder of the moraine is seen from the various topographical remnants associated with degradational processes occurring on ice cored terrain. The inactivity of these processes is due to the variation in depth of the overlying material rather than to variations in the influence of the local climatic parameters around the moraine. Fabric analysis performed on an ice core sample revealed that it was stagnant glacier ice. However extreme caution must be used when interpreting ice types from fabric analysis as different types may indeed possess similar fabric characteristics under certain circumstances. Where possible the largest number of crystals should be used in the analysis to increase the significance of any patterns observed and these

results should be corroborated with evidence revealed from other tests, such as chemical analysis for trace elements, for determining ice types.

The present day extent of the ice core could be revealed by some remote sensing technique such as seismic or electrical resistivity measurements, and these results could be used in determining more accurate temperature gradient data in the soil as well as revealing variations of the depth of the ice- till interface, from the depth of the thaw which was calculated to be 3.2 meters. Because of the sensitivity of soil thermal parameters, (i.e. thermal conductivity, diffusivity, volumetric heat), to changes of moisture content and soil type, this figure represents a very rough estimate, and caution must be used when reporting and interpreting such critical thickness values especially when working with such variable material as till. Thus no specific soil thermal parameters are given as being representative of this till type. Complete and detailed records of both climatic and soil conditions are recommended to increase the accuracy of the results, as well as a more detailed analysis of soil characteristics. Climatic data recorded on the moraine over the thaw period would allow a more accurate determination of the distribution of the thaw depth around the moraine.

Thermal probes extending down to the ice-till interface would provide a more accurate temperature profile through the soil and a better knowledge of debris thickness. It was extremely difficult to effectively sample the overlying debris, both surficially and at depth, because of the shifting of the till, i.e. flow tills, which occurs over the thaw season. Maximum melt out rates suggest that parts of the ice core of the Donjek end moraine could be completely wasted in 60 years. This rate is much higher than that given by McKenzie (1969), for a collapsing kame terrace in Alaska having approximately the same ice thickness (36 meters) buried under approximately 4 meters of washed gravel.

Melt water streams and ponds on the ice cored moraine surface are also effective triggering mechanisms for slumps and slides and indirectly are responsible for the same forms of mass movements becoming inactive. Glacial surge action may well have initiated ice core exposure on the lee area of the moraine, and because of melt water stream action of eroding and transporting the slurry debris from these exposures, they remain active throughout the thaw season.

The overall shape of the ice cored moraine conforms to similar features described elsewhere in the literature. The moraine is extremely massive in size having steeper distal

than proximal slope angles with the proximal side being ramp like in appearance. The slope angles were greater on the lee area than elsewhere and this, combined with a micro climate conducive to greater quantities of heat flow through the soil and a thinner material cover, has produced more active degradational processes here. The surface of this moraine is highly complex, both morphologically and in composition of the materials, reflecting the variety of environments which have or presently are operating there.

The size of the moraine, (especially on the western portion), and the quantity of till present on the moraine is deceiving both on air photographs and from a quick inspection in the field. Where exposures occurred on the moraine, it could be seen that the depth of overlying material was only a very thin mantle when compared to the quantity of ice beneath. Thus what may initially appear to be indications of a glacier, which is transporting exceptionally large quantities of debris, is misleading. Ice faces also showed that the form of the overlying debris conforms to that of the underlying ice. Due to differential ablation, caused to a degree by either/or climatic and soil thermal properties changing and mostly by variations in the depth of overlying material, the surface of the moraine has become hummocky in appearance. Thus as Loomis

(1970) has pointed out, buried ice cores can continue to change or effect morphologic development of the overlying material for many years as changes in the above enhance the process of ablation.

Despite the substantial appearance of the moraine form, it is apparent that small terrain disturbances may initiate periods of rapid degradation in localized areas. Sections on the moraine, with depths equal to or less than the thaw depth, bear evidence of the frequent activity of processes of degradation which in turn are influenced by the heat input into the moraine and its effect on the ice core. The quantity of heat being transmitted through the soil depends on both local soil thermal parameters and local climatic conditions. Thus the local climatic conditions of an area must be closely monitored if one is to understand more fully the rates, and to a degree, the distribution of certain degradational processes especially in those areas underlain by buried ice.

SELECTED BIBLIOGRAPHY

- Ahlmann, H. W. and Droessler, E. G., (1948). "Glacier Ice Crystal Measurements at Kebnekajse, Sweden." Journal of Glaciology, Vol. 1, pp. 268-274.
- Allan, C. R. Kamb, W. B. Meier, M. F. Sharp, R. P. (1960). "Structure of the Lower Blue Glacier, Washington." Journal of Geology, Vol. 68, No. 6, pp. 601-625.
- Anderson, J. L. and Sollid, J. L., (1971). "Glacial Chronology and Glacial Geomorphology In the Marginal Zones of the Glaciers, Midtdalsbreen and Nigardsbreen, South Norway." Norsk. Geogr. Tidsskr. Vol. 25, pp. 1-38.
- Anderton, P. W., (1970). "Deformation of Surface Ice at a Glacier Confluence, Kaskawulsh Glacier." Ice Field Ranges Research Project Scientific Results, Vol. 2, NY, Amer. Geog. Society, Montreal, AINA. pp. 59-76.
- _____ (1974). "Ice Fabric and Petrography, Meserve Glacier, Antarctic." Journal of Glaciology, Vol. 13, No. 68, pp. 285-306.
- Bader, H., (1951). "Introduction to Ice Petrofabrics." Journal of Geology, Vol. 59, pp. 519-536.
- Benedict, J. B., (1968). "Recent Glacial History of an Alpine Area in the Colorado Front Range, USA." Journal of Glaciology, Vol. 7, No. 49, pp. 77-88.
- Benjey, W., (1970). "Upper-Air Wind Patterns in the St. Elias Mountains, Summer 1965." IRRP Scientific Results, Vol. 2, 1970. pp. 3-16.
- Bishop, B. C., (1957). "Shear Moraines in the Thule Area, N. W. Greenland." U.S. - S.I.P.R.E. Res. Rep. 17, 46 p.
- Borns, H. W. and Goldthwait, R.P., (1966). "Late-Pleistocene Fluctuations of the Kaskawulsh Glacier." American Journal of Science, Vol. 269, No. 8, pp. 600-619.
- Boulton, G. S., (1967). "The Development of a Complex Supraglacial Moraine at the Margin of Sorbreen Ny Freisland, Vestspitsbergen." Journal of Glaciology, Vol. 6, No. 47, pp. 717-735.
- _____ (1968). "Flow Tillis and Related Deposites in some Vestspitsbergen Glaciers." Journal of Glaciology, Vol. 7, No. 51, pp. 391-412.

(1970). "On the Deposition of Subglacial and Melt Out Till at the Margins of Certain Svalbard Glaciers." Journal of Glaciology, Vol. 9, No. 56, pp. 231-246.

(1972). "Modern Arctic Glaciers as Depositional Models for Former Ice Sheets." Journal of the Geological Society, Vol. 128, Part 4, pp. 362-393.

Brunsdon, D., (1971). Slopes-Form and Process. Institute of British Geographers Special Publication No. 3, January 1971, 177 p.

Demorest, M.H., (1953). "Process of Ice Deformation within Glaciers." Journal of Glaciology, Vol. 2, No. 13, pp. 201-203.

Denton, G. H. and Stuiver, M., (1966). "Neoglacial Chronology, N.E. St. Elias Mtns, Canada." American Journal of Science, Vol. 264, No. 8, pp. 577-599.

(1967). "Late Pleistocene Glacial Stratigraphy and Chronology N.E. St. Elias Mtns, Yukon Territory, Canada." Geological Society of America, Bulletin, Vol. 78, No. 4, pp. 485-510.

Doornkamp, J. C. and King, C. A. M., (1971). Numerical Analysis in Geomorphology: An Introduction. London. 372 p.

Drew, J. V. Tedrow, J. Shanks, R. and Koranda, J., (1958). "Rates and Depth of Thaw in Arctic Soils." Amer. Geophysical Union, Trans., Vol. 39, No. 4, pp. 697-701.

Drewry, D. J., (1972). "A Quantitative Assessment of Dirt Cone Dynamics." Journal of Glaciology, Vol. II, No. 63, pp. 431-446.

Ekerbom, E. and Palosuo, E., (1963). "A Study of Ice Crystals at Storglaciaren, Kebnekajse." In Kingery, W. D. edition Ice and Snow, Properties, Processes and Applications, M.I.T. Press, Cambridge, Mass. 1963, 684 p.

Folk, R. L., (1968). Petrology of Sedimentary Rocks. The University of Texas, Geology, 370K, 383L. 383M. Austin, Texas. 83p.

French, H. M., (1971). "Slope Asymmetry of the Beaufort Plain, N. W. Banks Islands, N.W.T., Canada." Canadian Journal of Earth Sciences, Vol. 8, No. 7, pp. 717-731.

- _____ (1973). "Geomorphological Processes and Terrain Sensitivity, Banks Island." In report of activities April-October, 1972, Geological Survey of Canada, paper 73-1.
- _____ (1974). "Active Thermokarst Processes, Eastern Banks Island, Western Canadian Arctic." Canadian Journal of Earth Sciences, Vol. 11, No. 6, pp. 785-794.
- Geiger, R., (1966). The Climate Near the Ground. Harvard University Press, Cambridge, Mass. 611 p.
- Gell, A., (1973). "Ice Petrofabrics, Tuktoyaktuk, N.W.T. Canada." M.A. Thesis.
- Gold, L. W., (1963). "Deformation Mechanism in Ice." pp. 8-27. In Kingery, W.D. edition Ice and Snow - Properties, Processes and Applications, M.I.T. Press, Cambridge, Mass. 1963, 684 p.
- Goldthwait, R. P., (1951). "Development of End Moraines in East-Central Baffin Island." Journal of Geology, Vol. 59, No. 6, pp. 567-577.
- Gow, J. A., (1969). "On the Rates of Growth of Grains and Crystals in South Polar Firn." Journal of Glaciology, Vol. 8, No. 53, pp. 241-252.
- Gravenor, C. P. and Kupsch, W. O., (1959). "Ice-Disintegration Features in Western Canada." Journal of Geology, Vol. 67, pp. 48-64.
- Gray, D. M., (1970). Principles of Hydrology. Water Information Center, Inc., Port Washington, N.Y. 1973. Copyright 1970. National Research Council of Canada.
- Haff, J. C., (1938). "Preparation of Petrofabric Diagrams." The American Mineralogist, Vol. 23, pp. 543-574.
- Havens, J. M., Saarela, D. E., (1969). "Exploration Meteorology in the St. Elias Mtns." IRRP, Vol. 1, 1969, pp. 17-22.
- Hooke, R. L., (1968). "Comments on the Formation of Shear Moraines: an Example from South Victoria Land, Antarctica." Journal of Glaciology, Vol. 7, No. 50, pp. 351-352.
- _____ (1970). "Morphology of the Ice Sheet Margin near Thule, Greenland." Journal of Glaciology, Vol. 9, No. 57, pp. 303-324.

- _____ (1973). "Flow Near the Margin of the Barnes Ice Cap and the Development of Ice-Cored Moraines." Geological Society of America, Bulletin, Vol. 84, No. 12, pp. 3929-3948.
- Inman, D. L., (1952). "Measures for Describing the Size Distribution of Sediments." Journal of Sedimentary Petrology, Vol. 22, pp. 125-145.
- Johnson, P. G., (1971). "Ice Cored Moraine Formation and Degradation, Donjek Glacier, Yukon Territory, Canada." Geografiska Annaler, Vol. 53A, 3-4, pp. 198-202.
- _____ (1972). "A Possible Advanced Hypsithermal Position of the Donjek Glacier." Arctic, Vol. 25, No. 4, pp. 302-305.
- _____ (1972). "The Morphological Effect of Surges of the Donjek Glacier, St. Elias Mountains, Yukon Territory, Canada." Journal of Glaciology, Vol. 11, No. 62, pp. 227-234.
- _____ (1972). "Recent Crevasse Fillings at the Terminus of the Donjek Glacier, St. Elias Mtns, Yukon Territory." Geoscope, University of Ottawa, Vol. 3, No. 1, pp. 15-24.
- _____ (1972). "The Degradation of the Donjek Glacier Neoglacial Moraine, St. Elias Mtns., Yukon Territory, Canada." Research Notes No. 1. Department of Geography, University of Ottawa.
- _____ (1974). "Mass Movement of Ablation Complexes and their Relationship to Rock Glaciers." Geografiska Annaler, Vol. 56, Ser. A., pp. 93-101.
- Kamb, W. B., (1959 a). "Theory of Preferred Crystal Orientation Developed by Crystallization Under Stress." Journal of Geology, Vol. 67, pp. 153-170.
- _____ (1959 b). "Ice Petrofabric Observations from Blue Glacier, Washington, in Relation to Theory and Experiment." Journal of Geophysical Research, Vol. 64, No. 11, pp. 1891-1909.
- King, C. A. M., (1966). Techniques in Geomorphology. Edward Arnold Ltd., 342 p.
- Kizaki, K., (1962). "Ice Fabric Studies on Hamna Ice Fall and Honnorbrygga Glacier, Antarctica." The Antarctic Record, No. 16, pp. 1392-1412.
- _____ (1969). "Fabric Analysis of Surface Ice Near Casey Range, East Antarctica." Journal of Glaciology, Vol. 8, No. 54, pp. 375-383.

- _____ (1969). "Ice Fabric Study of the Mawson Region, East Antarctica." Journal of Glaciology, Vol. 8, No. 53, pp. 253-276.
- Krumbien, W.C., (1934). "Size Frequency Distribution of Sediments." Journal of Sedimentary Petrology, Vol. 4, pp. 65-77.
- Lachenbruch, A.H., (1957). "Probe for Measurement of Thermal Conductivity of Frozen Soils in Place." Trans. American Geophysical Union, Vol. 38, pp. 691-697.
- _____ (1959). "Periodic Heat Flow in a Stratified Medium with Application to Permafrost Problems." U.S. Geological Survey, Bulletin, 1083-A, 35 p.
- Lamonth, C. and St-Onge, D., (1961). "A Note on a Periglacial Erosional Process in the Isachsen Area, N.W.T." Geographical Bulletin, No. 16, pp. 104-113.
- Landim, P.M. and Frakes, L.A., (1968). "Distinction Between Till and Other Diamictos Based on Textural Characteristics." Journal of Sedimentary Petrology, Vol. 38, No. 4, pp. 1213-1223.
- Langway, C.C., (1958). "Ice Fabrics and the Universal Stage." SIPRE Tech. Report 62, Snow Ice Permafrost Res. Establishment, U.S. Army, 16 p.
- Lee, W.H.K. and MacDonald, G.F.E., (1963). "The Global Variation of Terrestrial Heat Flow." Journal of Geophysical Research, Vol. 68, No. 24, pp. 6481-6492.
- Leopold, L.B. Wolman, M.G. Miller, J.P., (1964) Fluvial Processes in Geomorphology. W.H. Freeman and Company, U.S.A., 522 p.
- Loomis, S.R. Dozier, J. Ewing, K.J., (1970). "Studies of Morphology and Stream Action on Ablating Ice." AINA, Res. Paper 57, pp. 1-167.
- MacKay, J.R., (1966). "Segregated Epigenetic Ice and Slumps in Permafrost, MacKenzie Delta Area, N.W.T." Geographical Bulletin, Vol. 8, pp. 59-80.
- _____ (1971). "The Origin of Massive Icy Beds in Permafrost, Western Arctic Coast, Canada." Canadian Journal of Earth Sciences, Vol. 8, pp. 397-422.
- Marcus, M.G., (1969). "Summer Temperature Relationships along a Transect in the St. Elias Mtns." IRRP, Vol. 1, pp. 23-31.

- Marcus, M.G. and Ragle, R.H., (1970). "Snow Accumulation in the Ice-field Ranges, St. Elias Mtns., Yukon." Arctic and Alpine Research, Vol. 2, No. 4, pp. 277-292.
- Matthes, F.E., (1948). "Moraines with Ice Cores in the Sierra Nevada." Sierra Club Bulletin, Vol. 33, pp. 87-96.
- McKenzie, G.D., (1969). "Observations on a Collapsing Kame Terrace in Glacier Bay National Monument, South-Eastern Alaska." Journal of Glaciology, Vol. 8, No. 54, pp. 413-425.
- Meier, M.F. Rigsby, G.P. Sharp, R.P., (1954). "Preliminary Data from Saskatchewan Glacier, Alberta, Canada." Arctic, Vol. 7, No. 1, pp. 3-26.
- Monthly Record - Meteorological Observations in Canada. (1971, 1972, 1973). Environment Canada.
- Muller, J.E., (1967). "Kluane Lake Map-Area, Yukon Territory (115G 115F E 1/2)." Geological Survey of Canada, Memoir 340. 137 p.
- Østrem, G., (1959). "Ice Melting Under a Thin Layer of Moraine, and the Existence of Ice Cores in Moraine Ridges." Geografiska Annaler, Vol. XLI, No. 4, pp. 228-230.
- _____ (1962). "Ice Cored Moraines in the Kebnekajse Area." Bjuletyn Peryglacjalny, NR11, pp. 271-278.
- _____ (1963). "Comparative Crystallographic Studies from Ice Cored Moraines, Snowbanks, and Glaciers." Geografiska Annaler, Vol. 45, No. 4, pp. 210-240.
- _____ (1964). "Ice Cored Moraines in Scandinavia." Geografiska Annaler, Vol. 46, No. 3, pp. 282-337.
- _____ (1964). "Ice Crystals from an Ice Cored Moraine on Baffin Island, N.W.T." Geographical Bulletin, Vol. 22, pp. 72-79.
- _____ (1965). "Problems of Dating Ice Core Moraines." Geografiska Annaler. Vol. XLVII, No. 1, pp. 1-38.
- Østrem, G. and Arnold, K., (1970). "Ice Cored Moraines in South British Columbia and Alberta, Canada." Geografiska Annaler, Vol. 52, No. 2, pp. 120-128.
- Patterson, W.S.B., (1969). The Physics of Glaciers. Pergman Press, 250 p.
- Penner, E., (1961). "Ice-Grain Structure and Crystal Orientation in an Ice Lens from Leda Clay." Geological Society of America, Bulletin. Vol. 72, pp. 1575-1578.

- Perey, F.G.J. and Pounder, E.R., (1958), "Crystal Orientation in Ice Sheets." Canadian Journal of Physics, Vol. 36, pp. 494-502.
- Phillips, F.C., (1954). The Use of Stereographic Projection in Structural Geology. Edward Arnold, 87 p.
- Porter, S.C. and Denton, G.H., (1967). "Chronology of Neoglaciatioin in the North American Cordellieria." American Journal of Science. Vol. 265, pp. 177-210.
- Prest, V.K., (1968). "Nomenclature of Moraines and Ice Flow Features as Applied to the Glacial Map of Canada." Geological Survey of Canada, Paper 67-57, 32 p.
- Price, R.J., (1970). "Moraines at Fjallsjokull." Arctic and Alpine Research, Vol. 2, No. 1, pp. 27-42.
- Rampton, V.N., (1970). "Neoglacial Fluctuations of the Natazhat and Klutlan Glaciers, Yukon Territory, Canada." Canadian Journal of Earth Sciences, Vol. 7, No. 5, pp. 1236-1263.
- Rampton, V.N. and MacKay, J.R., (1971). "Massive Ice and Icy Sediments Throughout the Tuktoyaktuk Penninsula, Richards Island, and Nearby Areas, District of MacKenzie." Geological Survey of Canada, Paper 71-72, 16 p.
- Rampton, V.N., and Walcott, R.I., (1974). "Gravity Profiles Across Ice-Cored Topography." Canadian Journal of Earth Sciences, Vol. 11, No. 1, pp. 110-122.
- Reid, J.R., (1969). "Effects of a Debris Slide on Sioux Glacier, South Central Alaska." Journal of Glaciology, Vol. 8, No. 54, pp. 353-367.
- _____ (1970). "Geomorphology and Glacial Geology of the Martin River Glacier, Alaska." Arctic, Vol. 23, No. 4, pp. 255-267.
- _____ (1970). "Late Wisconsin and Neoglacial History of the Martin River Glacier, Alaska." Geological Society of America, Bulletin, Vol. 81, pp. 3593-3604.
- Rigsby, G.P., (1951). "Crystal Fabric Studies on Emmons Glacier, Mt. Rainier, Washington." Journal of Geology, Vol. 59, pp. 590-598.
- _____ (1958). "Fabrics of Glacier and Laboratory Deformed Ice." Union Géodesique et Géophysique Internationale. Ass. Internat. d'Hydrologie Scientifique, Symposium de Chamonix, Vol. 16-24, Sept. pp. 351-358.
- _____ (1960). "Crystal Orientation in Glacier and in Experimentally Deformed Ice." Journal of Glaciology, Vol. 3, pp. 589-606.

- _____ (1968). "The Complexity of the Three Dimensional Shape of Individual Crystals in Glacier Ice." Journal of Glaciology, Vol. 7, No. 50, pp. 233-251.
- Schytt, W., (1959). "The Glaciers of the Kebnekajse Massif." Geografiska Annaler, Vol. 41, pp. 213-227.
- _____ (1968). "Notes on Glaciological Activities in Kebnekajse, Sweden during 1966-1967." Geografiska Annaler, Vol. 50, pp. 111-120.
- Scott, R.F., (1964). "Heat Exchange at the Ground Surface." CRREL. 11-A1, 49 p.
- Scott, J.S. St-Onge, D., (1969). "Guide to the Description of Till." Geological Survey of Canada, Paper 68-6.
- Seligman, G., (1949). "The Growth of the Glacier Crystal." Journal of Glaciology, Vol. 1, pp. 254-267.
- Sellers, W.D., (1967). Physical Climatology. The University of Chicago Press, Chicago and London, 272 p.
- Sharp, R.P., (1949). "Studies of Supraglacial Debris on Valley Glaciers." American Journal of Science, Vol. 247, No. 5, pp. 289-313.
- Shaw, J., (1971). "Mechanism of Till Deposition Related to Thermal Conditions in a Pleistocene Glacier." Journal of Glaciology, Vol. 10, No. 60, pp. 363-373.
- Shumskii, P.A., (1958). "The Mechanism of Ice Straining and Its Recrystallization." Union Géodesique et Géophysique Internationale. Ass. Internat. d'Hydrologie Scientifique, Symposium de Chamonix, Vol. 16-24, Sept. pp. 244-248.
- _____ (1964). Principles of Structural Glaciology. Dover Publications Inc., N.Y. 497 p.
- Souchez, R.A., (1966). "The Origin of Morainic Deposites and the Characteristics of Glacial Erosion in the Western SOR-Rondane, Antarctica." Journal of Glaciology, Vol. 6, No. 4, pp. 249-254.
- _____ (1967). "The Formation of Shear Moraines: an example from South Victoria Land, Antarctica." Journal of Glaciology, Vol. 6, No. 48, pp. 837-843.
- _____ (1971). "Ice-Cored Moraines in Ellesmere Isl., N.W.T." Journal of Glaciology, Vol. 10, No. 59, pp. 245-254.

- Swithinbank, C.W.M., (1949). "The Origin of Dirt Cones on Glaciers." Journal of Glaciology, Vol. 1, No. 8, pp. 461-465.
- Taylor, L.D., (1963). "Structure and Fabric on the Borroughs Glacier, S.E. Alaska." Journal of Glaciology, Vol. 4, pp. 731-752.
- Taylor-Barge, B., (1969). "The Summer Climate of the St. Elias Mtn. Region." IRRP, Vol. 1, pp. 33-49.
- Terzaghi, K., (1952). "Permafrost. In Contributions to Soil Mechanics 1941-1953." Boston Mass., Boston Society of Civil Engineers, pp. 319-394.
- Tuma, J.J. Abdel-Hady, M., (1973). Engineering Soil Mechanics. Prentice-Hall, Inc., New Jersey. 335 p.
- Wahrhaftig, C. and Cox, A., (1959). "Rock Glaciers in the Alaska Range." Geological Society of America, Bulletin, Vol. 70, pp. 383-426.
- Weertman, J., (1961). "Mechanism for the Formation of Inner Moraines Found Near the Edge of Cold Ice Caps and Ice Sheets." Journal of Glaciology, Vol. 3, pp. 965-978.
- Wendler, G. and Ishikawa, N., (1974). "Effect of Slope, Exposure and Screening on Solar Radiation." Journal of Glaciology, Vol. 68, No. 13, pp. 213-226.
- _____ (1974). "The Combined Heat, Ice and Water Balance of McCall Glacier." Journal of Glaciology, Vol. 68, No. 13, pp. 227-241.
- Whalley, W.B., (1974). "Rock Glaciers and Their Formation." Geographical Papers, Reading University, No. 24, 60p.
- Williams, P.J. and Nickling, W.G., (1971). "Ground Thermal Regime in Cold Regions." In Research Methods in Pleistocene Geomorphology. 2nd Guelph Symposium on Geomorphology, 1971. Yatsu, E. and Falconer, A. University of Guelph.
- Yong, R. and Warkentin, B., (1966). Introduction to Soil Behavior. The Macmillan Company, N.Y., 501 p.

APPENDIX1. Grain Size Analysis1.1 Statistical Analysisa) Mean Grain Size

Mean grain size was calculated for phi fractions between -0.5 phi and 4.0 phi. As mentioned earlier, the coarser fraction was not employed on the cumulative curves, and thus was not employed in calculation of either the mean or any other statistical parameter. The measures of central tendency are thus underestimated in this study. However some indication as to grain size variation may be gained by analyzing the -0.5 phi to 4.0 phi range.

The equation used to determine measure of central tendency was that of Folk and Ward 1957. (From King 1966).

$$Mz = \frac{\phi_{16} + \phi_{50} + \phi_{84}}{3}$$

where Mz = mean grain size

Each particular traverse showed an individual pattern of its own. Four traverses are presented here as examples

of the variation. Lines A and G were located on the northern portion of the moraine while M and B were taken on the west and east respectively.

A traverse shows coarsest material on the inside grading to finer material on the outside.

G traverse shows the coarsest material on the outside and finest on the inside.

M shows grading from fine, from both proximal and distal sides, to coarse material near the middle of the moraine.

B traverse showed a coarser fraction tending towards a finer fraction as one moves in towards the glacier. No statistical test of significance was performed on the mean values, and thus it is difficult to state for certainty that these results are showing significant differences and individual patterns. However, there is a variation in mean size within each traverse.

The average mean grain size along each traverse was determined and is shown in FIG. 36 .

The west side of the moraine tended to show the finest material (.28mm), while the east side showed the coarsest fraction (.45mm), and the north section of the moraine had a mean value of (.35mm)*.

The fact that the east side showed a larger mean value than the west side may partly be explained through the process of winnowing. The west side of the moraine has been shown to receive lower wind values than that on the northern section of the moraine, while the east side of the moraine would receive as much or higher wind values than those of the northern section. (Chapter 4). Thus a greater percentage of fines could be removed by the process of deflation on the eastern side than on the western section. Similar values of rainfall, on all sections of the moraine, show that there is a strong likelihood of surface wash removing relatively equal amounts of fines from the unvegetated inner portion of the moraine.

* All phi values were converted to mm by use of conventional charts relating phi values to Wentworth scale values.

However, it may also be that the morainic material was deposited in situ on the eastern side with a higher percentage of coarser fragments than on other sections of the moraine.

b) Sorting

The amount of variation or deviation from the mean was determined through the sorting coefficient. The formulae used to calculate the sorting values was

$$6\phi = \frac{\phi_{75} + \phi_{25}}{1.35} \quad (\text{King, 1966})$$

Although this formulae may not be as accurate as others (e.g. Folk 1968 Inclusive Graphic Standard Deviation), it was employed here because values were accurately plotted on cumulative curves more often within this range. Thus no extrapolation was required to obtain sorting values. Each individual traverse showed its own particular pattern (FIG. 36).

M traverse shows poorest sorting on both the proximal and distal sides of the moraine, and better sorting towards the middle area.

G becomes more poorly sorted towards the proximal side of the moraine.

A becomes better sorted towards the proximal side of the moraine.

B traverse showed poorer sorting towards the proximal side of the moraine.

The large variation within short distances on the moraine may be seen by a comparison of traverses A and G which are located within 47 meters of one; another yet have sorting values which increase and decrease respectively as one moves in towards the inner portion of the moraine.

The average mean values for each traverse show that the highest sorted values (i.e. those showing the worst sorting), are those found on the north and east areas on the moraine. However all values, i.e. mean and average means, show poor sorting values, and it may be concluded that the depositing agent did not possess enough energy to sort the individual fractions. The fact that some samples were better sorted than others suggests that more than one type of environment may have been operating on the moraine when the material was deposited, or that this material has been reworked.

c) Skewness

Values for skewness were determined by use of Inman's formulae by comparing the mean and median values.

$$\phi = \frac{M\phi - Md\phi}{6\phi} \quad (\text{From King, 1966})$$

The results are tabulated in FIG. 36 .

All samples showed a positive skewness, i.e. towards the finer fractions, except sample G_1 . This sample, located directly north of the present glacier snout on the distal side of the moraine, was taken from a fossil mudflow area and is highly skewed towards the coarser fraction. The western side of the moraine shows a more normal distribution than the east side, while the northern area contained both low and high skewed values showing the complexity of this area. G traverse showed a high skewness value on the distal side of the moraine; and became less skewed, or showed a more normal distribution, as one moves towards the proximal side of the moraine. M traverse becomes less highly skewed as one moves in towards the center of the moraine from both the proximal and distal sides. A and B traverses show least skewed values on the outside of the moraine; and became progressively more skewed as one moves towards the proximal side of the moraine.

The positive values of skewness may be biased in that they do not take into account the coarse fraction of the total sample; and the inclusion of the coarse fraction would certainly reduce the positive skewness. The presence of fines may indicate a general lack of fluvial action or reworking of the material following initial deposition.

d) Kurtosis

Kurtosis values were determined by use of the 'graphic kurtosis' formulae employed by Folk and Ward (1968) describing the peakedness of the frequency distribution curve.

$$K_g = \frac{\phi_{95} - \phi_5}{2.44 (\phi_{75} - \phi_{25})}$$

where K_g = graphic kurtosis

Values for K_g are shown in FIG. 36. Folk (1968) has suggested verbal limits of -

under .67 very platykurtic

.67 - .90 platykurtic

.90 - 1.11 mesokurtic

1.11 - 1.50 leptokurtic

1.50 - 3.00 very leptokurtic

over 3.00 extremely leptokurtic

M begins with a platykurtic curve on both the proximal and distal sides and grades to leptokurtic near the central ridge of the moraine. Thus the tails are better sorted near the outer portions of the moraine, while higher sorting (poorly sorted) values for the middle portion occur near the center of the moraine. A traverse shows a platykurtic curve value for the distal side of the moraine, becoming leptokurtic as one moves towards the proximal side. G values show a leptokurtic tendency on the distal side and becomes more normally peaked as one moves towards the proximal side.

All kurtosis values were normalized by use of an equation of Folk (1968). The normal curve has a value of .50 and most sediments occur between .40 and .65. An overall mean (average mean) value for individual traverses is shown in FIG. 36.

The western portion of the moraine shows, on the average, platykurtic values which tend to be bimodal with subequal amounts of the two modes. The eastern portion of the moraine shows leptokurtic values and tends towards a unimodal size distribution, while material in the northern portion of the moraine tends to be mesokurtic.

When all samples were looked at individually, the following observations were noted.

<u>KURTOSIS</u>	<u>FREQUENCY</u>	<u>% OF TOTAL</u>
Platykurtic	6	37
Mesokurtic	7	44
Leptokurtic	3	19

The high predominance of platykurtic over leptokurtic shows the possibility of bimodal distributions throughout the moraine. Platykurtic samples, according to Landim and Frakes (1968), reflect velocity fluctuations which affect the tails of the distribution much more significantly than the central portion, and thus indicates a more erratically fluctuating medium of transport.

e) Frequency Distributions - Histograms

Histograms were drawn for all samples analyzed, showing percentage distribution by weight. The coarse fraction was included, i.e. -1.0 phi and greater.

Samples M_1 and M_{11} represent the proximal and distal extremes on the western portion of the moraine. Both show relatively smaller coarser and larger fine values than samples between them. Both samples also show three distinct modes, i.e. coarse fraction, fine fraction, and another smaller mode at one phi. It may be presumed that even if the coarser and finer fraction were distributed over their respective remaining phi values, modes would occur within each fraction. The remaining samples between these two extremes show similar distributions, but have a higher coarser than finer fraction. The samples again show three modes in the coarser and finer areas as well as at one phi. A minimum value occurs in all samples at 4.0 phi.

Material in the proximal side of the moraine on the northern section shows large coarse fractions, with varying percentages of material in the finer fractions. In general there are three distinct modes, one coarse, another at one phi, and another at the fine fraction of 4.0 phi and greater. Material located near the top of the northern portion of the moraine shows a lower percentage of coarse material and a corresponding higher percentage of medium and fine material. Instead of three distinct modes, there are four or five (modes). The distal side of the moraine shows again three distinct modes similar to those for the proximal side.

Samples taken on the eastern side of the moraine show the same distribution as that for other areas along it. There is

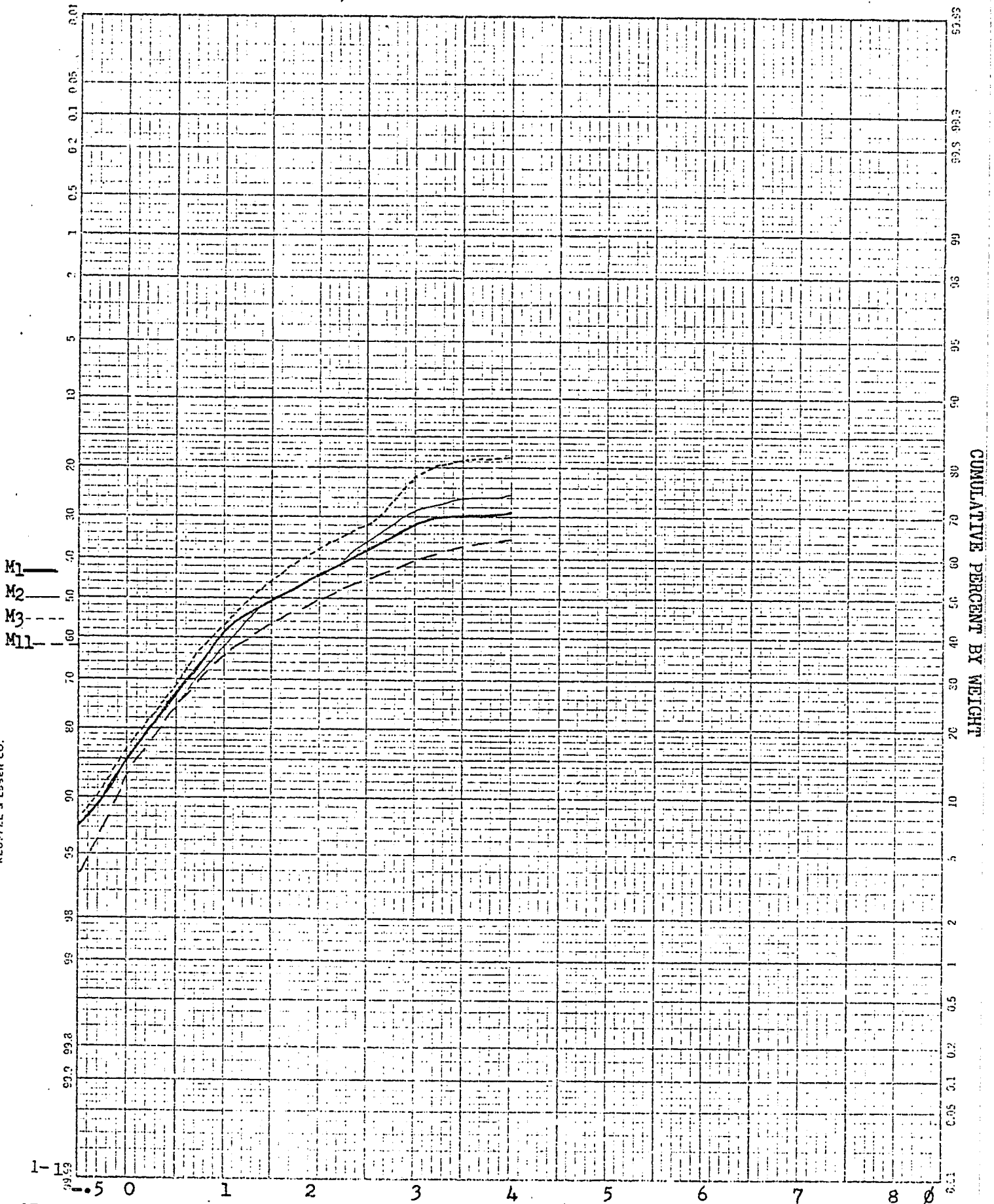
a large percentage of coarse material, another mode in the finer fraction (> 4 phi), and another mode at -0.5 phi.

Samples were taken at both A and B stations at each level concomitant with thermal depth probes. Material at the 15 cm level showed three distinct modes, coarse, zero phi, and fine fractions at both A and B. The percentage by weight varied to a degree in the medium fraction. The 31 cm depth showed a similar distribution to that at 15 cm, but had more variation in the medium fraction. A sample showed a higher percentage by weight in the 0 phi to 1.0 phi, and 3.0 phi range. Also A sample contains more modes than B sample, showing the complex nature of the material. Material at the 46 cm level, at both A and B, shows a similar tri modal distribution at < -1.0 phi, > 4.0 phi and -0.5 phi range.

A very similar distribution, i.e. tri modal, occurs throughout most of the moraine. However, there are variations within this pattern, both in terms of number of modes and percentage by weight composition. Higher percentages of fines are generally found on both the outer and inner extremes of the moraine than those between. Similar variations may be found on prominent features such as mudflows and prominent ridges. The percent by weight composition also varies with depth at both A and B stations, again showing the complexity of the character of the end moraine sediments.

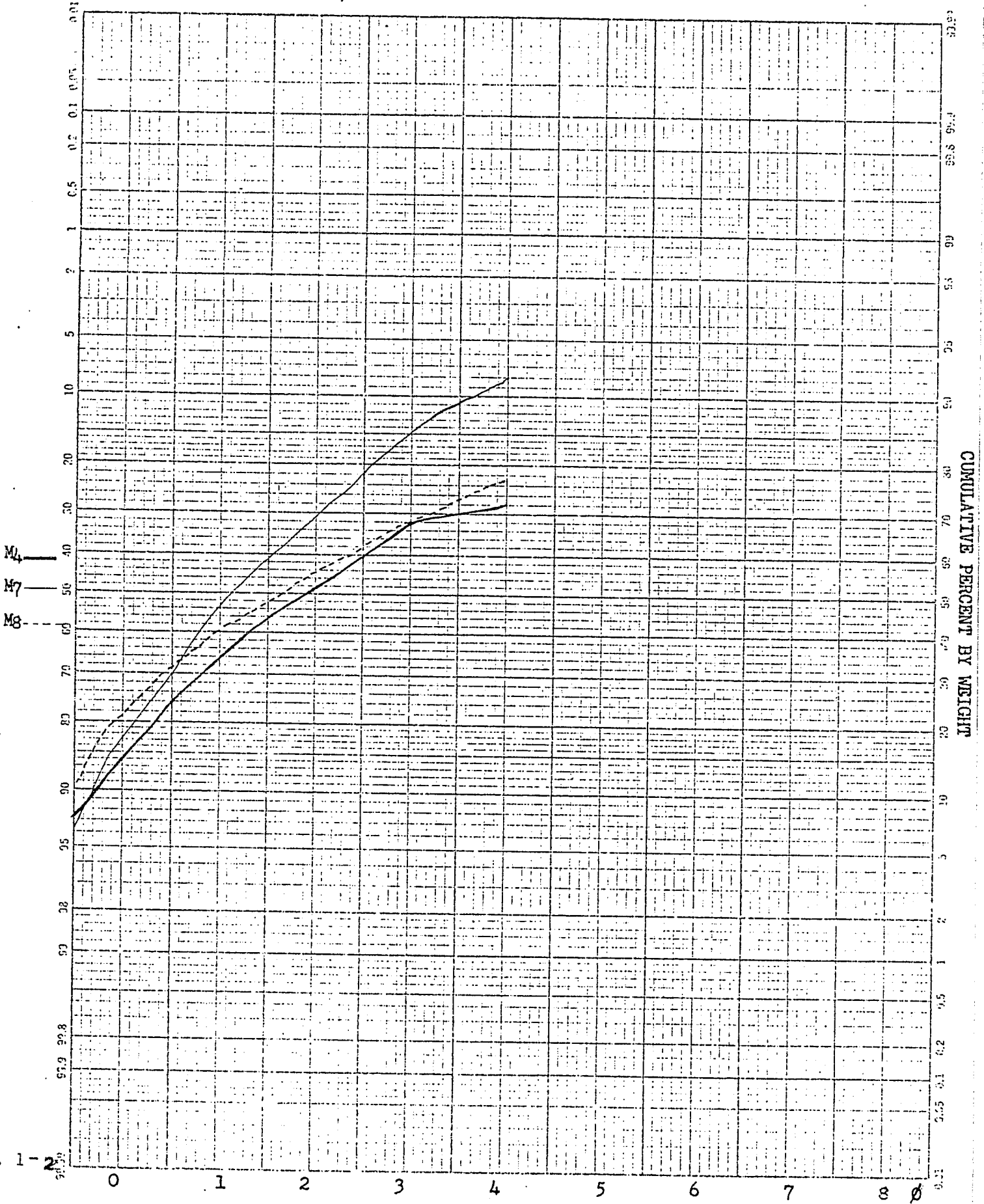
STATISTICAL PARAMETERS OF GRAIN SIZE ANALYSIS

<u>Sample</u>	<u>Mean Size</u>	<u>Sorting</u>	<u>Skewness</u>	<u>Kurtosis</u>	<u>Average Mean Size</u>	<u>Average Mean Sorting</u>	<u>Average Mean Skewness</u>	<u>Standardized Average Mean Kurtosis</u>
M ₁	.26	3.3	+ .25	.73	.28	3.1	+ .16	.45
M ₂	.26	3.6	+ .22	.83				
M ₃	.30	2.5	+ .25	1.10				
M ₄	.25	3.6	+ .05	.73				
M ₇	.40	2.1	+ .07	1.00				
M ₈	.26	3.0	+ .15	.76				
M ₁₁	.21	3.7	+ .12	.63				
G ₁	.38	2.2	-1.36	1.20	.32	2.4	- .20	.51
G ₂	.34	2.2	+ .42	1.0				
G ₄	.26	2.6	+ .14	.93				
G ₅	.28	2.7	0	.98				
A ₁	.28	3.1	+ .14	.70	.35	2.3	+ .18	.49
A ₂	.30	2.3	+ .17	.97				
A ₃	.48	1.5	+ .23	1.30				
B ₂	.30	2.2	+ .50	.98	.45	1.7	- .24	.57
B ₁	.60	1.1	- .03	1.70				



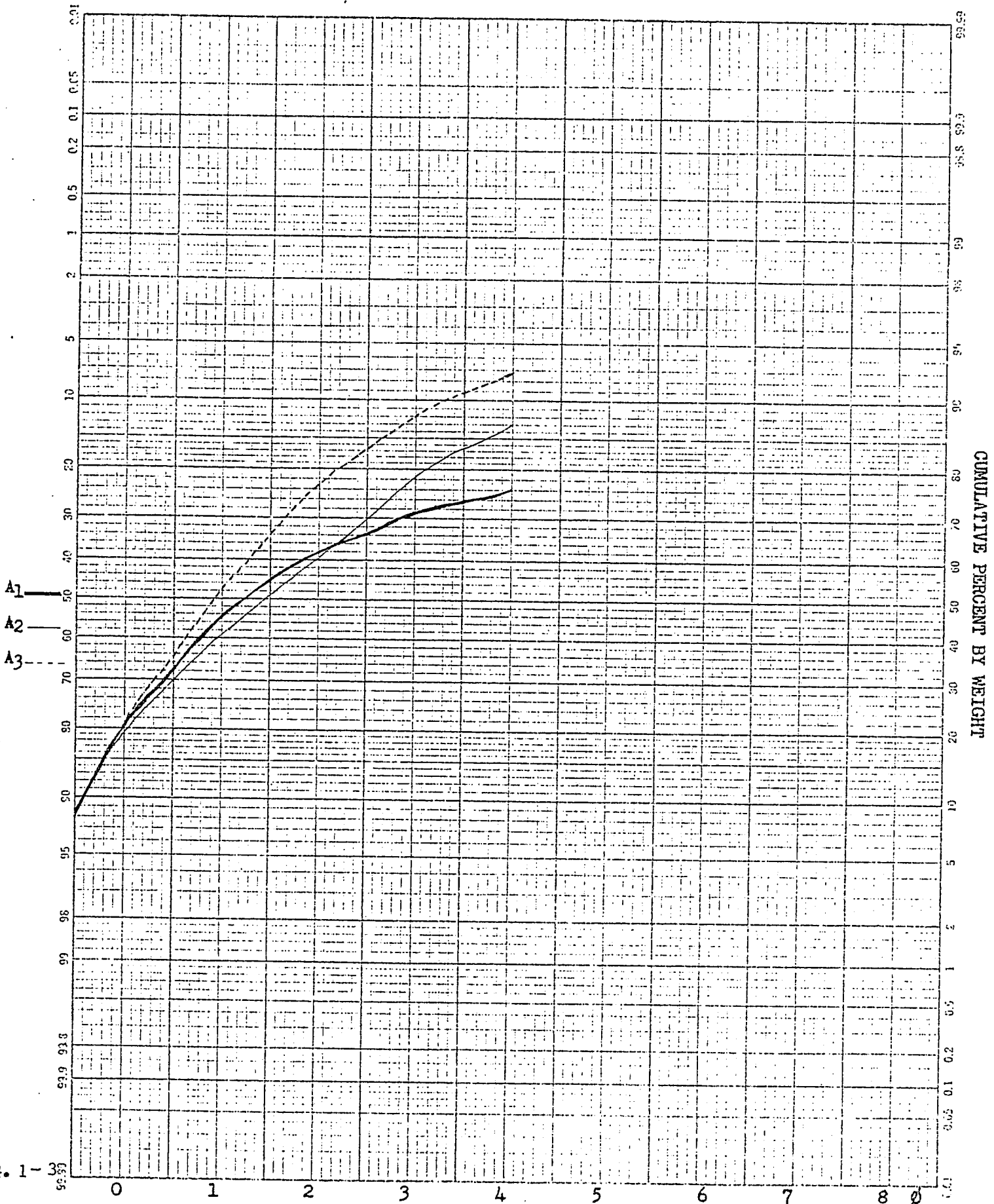
1000 X BU DIVISIONS
MADE IN U.S.A.
LUFTTEL & ESSER CO.

FIG. 37



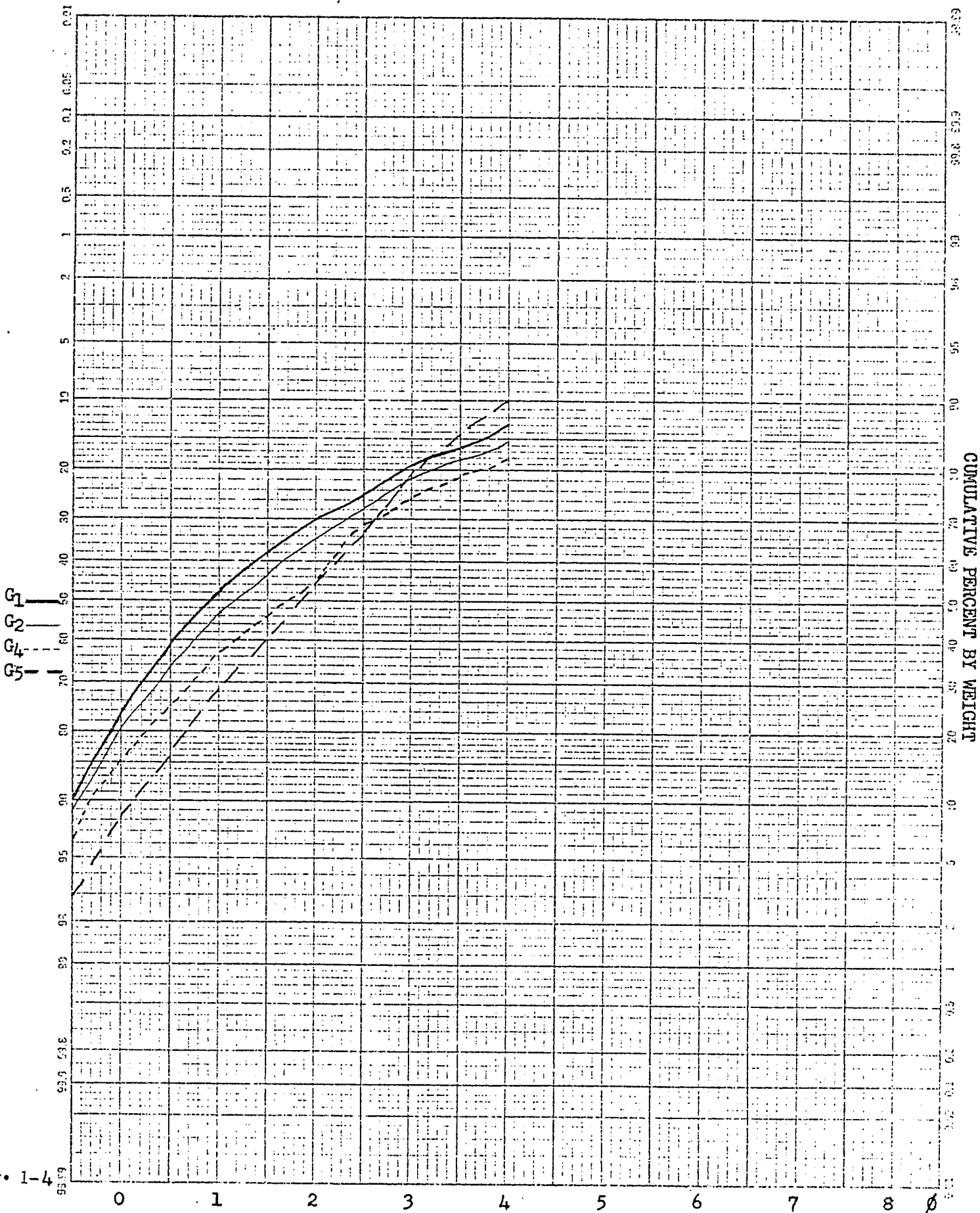
IN ALL X DIVISIONS MADE IN U.S.A.
NEUFEL & ESSER CO.

FIG. 1-2



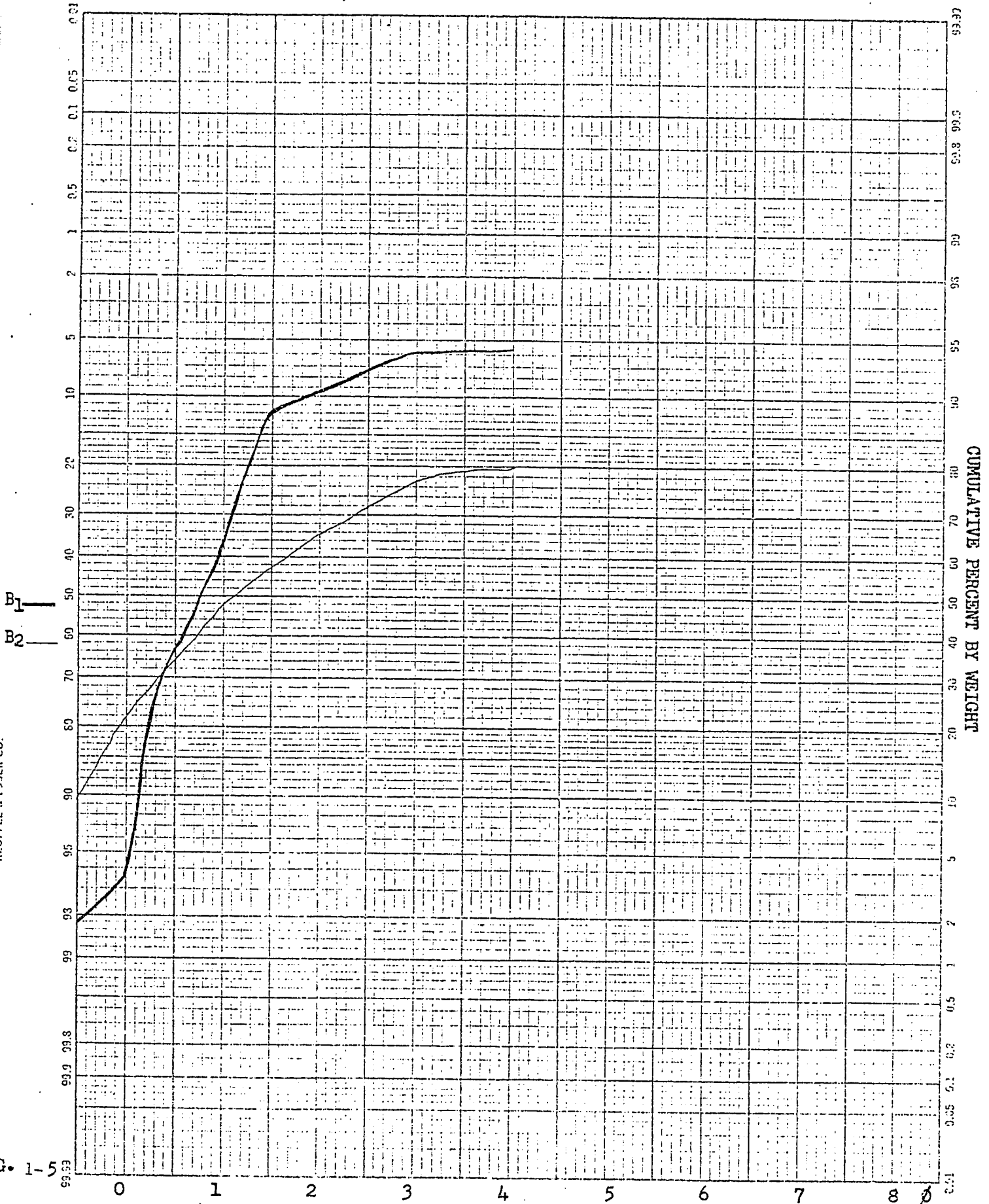
MECHANICAL DIVISIONS
MADE IN U.S.A.
NEUFULL & ESSER CO.

FIG. 1 - 33



GENERAL ELECTRIC CO.
MILWAUKEE, WIS.
DIVISION OF
ELECTRIC & ELECTRONIC DEPARTMENTS
MADE IN U.S.A.

FIG. 1-4



WILSON JONES
X 50 DIVISIONS
MADE IN U.S.A.
RUFFELL & ESSER CO.

FIG. 1-5

2. General Discussion of Heat Flow Through Soil

2.1 Soil Thermal Parameters

The transfer of heat through soil is a very complex problem involving many variables and sets of interrelationships, all of which could not be measured or taken into account in this work. However by using values obtained by others for certain variables not measured in the field, coupled with values which were obtained directly from field measurements together with general formulae derived for heat flux in soil, certain trends were apparent.

The rate at which heat flows through a soil at a depth Z below the surface is directly proportional to the vertical temperature gradient existing at that level. The equation

$$G_1 = -\lambda \frac{T}{Z} ,$$

gives the heat flow through a soil at a depth Z , where the heat flow is both positive and downward when the temperature decreases with depth. The constant of proportionality is called the thermal conductivity, and is a function of the composition, moisture content, and temperature of the soil. (Chang 1958, from Sellers 1967). The thermal conductivity of a soil is the rate at which the heat energy passes through a unit area of a given material in a given time when a temperature gradient of

$1^{\circ}\text{C cm}^{-1}$ exists. Values of thermal conductivity for various materials have been presented in Fig. 38, while Fig. 39 shows how it increases with increasing moisture content. The thermal conductivity is also higher for frozen than for unfrozen soil, e.g. Water (λ) = 0.0013, Ice (λ) = 0.005 cal. $\text{cm}^{-1} \text{sec}^{-1} \text{ }^{\circ}\text{C}^{-1}$. (Sellers 1967, Yong and Warkentin 1966).

Another factor influencing the rate of heat transfer through the soil is the heat capacity of the media. This term may be defined as the quantity of heat required to raise the temperature of a unit mass of the material by one degree F or C. The units are BTU $\text{ft}^{-3} \text{ }^{\circ}\text{F}^{-1}$ or cal $\text{cm}^{-3} \text{ }^{\circ}\text{C}^{-1}$. In reduced equation form the heat capacity may be defined by $c = 0.46x_m + 0.60x_o + x_w$ cal $\text{cm}^{-3} \text{ }^{\circ}\text{C}^{-1}$ where x_m , x_o and x_w are the volume fractions of minerals, organic matter, and water; and 0.46 and 0.60 are average values of the heat capacity of minerals and organic matter respectively at 10°C ; and the heat capacity of water is 1.0 cal $\text{cm}^{-3} \text{ }^{\circ}\text{C}^{-1}$.

Figure 40 shows the dependence of the heat capacity on the moisture content whose values are shown in terms of a ratio of volume fraction of water to the volume fraction of air in the oven-dry soil. It would appear from this figure that the heat capacity varies linearly with the moisture content. Also the heat capacity is greater for

THERMAL CONDUCTIVITY VALUES FOR VARIOUS SOIL CONSTITUENTS

Substance	T (°C)	λ (m cal cm ⁻¹ sec ⁻¹ C ⁻¹) 1 m cal = 10 ⁻³ cal)
Quartz	10	21.0
Clay Minerals	10	7.0
Organic Matter	10	0.60
Water	10	1.37
Ice	0	5.20
Air	10	0.06

Fig. 38 (Sellers, 1967, p. 127)

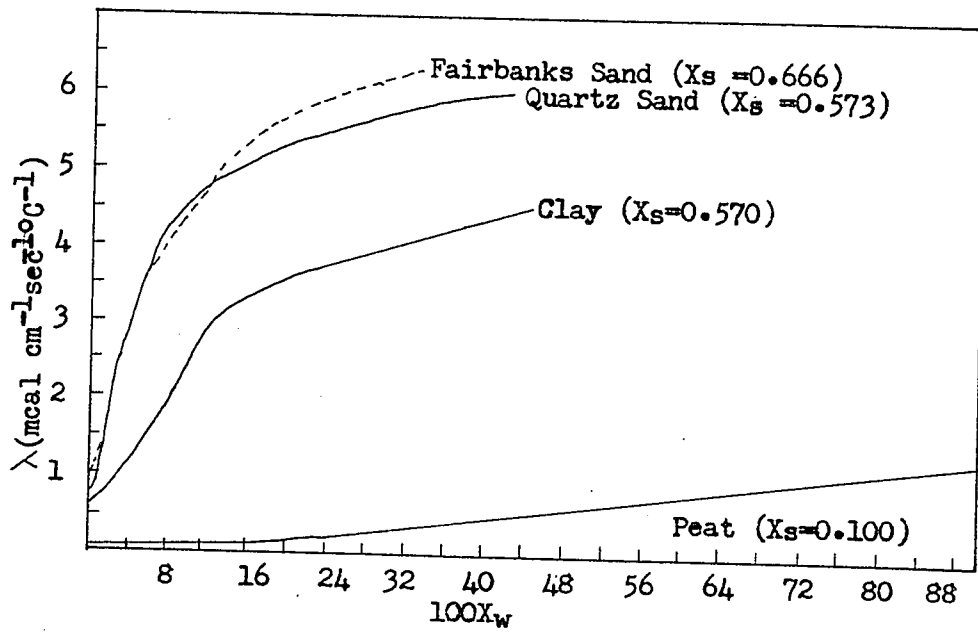


Fig. 39 DEPENDENCE OF THE THERMAL CONDUCTIVITY λ ON THE VOLUME FRACTION OF WATER X_w FOR FOUR DIFFERENT SOIL TYPES. (from Sellers, 1967, p.128)

DEPENDENCE OF HEAT CAPACITY ON THE MOISTURE CONTENT

Soil Type	X_s	C_s	X_w/X_{ad}				
			0	0.2	0.5	0.8	1.0
Sand	0.585	0.517	.302	.385	.510	.634	.717
Clay	.417	.576	.240	.357	.532	.706	.823
Peat	0.246	.602	.148	.300	.525	.751	.902

Fig. 40 (Sellers 1967, p. 132)

unfrozen soil than for frozen soil, e.g. Ice (C) =
 $0.46 \text{ cal cm}^{-3} \text{ }^{\circ}\text{C}^{-1}$ at 0°C .

In engineering practice, the term volumetric heat capacity is used and refers to the volumetric heat of soil-water; and is the product of the specific heat C and the dry density of the material.

$$C = \left(.17 + \frac{W}{100} \right) \rho_d \text{ BTU ft}^{-3} \text{ }^{\circ}\text{F}^{-1}$$

(Tuma and Abdel-Hady 1973)

As has been previously shown, the moisture content of soils plays a major role in determining heat flux and temperature profiles in soils. The moisture content of most soils normally lies between field capacity and the permanent wilting point. Gray (1970), defines field capacity as the amount of moisture retained by a soil initially at a higher water content, which is permitted to drain by gravity, for a specified period of time (usually 2 or 3 days). Gray also defines the permanent wilting point as the soil moisture content when plants permanently wilt. Sellers gives representative values of both the wilting point and field capacity in terms of the ratio expressed under heat capacity (Fig. 41). (If the volume of the soil particles is known, the wilting point and field capacity can be expressed in terms of percent volumetric fraction.)

REPRESENTATIVE MOISTURE CONTENTS AT THE WILTING POINT
AND AT FIELD CAPACITY FOR THIRTEEN SOIL TYPES

Soil Type	$\frac{X_w}{X_{ad}}$	
	Wilting Point	Field Capacity
Gravel	0.04	0.11
Coarse Sand	0.06	0.13
Medium Sand	0.10	0.26
Fine Sand	0.15	0.35
Sandy Loam	0.19	0.43
Fine Sandy Loam	0.25	0.56
Silt Loam	0.30	0.66
Silt Clay Loam	0.36	0.72
Clay Loam	0.32	0.74
Silt Clay	0.47	0.93
Clay	0.48	0.93
Heavy Clay	0.65	1.21
Peat	0.21	0.62

* Values are expressed in terms of the volume fraction of air, X_{ad} , in oven-dry soil.

2.2 Unidirectional Heat Transfer

It is assumed in this study that heat transfer does not occur horizontally but only in a vertical direction. Thus the rate at which a soil layer is warming or cooling can be determined by measuring the vertical flux at two different depths. If G_1 and G_2 are two depths within the soil, then

- (1) Vertical flux through the top layer is

$$G_1 = -\lambda_1 \left(\frac{\Delta T}{\Delta Z} \right)_1$$

λ = Thermal Conductivity
 T = Soil Temperature
 Z = Depth

- (2) Vertical flux through the bottom layer is

$$G_2 = -\lambda_2 \left(\frac{\Delta T}{\Delta Z} \right)_2$$

$$\text{and } G = G_1 - G_2 = \lambda_1 \left(\frac{\Delta T}{\Delta Z} \right)_1 - \lambda_2 \left(\frac{\Delta T}{\Delta Z} \right)_2$$

The rate of change determined above is directly proportional to the observed time rate of temperature change .

$$G = -C \frac{\Delta T}{\Delta Z} \cdot \Delta Z$$

C = Heat Capacity

Z = Soil Depth

T = Soil Temperature

t = time (hrs or months)

where

Sellers (1967) has rewritten the above equations in differential form and equated them.

$$\frac{\partial G}{\partial Z} = - \frac{\partial}{\partial Z} \left(\lambda \frac{\partial T}{\partial Z} \right) = -C \frac{\partial T}{\partial t}$$

Assuming the soil is homogeneous and thus thermal conductivity does not vary with depth, then

$$\frac{\partial T}{\partial t} = \frac{\lambda}{C} \frac{\partial^2 T}{\partial Z^2} = K \frac{\partial^2 T}{\partial Z^2}$$

where $K = \frac{\lambda}{C}$ is defined as the thermal diffusivity.

As previously mentioned the above equation represents one-dimensional heat conduction, i.e. vertical, and relates the warming or cooling of a soil column to the curvature of the temperature profile.

The thermal diffusivity determines the heating or cooling rate accompanying a given temperature profile. As with thermal conductivity and heat capacity, the

thermal diffusivity is dependent upon soil moisture content (Fig. 42). The figure reveals that k is greatest at moisture contents of between 8-20 percent by volume. Within this range, the thermal conductivity is not far removed from its maximum value and the heat capacity is relatively small. The soil conducts heat efficiently, and warms or cools readily for a given energy input or output. Due to the insulating effect of air between the soil particles, soils with low moisture contents reduce the heating or cooling rate. At high moisture levels, the heat capacity of the soil is greatly enhanced resulting in small temperature changes, and again low diffusivity values. Figure 43 shows some k values for various soil types. According to Sellers (1967 p. 140), the thermal diffusivity of most soils lies between .001 and .012 $\text{cm}^2 \text{sec}^{-1}$.

Because the temperature profile at depth or at the surface of soil takes on an approximate form of a sine wave, one may determine the diffusivity from the amplitude and phase equations.

$$k = \frac{1}{2W} \left(\frac{z_2 - z_1}{\Delta t \text{ max.}} \right)^2$$

where $W = \text{angular frequency of oscillation} = \frac{2\pi}{P}$

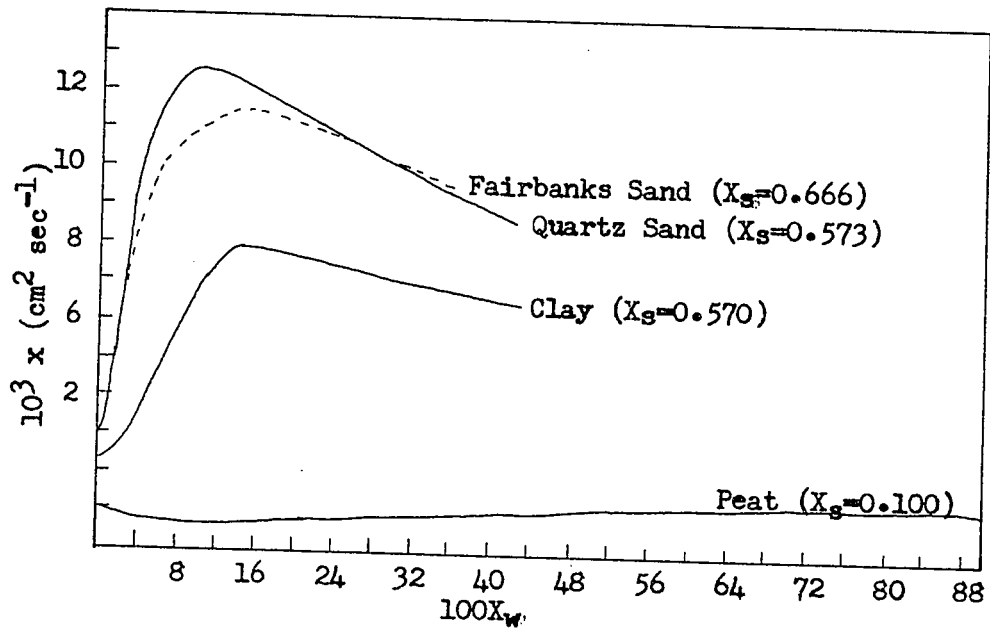


Fig. 42 DEPENDENCE OF THE THERMAL DIFFUSIVITY k ON THE VOLUME FRACTION OF WATER X_w FOR FOUR DIFFERENT SOIL TYPES. (from Sellers, 1967, p. 135)

THERMAL DIFFUSIVITY VALUES FOR VARIOUS SUBSTANCES

Substance	T (°C)	k (cm ² sec ⁻¹)
Quartz	10	.044
Clay Minerals	10	.015
Organic Matter	10	.001
Ice	0	.0114
Still Water	10	.0014
Stirred Water		
Very Stable		.1
Moderately Stable		50
Neutral		300
Still Air	10	.202
Stirred Air		
Very Stable		1.0 x 10 ³
Moderately Stable		1.0 x 10 ⁵
Very Unstable		1.0 x 10 ⁷

Fig. 43 (Sellers, 1967, p. 134)

where P = period of wave (24 hours or 12 months)

$Z_2 - Z_1$ = difference between two depths at which wave is recorded

t_{\max} = time of maximum or minimum temperature.

This above equation has been found to give satisfactory results for the annual cycle only. Another equation employing the delay $t_2 - t_1$ between the onset of a point on the wave at two depths Z_2 and Z_1 may also yield the k value.

$$t_2 - t_1 = \frac{Z_1 - Z_2}{2} \sqrt{\frac{T}{a \pi}}$$

where a = k = diffusivity

(Williams & Nickling 1972, p. 29)

Underlying Assumptions

1. Any horizontal temperature gradients are disregarded.
2. Unidirectional heat flow is either positive or negative and in a vertical direction.
3. Soil is homogeneous throughout.
4. The thermal conductivity is uniform throughout the profile.

5. Employment of maximum water content (field capacity) for moraine material.

6. Heat transfer is by conduction only. Other methods not mentioned are: a mass transfer in a liquid or vapour state such as during a rainstorm when downward percolation of water transfers heat to or removes it from near surface soil layers, or by evaporation or condensation occurring near the surface of soils in association with the migration of water vapour.

7. The thermal conductivity may change within a frozen soil (homogeneous) as the soil temperature changes.

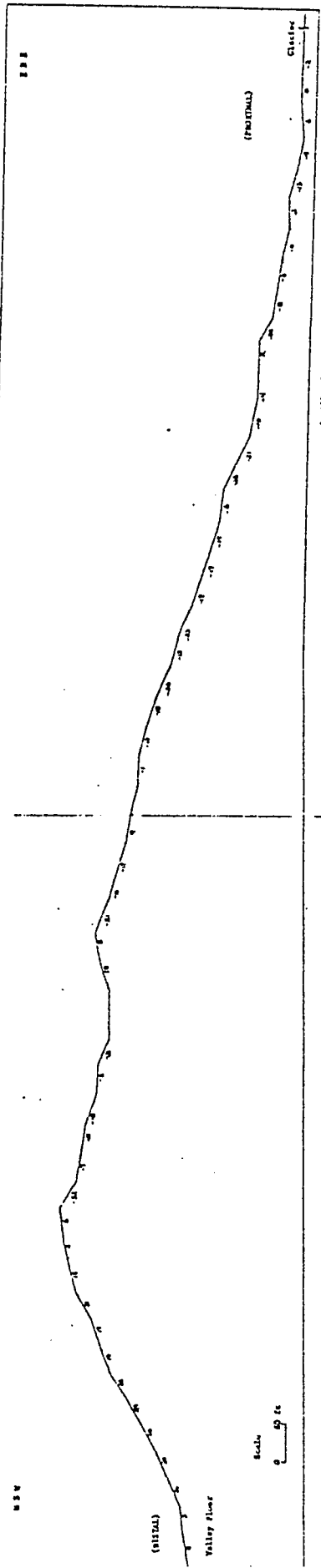


FIG. 13A. PROFILE 'J' ACROSS MESSERS OR LES PORTION MORAINES

- RESUME -

L'initiation et la répartition de certains processus de dégradation, liées à des changements topographiques qui s'ensuivent sur une moraine à noyau de glace, ont été étudiées en fonction des variations microclimatiques et des mouvements de progression qui agissent sur cette moraine. L'étude est conçue selon un modèle dynamique.

La région étudiée est localisée sur une moraine terminale à noyau de glace ayant une forme large et arquée, moraine qui borde le front du glacier Donjek et qui est située dans la vallée de la Donjek, montagne St-Elias, territoire du Yukon. Cette moraine terminale s'étend à une distance variant de 0.8 à 2.7 km. en aval de la position présentement occupée par le glacier dont elle en est détachée.

Le climat de la région fut déterminé à partir de données recueillies à une station de météorologie gouvernementale située non loin de là. Les données sur les variations climatiques en ce qui a trait à la surface de la moraine ou à faible profondeur, pour la période du 1^{er} juillet au 25 juillet 1972, ont été obtenues grâce à deux microstations météorologiques placées sur la moraine; ces données sont représentées ici sous la forme de graphiques indiquant les moyennes de température quotidienne. Des données sur le nombre de jours où une des stations enregistra une température plus élevée pour une journée complète et pour des intervalles de pluie de trois heures ont aussi été notées pour la durée de la période d'étude.

Le gradient de température des matériaux morainiques a aussi été mesuré aux deux stations météorologiques au moyen de thermomètres enregistreurs placés à des profondeurs de 15, 31 et 46 cm. Les moyennes de température quotidienne furent reportées sur des graphiques, alors que les valeurs moyennes de température furent enregistrées, pour l'ensemble de la période d'étude. Le niveau de pénétration des ondes thermiques, calculé en fonction des variations diurnes et saisonnières de température du sol en profondeur, ainsi que les alternances de gel et de dégel commandées par cette pénétration furent calculés. La quantité de chaleur fournie au sol, provenant du contact des masses d'air sur le sol, et la diffusion dans le sol de la température régnant à sa surface ont aussi été étudiées pour chaque observatoire météorologique au moyen d'équations standardisées utilisées par les services de génie. Ainsi, le niveau d'ablation du noyau de glace de la moraine est fonction des transferts de chaleur mentionnés ci-haut, des phénomènes de rayonnement et d'évaporation qui en résultent.

Les paramètres microclimatiques et les valeurs représentant le flux de chaleur sont reliés au processus de dégradation, c'est-à-dire à l'ablation, et aux autres processus qu'elle engendrent tels les coulées de boue (éboulements, glissements de terrain), et les cours d'eau fluvio-glaciaires et les étangs se formant sur la moraine. La distance de recul du mur de rimaye a été calculée aux lieux où il existe des affleurements de glace. Dans la plupart des cas mentionnés ci-haut, il est plus question de tendances que de valeurs spécifiques.

La morphologie de la moraine est représentée à la fois qualitativement et quantitativement par des mesures de l'angle de la pente du côté proximal et du côté distal de la moraine; les types de végétation et la fréquence de la présence de ces types de végétation sont reliés à l'occurrence de ces processus. Des échantillons de sol ont été pris sur la moraine et analysés pour leur granulométrie; les résultats furent utilisés dans les équations de transfert de chaleur.

Les données sur la progression des glaces en action sur la moraine furent déterminées à partir de photographies aériennes; les résultats de cette analyse furent enregistrés par rapport au recul du mur de rimaye, plus précisément par rapport aux affleurements de noyau de glace dont la présence est causée par ces avancées glaciaires.

Finalement, un échantillon de la glace enfouie provenant de la moraine à noyau de glace Donjek fut analysé pour sa texture afin de déterminer l'efficacité de cette méthode d'identification en ce qui a trait à la glace enfouie.

Les résultats de ces analyses ont montré que les variations microclimatiques se produisant sur la moraine n'expliquent pas entièrement la présence de certains types de dégradation. Par contre, l'initiation et l'accroissement des taux d'occurrence de ces processus peuvent être expliqués jusqu'à un certain point, par des accroissements similaires de certains paramètres microclimatiques tels la température ambiante, les précipitations, l'humidité relative, le rayonnement solaire, et par le

décroissement de certains autres paramètres tels l'évaporation et le vent. Les variations climatiques, et non les variations des types de sol, sont les agents responsables des variations dans la quantité de chaleur qui pénètre le sol aux deux stations et de leur taux d'ablation différentielle. Le caractère hétérogène du matériaux morainique ne nous a pas permis d'identifier des paramètres thermiques des sols.

La présence d'affleurements de noyaux de glace et des mouvements de masse qui y sont associés, dépendent principalement des variations de la profondeur des matériaux morainiques et des paramètres thermiques du sol. L'échelle du recul du mur de rimaye, calculée pour les éboulements actifs durant la période d'étude, est comparable, dans des conditions similaires, à ceux étudiés dans l'Arctique.

Dans les conditions climatiques actuelles, les taux maxima des eaux de fonte calculés pour cette moraine suggèrent la disparition du noyau de glace dans une soixantaine d'années.

Les cours d'eaux fluvio-glaciaires et les étangs qui se forment sur la moraine constituent des mécanismes de déclenchement d'éboulements et de glissements de terrain et sont responsables, par la suite, de l'inactivité de ces processus.

La moraine est très massive; sa pente distale est plus escarpée que sa pente proximale. Les angles des pentes situées sous le vent sont plus raides. Cette situation, combinée avec un microclimat d'autant plus propice à des quantités plus grandes de chaleurs transmises dans le sol

et un couvert morainique mince, a favorisé une présence active des processus de dégradation dans cette région. La surface de la moraine est très complexe du point de vue morphologique et au niveau de la nature des matériaux en présence, reflètent les nombreux environnements qui agissent présentement ou ont déjà agi sur elle. Les dimensions de la moraine et la quantité de till qui la compose sont décevantes puisque la masse des matériaux morainiques, dans la partie ouest de la moraine, ne constitue qu'une couverture très mince reposant sur une énorme masse de glace sous-jacente. L'ablation différentielle du noyau de glace a déterminé la relation de la morphologie des matériaux du surface avec la morphologie de la glace sous-jacente et le bosselage de la moraine.

L'analyse de la texture de l'échantillon de glace a révélé que s'était de la glace de glacier. Par contre, puisque d'autres types de glace peuvent avoir des caractéristiques semblables dans des circonstances particulières, il est nécessaire d'être prudent dans l'utilisation de cette méthode.